8-3-2017

Underwater Energy Storage - Emphasis on Buoyancy Technique

Kyle Patrick Bassett
University of Windsor

Underwater Energy Storage - Emphasis on Buoyancy Technique

by

Kyle Patrick Bassett

A Dissertation
Submitted to the Faculty of Graduate Studies
through the Department of Civil & Environmental Engineering
in Partial Fulfillment of the Requirements for
the Degree of Doctor of Philosophy
at the University of Windsor

Windsor, Ontario, Canada
2017

Underwater Energy Storage: Emphasis on Buoyancy Technique

by

Kyle Bassett

APPROVED BY:

_____

D. Millar, External Examiner
Laurentian University

_____

A. Sobiesiak
Department of Mechanical, Automotive & Materials Engineering

_____

E. Tam
Department of Civil & Environmental Engineering

_____

R. Balachandar
Department of Civil & Environmental Engineering

_____

D. Ting, Co-advisor
Department of Mechanical, Automotive & Materials Engineering

_____

R. Carriveau, Co-advisor
Department of Civil & Environmental Engineering

June 6, 2017

DECLARATION OF PREVIOUS PUBLICATIONS

This thesis includes 4 original papers that have been previously published/under review for publication in peer reviewed journals, as follows:

Thesis Chapter	Publication	Status
Chapter 2	Underwater Energy Storage through application of Archimedes Principle. Journal of Energy Storage, Volume 8, Pages 185-192, November 2016	Published
Chapter 3	Experimental Analysis of Buoyancy Based Energy Storage. IET Renewable Power Generation Volume 10, Issue 10, Pages 1523-1528, November 2016	Published
Chapter 4	Integration of Buoyancy Battery Energy storage with Utility Scale Wind Energy Generation. Journal of Energy Storage	Accepted. In Press.
Chapter 5	Energy Arbitrage Opportunities for Energy Storage Facilities in Ontario.	To Be Submitted
Chapter 6	Drag and work Evaluation of Buoyancy Energy Storage System. Journal Energy Storage	To Be Submitted

I am the primary, Lead author of each of the listed works. Contributions by co-authors Dr. Rupp Carriveau and Dr. David Ting were made in editing, proofreading, and supervisory capacity.

I certify that I have obtained a written permission from the copyright owner(s) to include the above published material(s) in my thesis. I certify that the above material describes work completed during my registration as graduate student at the University of Windsor. I declare that, to the best of my knowledge, my thesis does not infringe upon anyone's copyright nor violate any proprietary rights and that any ideas, techniques, quotations, or any other material from the work of other people included in my thesis, published or otherwise, are fully acknowledged in accordance with the standard referencing practices.

Furthermore, to the extent that I have included copyrighted material that surpasses the bounds of fair dealing within the meaning of the Canada Copyright Act, I certify that I have obtained a written permission from the copyright owner(s) to include such material(s) in my thesis.

I declare that this is a true copy of my thesis, including any final revisions, as approved by my thesis committee and the Graduate Studies office, and that this thesis has not been submitted for a higher degree to any other University or Institution.

ABSTRACT

The present document is a manuscript-based dissertation covering Kyle Bassett's PhD research from January, 2015 to January 2017. The research was particularly focused on studying and developing an emerging energy storage technique known as Buoyancy Battery Energy Storage (BBES). The buoyancy energy storage technique is presented and primary components are described and discussed. An idealized system was analyzed to determine governing equations of operation as well as ideal energy storage density.

Experimental analysis was conducted to confirm properties of constant discharge force with respect to both float position and storage duration. Discharge testing was conducted with a developed scale system installed in the offshore testing tank and the University of Windsor.

To evaluate the scalability of the technique, a utility scale BBES system was designed with power output capacity of 1 MW and energy storage capacity of 1MWh. Several commercially available marine lift bags were considered and evaluated for volume requirements and drag effects at various float speeds. Theoretical roundtrip efficiency for this designed system was found to be 83% based on results from drag calculations, pulley losses and electrical efficiency losses. Numerical simulations of system performance were completed to determine the revenue generation of the designed system based on 2015 Ontario market energy prices. To validate system operation in a marine environment, open water testing was conducted in Lake Huron. Testing validated surface deploy ability and steady state float motion was achieved.

To further investigate the market opportunities and challenges facing the grid scale integration of energy storage, an analysis of market conditions was performed using Ontario, Canada as a case

study. Ten years of Hourly Ontario Energy Price was analyzed using Fourier transform to reveal periodic trends within the data. It was found that the introduction of Time-of-use billing for electricity was effective in changing energy consumption behavior, improving balance for the electricity grid. Revenue generation simulations were completed for utility scale energy storage systems of various technologies (and thus various roundtrip efficiencies) using historic 2015 energy price data. Simulations included single and multi-cycle storage programs. It was determined that energy storage facilities are not currently financially viable, due to the minimal revenue produced through energy arbitrage transactions. The development of energy storage in Ontario will depend greatly on governmental subsidies and additional revenue-generating ancillary services such as regulation and black start capability.

Additional experimental analysis was performed using a modified BBES system designed to convert input energy into mechanical work such that each quantity could be controlled and measured. Three float shapes of interest were tested including a horizontally configured cylinder, a vertically configured cylinder as well as a sphere. Discharge efficiencies greater than 90% were achieved. Roundtrip efficiencies of 78% were recorded. Results suggest that with improved conversion pulleys and component scaling, experimental roundtrip efficiencies should approach the theoretical efficiency used in the 1 MW BBES system designed.

To the scientists, engineers and students
working towards improved sustainability on this planet.
I hope this helps.

ACKNOWLEDGEMENTS

I would like to express my sincere gratitude to Dr. David Ting and Dr. Rupp Carriveau for their excellent guidance and support during my PhD program. The invaluable comments and assistance from the committee members Dr. Tam, Dr. Balachandar and Dr. Sobiesiak are gratefully acknowledged. I would also like to thank external examiner Dr. Dean Millar for offering his time to review and provide input on this work.

I would like to also acknowledge Captain Grant Warga for his help in the open water testing, for allowing us to perform testing on his ship and also for the great discussions and brain-storming sessions on the topic of storing energy in the marine environment.

I would also like to express my gratitude for all the friends and family in my life who have supported my pursuit for a higher understanding of the beautiful world around us.

My Wife Elizabeth, who has witnessed and supported the madness of discovery and graciously decided to accompany me in this life long journey. Love is metaphysical gravity.

My mother Sandy, for all her support through my scholarly and scientific pursuits.

My brother Jeff, for helping me escape my desk to unwind, breathe fresh air, have a laugh, and maybe catch a pike or two.

My late grandmother Victoria Bassett-Hoffman, who told me at a young age to focus on what I was good at; math and science.

My late Father Blair, for teaching me the beauty of machines and for inspiring curiosity.

TABLE OF CONTENTS

LIST OF TABLES

Chapter 2

Chapter 3

Chapter 4

Chapter 5

Chapter 6

Appendix C

Appendix D

LIST OF FIGURES

Chapter 2

Chapter 3

Chapter 4

Chapter 5

Chapter 6

Appendix E

LIST OF APPENDICES

Chapter 1

Introduction

1.1 - Overview

This thesis documents the work completed for the formation, development and testing of a new energy storage technology known as Buoyancy Battery Energy Storage. The research in this study is presented in a series of five research papers which are currently in various stages of publication and review by engineering journals.

1.2 - Research Phases

The work presented in this thesis proceeded through various research phases as discoveries during numerical and experimental investigation into the BBES technique motivated further investigation in certain areas of the concept.

During the period of study the author attended the Offshore Energy Storage conferences for 2015 and 2016 in Edinburgh, Scotland and Valletta, Malta respectively. These learning opportunities allowed for feedback on the BBES concept as well as guidance as to what areas warrant further research. Feedback and discussion with the defence committee during the dissertation proposal also provided valuable guidance.

1.2.1 - Literature review of Energy Storage Technologies

To begin understanding the potential need for a new alternate form of underwater energy storage a literature review was completed to become familiar with the state-of-the art in the area. Existing ES technologies for both on and offshore environments were considered during this review. Technologies reviewed included Chemical Batteries, Supercapacitors, Flywheels, Pumped hydro, Compressed air, and Underwater Compressed Air.

Considering the limited application of many of these technologies for grid-scale energy storage greater than 1 MWh, it was determined that there exists a technological as well as academic need to further investigate alternate ES techniques capable of achieving these high storage capacities. Literature review is presented in Chapter 2 of this document.

1.2.2 - Formation of BBES concept

Inspiration for the energy storage technique which is the topic of this study, came to the author during an outdoor camping trip in 2011. At the time of conception the idea was quickly sketched on a piece of newspaper. The concept and sketch was left in a folder for years before reevaluation in 2015 when the author's PhD studies commenced.

In 2015, formal description of the BBES concept began with first establishing the mathematical foundations upon which the system operates. An idealized buoyancy system was presented and the force balance at the float component evaluated to determine equations for charge and discharge energy. Equations for charge and discharge power, as well as cycle time were

determined. The ideal theoretical energy density of the technique was calculated. Assumptions and idealizations used in the ideal equations of motion were discussed and qualified.

Two properties fundamental to the system operation discharge force independance of both time and position were validated experimentally. The work from this first research phase is presented in Chapter 2 of this document.

1.2.3 - First Experimental Analysis

To begin evaluating operational characteristics and performance properties of BBES, a experimental system was developed, fabricated and installed in the Offshore Testing Tank at the University of Windsor Turbulence and Energy Laboratory. A spherical float was tested for discharge power and float velocity with various loads. The influence of hydrodynamic drag as well as residual kinetic energy is defined. The work from this second research phase is presented in Chapter 3 of this document.

1.2.4 - Investigation into integration of BBES on Utility Scale

With aspects of BBES performance established through testing, an investigation into the scalability of the technique was undertaken. Commercially available marine salvage lift bags were considered as the basis for float design. Discharge forces were calculated for a range of floats. To connect multiple cylindrical floats together to form a single buoyant unit, an array configuration was defined where rows of multiple floats are arranged on a frame with a diametric distance between them. The work from this third research phase is presented in Chapter 4 of this document.

1.2.5 - Analysis of Energy Market opportunities for ES facilities

To understand the market environment in which prospective energy storage facilities will operate, a market analysis was completed for the Ontario, Canada electricity grid. IESO policy and market rules were reviewed and opportunities for ES discussed. ES interaction with the grid through energy arbitrage is defined mathematically. The concept of electricity price Global adjustment is presented and discussed with how it affects intermittent generators.

Historic Ontario Hourly price data for 2005-2015 was investigated using Fourier analysis to reveal the frequencies of price variation.

Revenue simulations are completed using 2015 price data to evaluate the income potential of operating energy storage facilities. Single as well as multi-cycle time shifting algorithms were considered. The work from this fourth research phase is presented in Chapter 5 of this document.

1.2.6 - Open Water Testing in Lake Huron

To verify that steady state operation and float velocity control could be completed, open water testing was conducted. A small scale float array featuring three cylindrical floats of similar ratios to the cylinders used in the simulated 1 MWh system was tested in Lake Huron. Tests were conducted in Blind Bay, located near Killbear provincial park in Parry Sound, Ontario. Discharge cycle testing was completed with various resistive loads. The work from this fifth research phase is presented in Chapter 4 of this document.

1.2.7 - BBES experiments with mechanical loading

In order to validate the performance of a scale BBES system under mechanical loading conditions, experiments evaluating the conversion of energy stored in Buoyancy to gravitational potential energy were completed. Cylindrical floats were analyzed in vertical and horizontal configuration. A spherical float was also evaluated. Charge and discharge performance was evaluated and experimental roundtrip efficiencies presented. The work from this sixth research phase is presented in Chapter 6 of this dissertation.

1.3 - Scope of Study

Objectives for this study are summarized in points presented below.

- Review state of literature of existing storage technologies
- Determine governing equations and theoretical limits of operation for Buoyancy Battery Energy storage (BBES)
- Execute scale tank testing to confirm overall functionality in storing and discharging energy.
- Determine relationships between storage discharge force and charge depth as well as discharge force and time
- Investigate scalability of system through design of a battery system for integration with a 2.3 MW wind turbine
- Determine theoretical round trip efficiency for developed system including drag losses
- Investigate 10 year historic data for Ontario HEP using Fourier analysis to reveal trends
- Complete revenue generation simulations for 1 MWh energy storage system operating in

Ontario market using 2015 HOEP data

- Perform experimentation and determine experimental efficiency for scale system consisting of cylindrical float in horizontal and vertical configuration

Chapter 2

Underwater Energy Storage Through Application of Archimedes Principle

.

2.1– Introduction

Wind and Solar Electricity generation is intermittent in nature, varying in both power quantity and time. International installed capacity of each has increased significantly and market trends indicate continued growth in the future [1- 6]. Intermittent power output can be optimized through the application of energy storage systems that store energy at times of low demand, and discharge energy at times of high demand. Due to the increased profit potential of supplying energy at times of peak market demand, there is motivation to couple renewable generation with grid-scale energy storage [7-9].

Several different energy storage techniques are currently under development including, but not limited to, flywheels [10-14], pumped hydro [15-18] supercapacitors [19-21], compressed air energy storage [1, 22-25] and underwater compressed air energy storage [26-29].

Flywheel energy storage (FES) involves the forced rotation of a large mass mounted to a shaft such that energy is stored in the form of rotational kinetic energy. While flywheels are common within industrial machine and automotive industries as a means to smooth the mechanical output of a motor, their application for energy storage, particularly for handling utility scale intermittent

energy sources is very new. A 5 MWh flywheel storage system has been proposed by Bornemann and Sander [12] for utility scale application utilizing superconducting bearings and a liquid nitrogen cooling process. While the system could not meet peak demand, it can be applied as a spinning electricity reserve. FES is typically used for short duration intermittence. Flywheel developers Temporal Power offer a 500 kW flywheel module for integration with existing renewable energy generation centers [14].

Pumped hydro energy storage (PHES) is the oldest form of mechanical hydro storage performed by pumping water from low to high elevation. There are currently about 280 pumped hydro storage stations worldwide with a total power of 90 GW [18]. Pumped hydro is typically used for bulk storage of large amounts of energy.

Supercapacitors are a type of electrochemical capacitor designed to handle high charge and discharge rates. Large supercapacitors for utility scale energy storage have been analyzed when coupled with a wind turbine generator system [20]. This application has shown promise for addressing short-term transients and extreme voltage events.

Compressed air energy storage (CAES) utilizes geologic formations such as solution mined salt domes or confined aquifers in order to store large volumes of compressed air. Energy is stored through the compression of air into the formations and discharged by expanding the compressed air through a turbine. Currently operational CAES plants are located in McIntosh Alabama, USA (110MW) and Huntorf, Germany (220 MW) [23]. A distinct limitation of CAES is the specific geologic configuration required. Further, there is increasing competition for potential CAES geologic units, as many are also well suited to the storage of natural gas or sequestered carbon.

Underwater compressed energy storage is similar to CAES , with the major difference being that the air is compressed in a container located underwater. Several approaches to UWCAES are under development including the utilization of distensible air container also referred to as an Energy Bag [28 , 29]. The abundance of underwater space available addresses the CAES limitation of required underground caverns. One developer, Hydrostor Inc. completed installation of a grid connected UWCAES system in November 2015 [30]. This system is deployed within Lake Ontario. Performance details of this system have yet to be published.

ORES (Ocean Renewable Energy Storage) is another approach to offshore energy storage which utilizes large concrete spherical structures mounted to waterbed [31, 32]. Water is pumped from these large containers during charge phase and is allowed to reenter the container through a turbine on discharge phase. Presently, no utility scale applications of ORES have been completed.

Presently installed renewable, intermittent, energy generation capacity far exceeds available storage, which indicates that energy storage has not received the same level of research, development and investment. No single technology provides a clear solution to the challenges faced as intermittent energy sources increase penetration rates onto existing electricity grids. The variety of operational environments of existing grids creates opportunity for a variety of storage methodologies to be applied where appropriate and thus there is motivation for further researching alternate energy storage methods not discussed thoroughly in literature.

This paper investigates one such alternate energy storage technique which utilizes an object's buoyancy as a means of energy storage known as Buoyancy Battery Energy Storage (BBES).

The technique utilizes the force of a buoyant object (buoy) submerged in water through a pulley and reel system [33, 34]. The buoyant object is affixed to a cable and rigged through a pulley mounted at the bottom of the water body. The cable then passes to a surface mounted reel unit. As the reel is turned in one direction by an external force, the buoy is forced below the water surface and locked for the desired charge period. When the force acting on the reel is removed the buoy will rise and perform work on the reel. The basic buoyancy storage system is depicted in Figure 2-1.

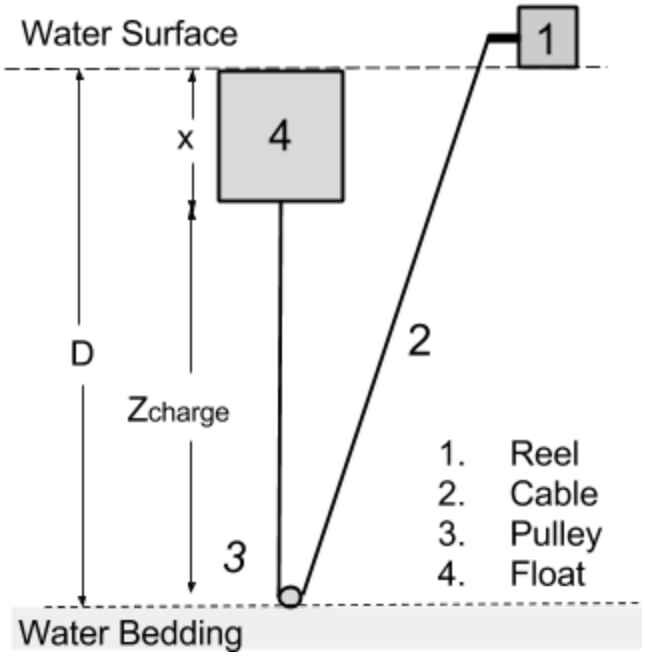

Figure 2-1 - Basic Buoyancy Energy Storage System

Research into the uses of buoyancy force for storing energy is in it's infancy. Experimental research by Alami involved the small scale testing of styrofoam buoys [34, 35]. This research featured a unique float composed of two truncated cones designed to introduce rotation as the float rises. This was accomplished by carving helix shaped grooves along the styrofoam buoy

shape. This project was successful in extracting energy from a small scale model and thus motivating future investigation into the concept. The rotational component in the kinetic energy of the buoy does increase the complexity of system dynamics, and thus there is value in evaluating the system without rotational effects.

A past patent application [33] states a potential system roundtrip efficiency of 90%, which was calculated based on an estimated generator efficiency of 95%, motor efficiency of 97%, and pulley efficiency of 99%. No experimental testing, research, or validation has been presented in the patent application to qualify or prove these claims.

The concept of buoyancy as presented in this research is distinct from the buoyancy energy storage system as presented by Klar et al. [36]. The system presented in [36] utilizes a buoyant platform acting as a reservoir for pumped hydro storage.

There are several inherent characteristics of this storage technique which make it attractive and worthy of further investigation. The BBES system can be installed within a body of water without subsurface connections, thus eliminating the requirements for remotely operated underwater vehicles (ROV) or compression diving. Also, the machinery required for BBES includes simple electric motor/ generator and cable reel each of which could be easily adopted from existing technology in renewable energy and offshore industries. Storage capacity is dependant on float volume, making the system adaptable for both shallow and deep water applications. Thermodynamic considerations are also simplified for BBES as temperature of ambient volume is unaffected by the storage and discharge cycles.

The fundamental buoyancy storage principle as depicted in Figure 1 has yet to receive sufficient research to determine its practical viability. Possible applications for integration in offshore and onshore environments have also yet to be presented and discussed in literature. The following sections outline the general theory of buoyancy energy storage and discusses the applicable losses and inefficiencies. Other characteristics of interest for BBES such as experimentally achievable efficiencies, cost per kWh storage and cost per kW of power capacity require a thorough feasibility analysis of a designed utility scale BBES system which is beyond the scope of this paper. This is a topic of ongoing research to be released in a forthcoming study. Applications are discussed in the context of possible large scale applications of the buoyancy energy storage principle.

2.2 – Idealized BBES System

The following contains the analysis of an ideal BBES system using the following assumptions and simplifications. These will be further discussed and qualified in section 2.3.

1. Ambient fluid is ideal.
2. Ambient fluid is at rest.
3. Float Volume is constant.
4. Change in total mass due to change in cable length is negligible.
5. Cable does not stretch.
6. Cable does not interfere with float.
7. No slip condition for cable on reel.
8. Reel anchor rigidly fixed to an independently supported structure.
9. Pulley anchored rigidly to water bed.
10. Friction of reel bearing assembly is negligible.
11. Friction between cable and pulley is negligible.
12. Drag losses from float motion negligible

2.2.1 Analysis of ideal system

As the reel in Figure 1 is turned, the cable is wound around the reel shaft and length of cable is decreased at a rate proportional to the reel shaft radius.

$$\Delta Lcable = 2\pi REV\, r \qquad \textbf{(1)}$$

Where $\Delta Lcable =$ change in cable length, REV= number of reel revolutions, r= radius of reel. Float has properties of mass, volume and dimensions of height, width and length. Float position is measured from bottom of float where cable is affixed. A Datum is set at the position where the full volume of float is submerged below the water's surface. Charge displacement ΔZ_{charge} is defined as the distance float can travel from initial position to the depth of water bedding D.

$$\Delta Z_{charge} = D - x \qquad \textbf{(2)}$$

The total number of revolutions for a given depth is then written by equating the change in cable length to the depth of charge through assumption 11.

For the reel to be wound a moment is applied to the shaft. The systems status is defined based on the balance of moments acting on the shaft at any given instant. The three system states of motion are expressed in equation 3 below. System at equilibrium (i.e. stationary or proceeding at constant velocity) can be expressed;

$$\sum Mx = ma = T_a - C\, r \qquad \textbf{(3)}$$

If $T_a = C\, r$, System at rest or proceeding with constant velocity.

If $T_a > C\,r$, Reel winding in positive direction, displacement of float positive downward.

If $T_a < C\,r$, Reel unwinding in negative direction, displacement if float negative upward.

where Ta is the applied torque to the reel shaft and C is the tension force in the cable. Considering the system beginning at rest, the reel will begin to be wound in the positive direction as the applied torque becomes greater than the torque caused by cable tension acting in the negative direction.

The cable tension can be found by considering the balance of forces acting on the float at equilibrium.

$$0 = F_b - mg - C \qquad \textbf{(4)}$$

Where F_b is the buoyancy force acting on the float, m is the mass of float, and g is gravitational acceleration. Buoyancy force can be calculated using the familiar form of the Archimedes equation [37].

$$F_b = -\rho_f g V \qquad \textbf{(5)}$$

Cable tension C, can then be found by inserting buoyancy force equation into (4) and rearranging.

$$C = \rho_f g V - mg \qquad \textbf{(6)}$$

The torque required to wind the reel at constant velocity is then calculated by inserting (6) into (3) and as this torque is applied, work is performed. The total work that can be performed for a

given water depth can then be defined. To simplify calculations the work can also be calculated by considering the linear displacement of the float.

$$W = \int_{Z1}^{Z2} C \, dz \qquad \textbf{(7)}$$

Thus the work that can be input into the system is proportional to float volume, float mass, and float displacement. The maximum work that can be performed given a specific water depth can then be expressed;

$$W_{max} = E_{charge} = C \, \Delta Z_{charge} \qquad \textbf{(8)}$$

The power input during the charge cycle and the charge time required given a desired power input can then be defined in terms of rotational motion at reel or linear motion of the float.

$$P_{charge} = C \, r \, \omega = C \, V_c \qquad \textbf{(9)}$$

$$t_{charge} = \frac{Z_{charge}}{4\pi^2 \, C \, r^2} P \qquad \textbf{(10)}$$

The above equations express the mechanism of the charge cycle, with energy input through the force of an applied torque on the shaft acting for a given time period. Using a mechanical lock on the reel shaft, the float can be held at a desired position for an indefinite period of time.

When it is desired that the stored energy be released, the balance of moment in (3) is shifted and the torque caused by the net upward force will cause the float to accelerate in the negative Z direction (towards the water surface) . A load torque T_L can then be applied to the reel such that the energy can be extracted from the system. This torque can be applied through mechanical or

electrical loading. $E_{discharge}$, $P_{discharge}$, $t_{discharge}$ can be found by evaluating the equations derived for charge operation at the relevant discharge velocity.

The derived equations form the basis for buoyancy storage system design as energy storage capacity can be estimated for a given water depths and float volumes along with discharge times and power levels.

An ideal storage capacity can now be calculated using (9) with a unit volume float cube and a 1 meter charge depth submersed in room temperature water. For this ideal storage capacity it is also assumed that the buoyancy force is much greater in magnitude compared to float weight such that M_{float}=0. BBES can be applied in both freshwater or seawater.

$$E_{ideal} = \rho_f g V \Delta Z_{charge} = (999.7 \tfrac{kg}{m3})(1m^3)(9.81 \tfrac{m}{s2})(1m) = 2.72 \text{ Wh}$$

This energy density is equivalent to that of pumped hydro energy storage. Density of freshwater has been used to calculate the ideal limit for BBES applied in a lake as the authors are developing the concept for applications in Canadian Great Lakes. . To determine a more realistic model of BBES, analysis of inefficiencies and losses are further discussed below.

2.2.2 - Inefficiencies and losses

In order to consider a more realistic buoyancy storage model, the idealizations and assumptions presented in 2.0 must be qualified and discussed.

2.2.2.1 - Hydrodynamic Losses

Assumption 1 regarding the idealization of the ambient fluid can be further complicated by considering the hydrodynamic forces acting on the float through its motion during charge and discharge phases. In a realistic model, the float will perform work to the fluid proportional to the hydrodynamic drag force opposing the float's motion. Drag force is expressed below.

$$F_d = \tfrac{1}{2}\,\rho A v^2 C_d \qquad \textbf{(11)}$$

Where A is the area of float perpendicular to motion, C_d is drag coefficient, and F_d is the drag force acting opposite direction of float velocity. Since F_d is acting against the float motion for both the charge and discharge phases the total energy loss will be the sum of the losses for charge and discharge.

$$E_{drag} = (F_{d1} + F_{d2})\,z = \tfrac{1}{2}\rho A\,(V_c^{\,2}\,C_{d1} + V_{dc}^{\,2} C_{d2})\,z \qquad \textbf{(12)}$$

Where V_c = charge velocity, V_{dc} = discharge velocity, C_{d1} =Drag coefficient at charge velocity V_c, C_{d2} =Drag coefficient at discharge velocity V_{dc}. For cases where charge velocity equals discharge velocity and float is symmetric about horizontal plane;.

$$E_{drag} = (\rho A V_c{}^2 C_{d1})\, z \qquad \textbf{(13)}$$

Assumption 2 regarding the ambient fluid at rest holds true for cases where ambient fluid is in a container or tank. For BBES in an open water body (i.e. lake or ocean) this assumption can be approached through proper site selection to find locations where ambient fluid velocities are at a minimum. Ambient fluid velocity greater than zero will result in an increase in cable tension for both charge and discharge phases. During charge phase the hydrodynamic drag will exert a force parallel to ambient fluid flow. This will increase the cable tension and in turn increase the reel input force required to submerge the float. If the ambient fluid velocity remains constant, the additional energy input will be recovered during discharge phase as the hydrodynamic drag contributes to the output torque on the reel. Thus for constant ambient fluid velocities, round trip efficiency of BBES is not affected.

In cases where ambient fluid velocity is variable, efficiency can be affected in both positive and negative ways. Efficiency will be affected positively in a case where ambient fluid velocity is low or zero during charge phase and greater during discharge. In this case the hydrodynamic drag does not affect charge cycle but increases output for discharge. Efficiency will be affected negatively when ambient fluid velocity is high during charge phase but low or zero during discharge. In this case additional work performed during charge is not recovered during discharge.

2.2.2.2 - Tidal Considerations

Although primarily designed for the storage of energy, the BBES system has potential for energy generation through the harvest of tidal energy. By charging at time of low tide and discharging at

high tide, additional depth is gained through which the float can travel during discharge resulting in additional generated energy. While all water bodies are affected by tides through gravitational pull due to lunar forces, the locations where the water level variation is large enough to be considered useful in energy generation are limited primarily to oceanic coastal areas . The largest tidal variation on the planet is 16.1 m occurring at the Bay of Fundy on the Eastern coast of Canada. The additional energy generated due to tidal effects can be calculated using equation (8) with the Z value equal to the difference between high tide and low tide water levels. An ideal location for tidal generation coupled with energy storage requires both sufficient depth, allowing for bulk energy storage, as well as significant tidal variation in water level. This is problematic as tidal effects are diminished as water depth increases.

2.2.2.3 - Acceleration Losses

Energy will also be lost at the beginning of both the charge and discharge cycles as force is required to accelerate the float to the speed required to meet desired power input or output. This energy can be recovered for the charge phase by removing the reel input torque before the desired charge depth, such that the final metres of charge depth are gained through float inertia. The same principle must be applied at the end of discharge phase with the final meters achieved under increased reel torque.

The level of control required to recover the acceleration losses is easily obtainable using modern motor control algorithms. While this controller does complicate the system operation, it should

not be reviewed as a significant challenge to implementation as complex control algorithms are widely used through heavy machine industry including utility scale wind turbines.

2.2.2.4 Cable Idealizations

Assumptions 3 through 5 should be easily addressed through correct selection of cable size and material by applying existing design principles. The cable weight is several magnitudes smaller than the net float buoyancy and thus the change in total cable weight between charge and discharge has minimal effect on overall system performance. State of the art of cable technology should be considered such that the cable will not stretch during system operation.

2.2.2.5 Mechanical Losses

Friction at both the reel bearing assembly and pulley will increase the force required during charge and reduce the output force during discharge. This will negatively affect overall efficiency at a rate proportional to angular speed of the reel and pulley assemblies. Losses can be calculated for a given bearing assembly using well established equations of bearing design.

2.2.2.6 Reel and Pulley Anchorage

Rigid anchorage of reel can be accomplished using principles in use for offshore wind turbines and offshore oil drilling operations. While fixed anchorage of the reel structure to the water bed may not feasible in cases of great water depth, a floating platform can be utilized. In case of floating platform, the effects of rising waters due to wave and tidal motion must be considered.

The anchorage required for the pulley can be achieved through the use of a large foundation mass to which the pulley is attached. This foundation mass can be a concrete structure or large

rock basket. The required foundation mass will be proportional to ambient fluid velocity, float volume, and design safety factor. For zero ambient fluid velocity mass required can be expressed.

$$M = \frac{2((\rho V g - mg)Sf)}{g} \qquad \textbf{(14)}$$

Where M is foundation mass, Sf is safety factor. With the foundation mass correctly designed, the pulley can be deployed from the water surface and left to fall under its own weight to its final position at the water bed. Torpedo piles, a promising means of offshore anchorage using large torpedo like anchor piers could also be used as a cost effective means of deployment. Compared to UWCAES, where significant deployment costs are incurred due to the requirements of divers, or underwater robots to anchor the accumulators at water bed, BBES holds a specific advantage as all equipment can be deployed from water surface.

2.2.2.7 - Float Considerations

As seen in the discussion of hydrodynamic losses above, the float design is critical for reducing losses associated with drag. In order to balance drag forces, the float should be symmetrical about both the horizontal and vertical axis and a shape should be selected with a minimum drag coefficient. The structural design of the float is also critical in maintaining assumption 11 - constant float volume. Due to the increase in hydrostatic forces with depth, if a distensible type float (similar to a balloon) were used, the float would decrease in volume as submerged, losing energy. To maintain volume, the float must have an internal structure to support its shape against the external hydrostatic force. A balloon-type float with internal pressure greater than the maximum hydrostatic pressure at max float depth could also be utilized as a constant volume

float. Computational fluid dynamics and experimental analysis should be applied to determine optimal float shapes in reducing drag due to both operation and ambient fluid velocity.

2.2.2.8 - Spatial Considerations

Utilizing the calculated energy density for a freshwater BBES system, float volume requirements can be estimated for an ideal offshore storage system of a required energy storage capacity. For a unit-radius cylindrical float, a float length of 1.17 m is required for the storage of 1 KWh when deployed in a water depth of 100 m. This can further be expanded to calculate the marine area, i.e. marine footprint, required for storage. Once again considering the cylindrical unit radius float, a marine area of 2.34 m^2 is required per 1 KWh of storage. Expanding upon these values, a float length of 1170 m and marine footprint of 2340 m^2 is required for 1 MWh of energy storage capacity. These values are based on the ideal assumptions listed in Section 2-2 and thus do not include drag losses. This required area, although large compared to other ES technologies, is not technically problematic as the marine area is more abundant and has significantly fewer competing uses when compared to land area. The social considerations of obtaining permission from marine area stakeholders for BBES installation is a separate challenge and is beyond the scope of this study.

2.2.2.9 Electrical Losses

When an electric motor and generator are used in connection to the reel such that electrical energy can be stored and discharged using BBES, additional losses will be experienced. The

power input or output from the motor unit will be proportional to system voltage and current. The required power level and thus amperage can be calculated for a given float and water depth through (11) which results in

$$I = \frac{(\rho V g - mg) V c}{Q} \qquad \textbf{(15)}$$

Where I is amperage (amps) and Q is system voltage (volts). The resistive losses within the motor are related to amperage through

$$E_{elec} = \left(\frac{C V_c}{Q}\right)^2 R \ t \qquad \textbf{(16)}$$

Where R is the total resistance of the electric motor coils, E_{elec} is electrical loss and t is time. Substituting t, we arrive at

$$E_{elec} = \frac{C^2 V_c R z}{Q^2} \qquad \textbf{(17)}$$

For equal charge and discharge power levels, and when charge and discharge occurs through the same electric motor (i.e. equal resistance of both charge and discharge phases) , the total loss can be expressed as twice the value of (17).

These electrical losses will be present for any energy storage scheme involving the conversion of rotational energy to electrical energy or vice versa including CAES, UWCAES, FES, and PHES. Theses losses can be minimized through proper motor selection such that high system voltages are used and electric motor winding resistance is minimized. This does not include inductance losses which require motor specifications for calculation.

It is also to be determined and analyzed whether it is ideal to have a single electronic device operating as both the motor and generator for the system.

2.2.3 Total Round trip Efficiency

With all major system losses accounted for the total round trip efficiency, η, of BBES system can be expressed;

$$\eta = 1 - \frac{\rho A V c^2 C d}{C} - \frac{2 C V c R}{Q^2} \qquad \textbf{(19)}$$

Which is applicable for cases of equal charge and discharge speed, and a symmetric float geometry.

2.2.3.0- Potential Applications for BBES

Considering the current state of renewable energy technology and the current challenge faced by engineers in integrating this intermittent energy onto existing electricity grids, buoyancy based energy storage may offer a useful tool in achieving the desired balance. By expanding on the basic system presented in Figure 1, several configurations can be developed for applying BBES in a variety of environments. The overall cost effectiveness and feasibility of each of these configurations are interesting and essential topics of further research. For each of the configurations presented the implementation and deployment of the energy storage system is paramount in considering the practicality of BBES in comparison to other ES schemes.

For locations with a high density of wind turbines located onshore in a coastal area, a BBES system with an onshore reel and generator unit can be utilized as depicted in Figure 2-2a.

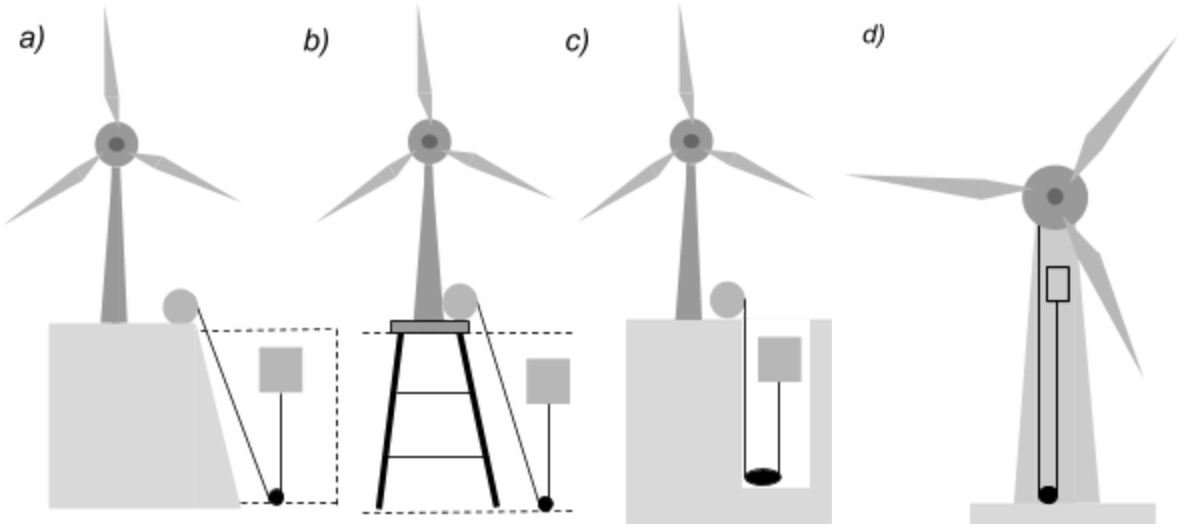

Figure 2-2 - Configuration of BBES. a - Onshore resource, offshore storage, b - Offshore resource, offshore storage, c - Onshore resource, Onshore storage, d - Storage within turbine tower

This configuration would have the advantage of reduced implementation costs for locations where an appropriate water depth is within a practical distance from shore. No underwater transmission cables would be required as existing grid infrastructure at shore would be utilized for discharging stored energy onto grid. Elaborate discussion on the use of underwater tension cables for sub-surface energy transmission is topic of future publication.

BBES can also be applied for offshore wind turbines with the reel and generator anchored to a support structure similar to an offshore wind turbine foundation as depicted in Figure 2-2b. A

sloping water bed, or a steep, nearshore, drop in water depth would be ideal environments for this application.

For the unique situation where energy storage is required, and viable water bodies are not within proximity of the energy source, the BBES system can be applied for onshore storage as depicted in Figure 2-2c. An alternate approach to this configuration would be the utilization of boreholes drilled into the ground surface to a specified depth. A casing would be applied to the borehole, and pulley anchorage installed such that the borehole could act as a container into which the ambient fluid would be poured and float would be suspended. While utility scale storage may not be achievable using standard auger and drilling equipment, this approach does present significant research potential for investigation of BBES. This approach can facilitate testing of small floats submersed to significant depths unachievable in lab settings while also eliminating the significant environmental and regulatory concerns of testing in an open body of water such as a lake. Utilization of the wind turbine's tower as a container for ambient fluid allows for energy to be stored within direct vicinity of generation as depicted in Figure 2d.

For onshore storage configurations the ambient fluid within the turbine tower does not need to be water but designers can select from a variety of available fluids with varying densities and viscosities. This will affect the overall storage capacity for a given depth as expressed in the governing equations presented above. Water with high dissolved salt content is an example of fluid which would increase the storage capacity for an enclosed system.

For each of the configurations presented, detailed design and cost analysis is required to determined each configurations viability as a practical energy storage scheme. Environmental

considerations such as the float, pulley and cable impact on marine plants and animals must be taken into account. For offshore configurations, technology and experience developed in the offshore oil industry must be applied such that BBES can benefit from previous industry advances.

4.0 – Experimental Testing

Before any of the above applications can begin to be realized or further investigated, the basic operation of the buoyancy storage system needs to be tested and evaluated in a controlled laboratory environment. Basic experimental analysis has been conducted to test a proof of concept buoyancy model as presented by the authors in [40]. This testing involved the confirmation of a basic buoyancy system's ability in storing and discharging mechanically introduced energy. For more serious theoretical and analytical evaluation of buoyancy storage and it's potential for utility scale energy storage to continue, there is significant value in confirming the most fundamental parametric relationships involved. Of particular interest for experimental validation in this paper are the relationships of discharge force, depth and storage time.

To begin testing the various fundamental performance aspects of buoyancy storage an appropriate apparatus and testing facility was required. The Turbulence and Energy Laboratory offshore testing tank was utilized for this series of testing. A basic reel system was designed and fabricated along with a pulley mount dead loaded to the tank floor. The testing tank and buoyancy apparatus are depicted in Figure 2-3. The system was successfully installed following

the surface deployment method. Properties of the testing tank as well as float specifications are presented in Table 1-1.

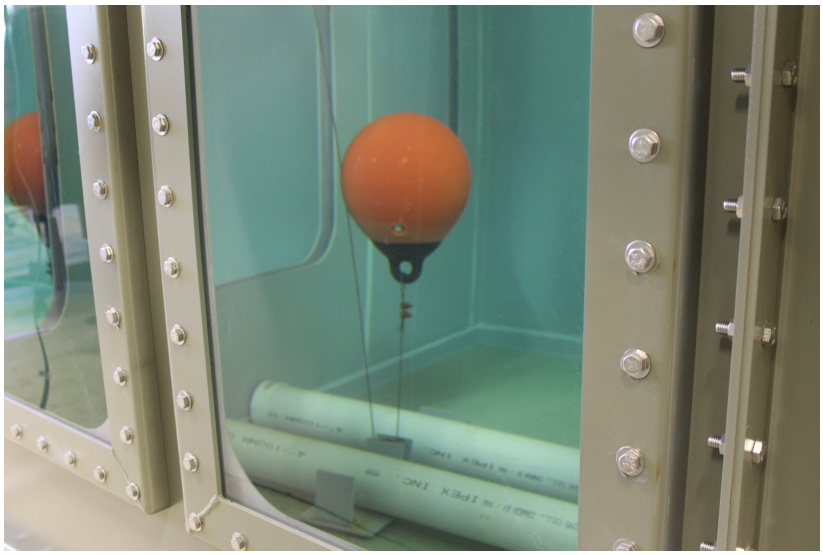

Figure 2-3 - Buoyancy testing in offshore tank

Table 2- 1 - Properties for tank testing

Tank Volume	25.4 m^3	**Float Height**	0.33 m
Water Depth	2 m	**Float Volume**	0.014 m^3 ± 2%
Charge Depth	1.67 m ± 0.6%	**Float Shape**	Spherical

Discharge force was measured at various submerged depths with force gauge measuring cable tension. Results for discharge force testing are displayed in Figure 2-4. The float was submerged at 0.1 m intervals and the discharge force was measured through the cable at the water's surface.

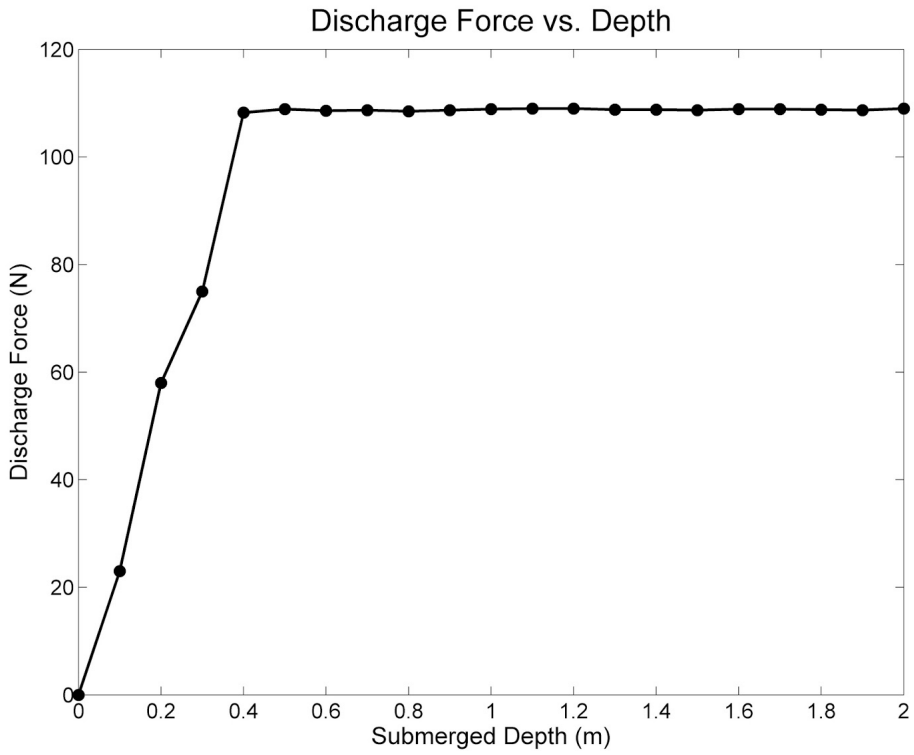

Figure 2-4 - Discharge Force vs. Charge Depth

Following the initial discharge force tests the relationship between discharge force and time was examined. The float was locked in the fully charged position and the discharge force measured at 0.5 hr intervals for a ten hour period. Results for temporal discharge force is displayed in Figure 2-5.

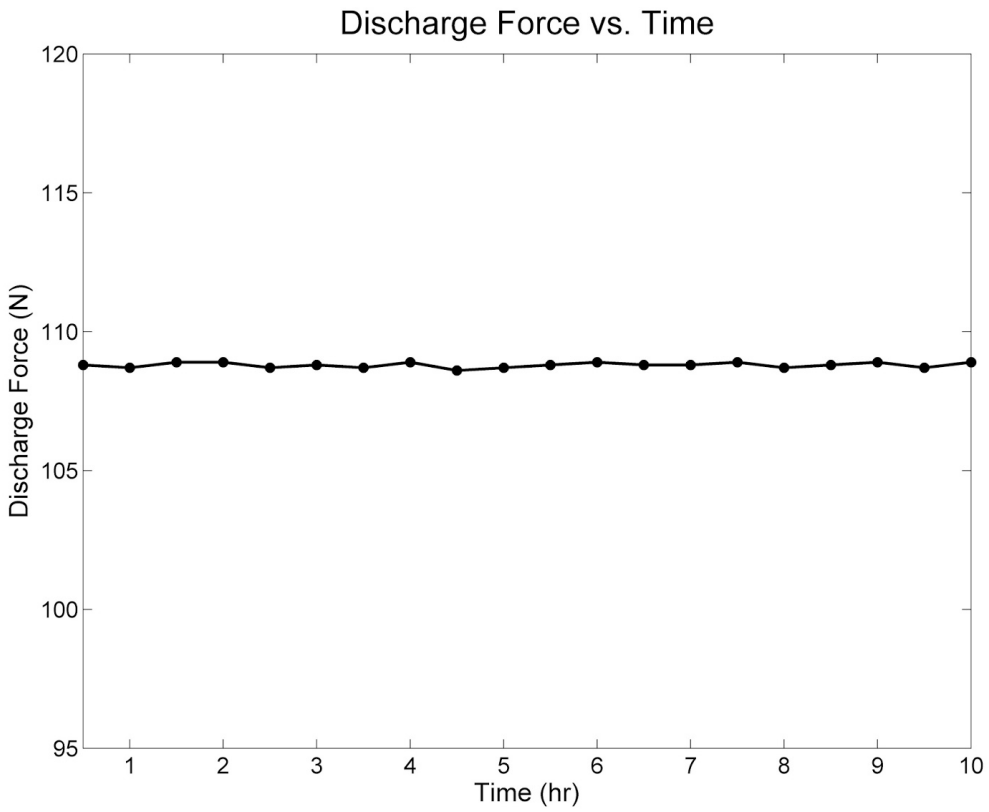

Figure 2-5 - Discharge Force vs. Time

2.4.1 – Experimental Observations

As can be seen in Figure 2-4, once the float was fully submerged the discharge force remained constantly within a 2 N-M range regardless of charge depth. All measurements at intervals of charge depth were within the margin of measurement error for the fully submerged float. As the float emerges beyond the water surface, the discharge force decreases rapidly and, reducing to zero at the point where the float is fully floating atop of water. From this testing it can be concluded that discharge force is constant with depth.

As can be seen from Figure 2-5, the discharge force was found to be independant of charge time for the durations tested as this is consistent with experimental results as well as the Archimedes principle on which this systems operations is based. Measured quantities were within expected variation for measurement and considering influencing factors such as friction within pulley. This time-independence of the discharge force implies that a BBES system can be used for extended-duration energy storage. This is also positive for lifetime cycling characteristics of BBES as the system performance over time will depend solely on the design life of it's mechanical (pulley, reel) and electrical components (motor, generator) as the medium for storage, buoyant potential energy, does not dissipate or degrade with cycling.

2.5.0 - Conclusions

An energy storage system utilizing buoyancy force, has been presented. Governing equations of operations have been developed through application of Archimedes principle of buoyancy for an ideal system. An ideal storage limit has been calculated to be 2.7 Wh per each meter of submersion. Formulas for total energy storage, charge and discharge power along with discharge time have been defined to serve as a basis for BBES system design.

Idealizations and assumptions used for equation development have been qualified and discussed; and a realistic model for ideal round trip efficiency has been presented; accounting for hydrodynamic, mechanical and electrical losses.

Several applications of BBES have been presented, outlining how this system of energy storage can be configured for both onshore and offshore energy resources.

Several conclusions can be drawn regarding BBES considering the equations and discussions presented as outlined below

- Energy storage capacity at a given location is proportional to float volume and water depth

- Energy stored is non-dissipative (i.e. Discharge force does not vary with time)

- Performance of a BBES system over it's design life will depend on fatigue characteristic mechanical and electrical components which make up the system. The medium of storage, buoyant potential energy, does not dissipate or degrade with cycling

- Energy can be extracted at various power levels by regulating the float speed

- There are no temperature or pressure changes within ambient fluid thus minimal thermodynamic considerations are required

- Black start capable (i.e. The system can be discharged without additional input energy)

- Round trip efficiency is independent of float mass

- BBES can be implemented offshore from water surface without divers lowering implementation costs.

Conclusions have not been drawn as to the achievable round-trip efficiency of BBES as this is subject for further research utilizing a more elaborate experimental apparatus. Further investigation into the hydrodynamic drag effects acting on float will be critical in determining the achievable round trip efficiencies of this system.

Overall, results of initial theoretical and proof of concept investigation into BBES is promising as the operation principle of buoyancy energy storage has been confirmed. Further research is required to further investigate how BBES can be applied for utility scale energy storage and quantifying the achievable round trip efficiencies for the system.

References

[1] Cavallo A., Controllable and affordable utility-scale electricity from intermittent wind resources and compressed air energy storage (CAES), Energy, Volume 32, Issue 2, February 2007, Pages 120-127,

[2] Barker, P.P.; Bing, J.M., Advances in solar photovoltaic technology: an applications perspective, Power Engineering Society General Meeting, 2005. IEEE , vol., no., pp.1955,1960 Vol. 2, June 2005, Pages 12-16.

[3] Bhubaneswari Parida, S. Iniyan, Ranko Goic, A review of solar photovoltaic technologies, Renewable and Sustainable Energy Reviews, Volume 15, Issue 3, April 2011, Pages 1625-1636.

[4] Devabhaktuni, V., et al., Solar energy: Trends and enabling technologies, Renewable and Sustainable Energy Reviews, Volume 19, March 2013, Pages 555-564.

[5] Hoffmann W., PV solar electricity industry: Market growth and perspective, Solar Energy Materials and Solar Cells, Volume 90, Issues 18–19, 23 November 2006, Pages 3285-3311.

[6] Changliang X., Zhanfeng S., Wind energy in China: Current scenario and future perspectives, Renewable and Sustainable Energy Reviews, Volume 13, Issue 8, October 2009, Pages 1966-1974.

[7]Liliana E. Benitez, Pablo C. Benitez, G. Cornelis van Kooten, The economics of wind power with energy storage, Energy Economics, Volume 30, Issue 4, July 2008, Pages 1973-1989,

[8] Pavlos S. Georgilakis, Technical challenges associated with the integration of wind power into power systems, Renewable and Sustainable Energy Reviews, Volume 12, Issue 3, April 2008, Pages 852-863.

[9] Barton, J.P.; Infield, D.G., Energy storage and its use with intermittent renewable energy, in *Energy Conversion, IEEE Transactions on*, vol.19, no.2, June 2004, Pages 441-448.

[10] Cimuca, G.O.; Saudemont, C.; Robyns, B.; Radulescu, M.M., Control and Performance Evaluation of a Flywheel Energy-Storage System Associated to a Variable-Speed Wind Generator,"Industrial Electronics, IEEE Transactions on , vol.53, no.4, June 2006, Pages 1074-1085.

[11] Ahrens, M.; Kucera, L.; Larsonneur, R., "Performance of a magnetically suspended flywheel energy storage device," Control Systems Technology, IEEE Transactions on , vol.4, no.5, Sept. 1996, Pages 494-502.

[12] Bornemann, H.J.; Sander, M., Conceptual system design of a 5 MWh/100 MW superconducting flywheel energy storage plant for power utility applications, Applied Superconductivity, IEEE Transactions on , vol.7, no.2, June 1997, Pages 398,401.

[13] Bolund, B., Bernhoff, H., Leijon, M. Flywheel energy and power storage systems, Renewable and Sustainable Energy Reviews, Volume 11, Issue 2, February 2007, Pages 235-258.

[14] Temporal power, A flywheel like no other, published online http://temporalpower.com/what-we-do/technology/flywheels/, accessed Oct 27, 2015

[15] J.P. Deane, B.P. Ó Gallachóir, E.J. McKeogh, Techno-economic review of existing and new pumped hydro energy storage plant, Renewable and Sustainable Energy Reviews, Volume 14, Issue 4, May 2010, Pages 1293-1302.

[16]Yang, C.,V., Jackson, R., Opportunities and barriers to pumped-hydro energy storage in the United States, Renewable and Sustainable Energy Reviews, Volume 15, Issue 1, January 2011, Pages 839-844.

[17] Dimitris Al. Katsaprakakis, Dimitris G. Christakis, Arthouros Zervos, Dimitris Papantonis, Spiros Voutsinas, Pumped storage systems introduction in isolated power production systems, Renewable Energy, Volume 33, Issue 3, March 2008, Pages 467-490.

[18] Leonhard, W.; Grobe, M., "Sustainable electrical energy supply with wind and pumped storage - a realistic long-term strategy or utopia?," Power Engineering Society General Meeting, 2004. IEEE, Volume.2, June 2004, Pages 1221-1225.

[19] Peterson, H.A.; Mohan, N.; Boom, R.W., "Superconductive energy storage inductor-converter units for power systems," Power Apparatus and Systems, IEEE Transactions on , Volume94, no.4, July 1975, Pages 1337-1348.

[20] Chad, A.,, and Joos, G., Supercapacitor energy storage for wind energy applications. IEEE Transactions on Industry Applications Volume 43 Issue 3 2007: Pages 769.

[21] Wei, L., Joós, G., and Bélanger, J., Real-time simulation of a wind turbine generator coupled with a battery supercapacitor energy storage system. Industrial Electronics, IEEE Transactions on Volume 57, Issue 4, 2010, Pages 1137-1145.

[22] Lund, H., Salgi, G., The role of compressed air energy storage (CAES) in future sustainable energy systems, Energy Conversion and Management, Volume 50, Issue 5, May 2009, Pages 1172-1179.

[23] Konrad, J. Carriveau, R., Ting. D., S-K. et al. Geological compressed air energy storage as an enabling technology for renewable energy in Ontario, Canada. International Journal of Environmental Studies, Issue 2, Vol 69. 2012

[24] Dicorato, M.; Forte, G.; Pisani, M.; Trovato, M., "Planning and Operating Combined Wind-Storage System in Electricity Market," Sustainable Energy, IEEE Transactions on , vol.3, no.2, pp.209,217, April 2012

[25] Denholm, P., Sioshansi, R., The value of compressed air energy storage with wind in transmission-constrained electric power systems, Energy Policy, Volume 37, Issue 8, August 2009, Pages 3149-3158.

[26] Cheung, B., Carriveau, R., Ting. D., S-K. et al. Distensible air accumulators as a means of adiabatic underwater compressed air energy storage. International Journal of Environmental Studies Volume 69, Issue 4, 2012, Pages 566-577.

[27] Pimm, A. J., S. D. Garvey, and R. J. Drew. "Shape and cost analysis of pressurized fabric structures for subsea compressed air energy storage."Proceedings of the Institution of Mechanical Engineers, Part C: Journal of Mechanical Engineering Science, Volume 225, Issue 5, 2011, Pages 1027-1043.

[28] Pimm, A. J., S. D. Garvey, and Jong, M., Commercial grid scaling of Energy Bags for underwater compressed air energy storage. International Journal of Environmental Studies 71.6 (2014): 804-811.

[29] Maxim de Jong, Design and testing of Energy Bags for underwater compressed air energy storage, Energy, Volume 66, 1 March 2014, Pages 496-508.

[30] Blackwell R., "Hydrostor launching compressed air power storage off Toronto Island" The Globe and Mail, November 17, 2015.
http://www.theglobeandmail.com/report-on-business/industry-news/energy-and-resources/hydrostor-launches-compressed-air-power-storage-system-off-toronto-island/article27306527/ Accsesed online February 2, 2016

[31] Slocum, A.H.; Fennell, G.E.; Dundar, G.; Hodder, B.G.; Meredith, J.D.C.; Sager, M.A., Ocean Renewable Energy Storage (ORES) System: Analysis of an Undersea Energy Storage Concept, *Proceedings of the IEEE* , Voume.101, Issue.4, April 2013, Pages 906-924.

[32] Slocum, A., Gregory H., Fennell E. , and Alison S. Greenlee. "Offshore energy harvesting, storage, and power generation system." U.S. Patent No. 8,698,338. 15 Apr. 2014.

[33] Morgan, J.P., Buoyancy energy storage and generation. US Patent US 20100107627 A1. 6 May 2010

[34] Alami, A.,. Analytical and experimental evaluation of energy storage using work of buoyancy force. Journal of Renewable and Sustainable Energy Volume 6, Issue 1, 2014, Pages 131-137.

[35] Alami, A.,, Experimental assessment of compressed air energy storage (CAES) system and buoyancy work energy storage (BWES) as cellular wind energy storage options, Journal of Energy Storage, Volume 1, June 2015, Pages 38-43.

[36] R. Klar, M Aufleur, M Thene, "Buoyancy Energy – Decentralized energy storage in European Power Plant Park" University of Innsbruck, Unit of Hydraulic Engineering, published online http://www.buoyant-energy.com/files/buoyant_energy_at_a_glance.pdf

[37] "The works of Archimedes". p. 257. Retrieved 11 March 2010.

[38] Trapani, K., L. Millar, Proposing offshore photovoltaic (PV) technology to the energy mix of the Maltese islands, Energy Conversion and Management, Volume 67, March 2013, Pages 18-26.

[39] Kim Trapani, Dean L. Millar, Helen C.M. Smith, Novel offshore application of photovoltaics in comparison to conventional marine renewable energy technologies, Renewable Energy, Volume 50, February 2013, Pages 879-888.

[40] Bassett, K., Carriveau, R., Ting. D., S-K., Experimental Analysis of Buoyancy Based Energy Storage System. Offshore Energy Storage 2015, Edinburgh Scotland, July 1-4, 2015.

Chapter 3

Experimental Analysis of Buoyancy Based Energy Storage

3.1 - Introduction

Recent advances in utility scale wind turbine technology along with improved manufacturing and installation techniques have increased wind energy's position as a potentially significant and affordable energy source. Available wind resources have been assessed for the majority of our planet and it has been determined that available resources are sufficient to meet all of planet's energy needs for usage projections to 2025 [1]. Photovoltaic solar energy technologies have also undergone significant technological improvements to solar cells, inverters and associated balance of system components [2 -4]. Solar energy has also seen a boost in both residential and utility scale installations as political adoption of Feed In Tariff (FIT) programs has created increased incentive [5,6].

With abundant resources at our disposal, engineers and scientists are posed with the task of effectively integrating these energy sources onto an existing electricity grid featuring a variety of other energy sources including nuclear, natural gas, coal and hydro energies. When considering the intermittency of solar and wind resources in conjunction with grid demand intermittency and the unique operating characteristics of each of the other energy sources, the challenge of achieving balance is complex.

One particular approach to addressing intermittency of an energy resource is through Energy Storage (ES). Many different methods and techniques for achieving ES exist, each with particular application requirements. Although the various methodologies can vary greatly, the overall principle remains consistent. Energy is stored at times of high supply/low demand and retained for a time period. When the supply/demand balance changes and the stored energy can be effectively used on the electricity grid, the energy is discharged from the storage system. Several different energy storage techniques are currently under development including, but not limited to, flywheels [7], pumped hydro [8] supercapacitors [9], compressed air energy storage [10-13] and under water compressed air energy storage [14-16].

3.2 - Buoyancy Based Energy Storage

There exists an alternate approach to underwater energy storage, which has yet to receive thorough research, named buoyancy based energy storage (BBES). The system involves the utilization of buoyancy force of an object submerged in water via a reel and pulley system [17, 18]. In its simplest form a buoyant object is tethered to a cable and strung through a pulley mounted at the floor of a body of water. A single pulley or multiple pulleys can be used. The cable is then wrapped around a reel. As the reel is wound via an external force, the length of the cable is shortened and the buoyant object is forced below the water surface. When the force on the reel is removed the buoyancy object will rise due to buoyancy force acting on the object. This system is very distinct from the floating hydraulic energy storage adapted from pumped hydro

technologies as described in [19]. The basic storage system and components are illustrated and identified in Figure 3-1.

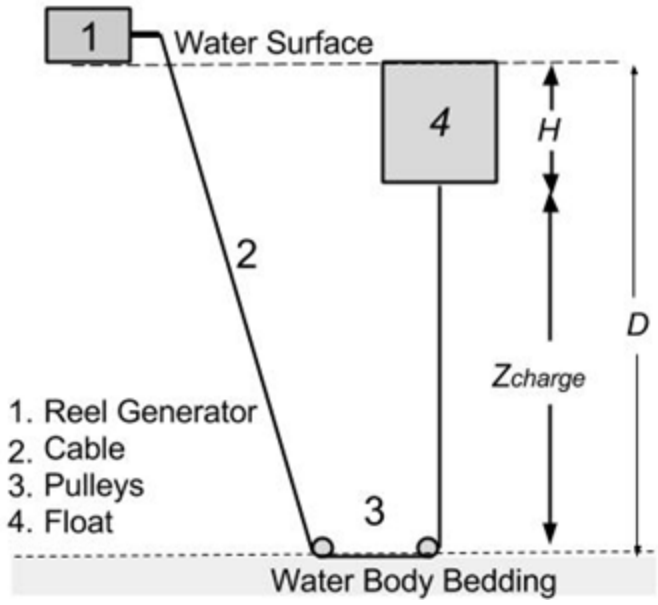

Figure 3-1 – Basic Buoyancy Energy Storage System with multiple anchorage pulleys

This system has several attractive qualities in terms of machinery requirements, the physics driving operation as well as deployment considerations. The primary mechanical device used to accomplish system operation is the reel mechanism used to convert the linear motion of the float into rotational motion to be harnessed by the generator. Reels of this type are used extensively throughout industry in cranes and winches and the design and operation of these reels is well understood. Logistically speaking, there is opportunity for a buoyancy battery system to be installed from the water's surface. No subsurface connections or underwater construction is required and thus deployment costs can be reduced by eliminating the requirements for compression diving and Robotic Autonomous Vehicles (ROVs). The main physical phenomenon

driving operation of this system is buoyancy force, which is related to the fundamental force of gravity. The buoyancy behavior of objects is well understood and highly predictable, thus allowing for straightforward calculation of energy storage capabilities under ideal conditions.

The buoyancy energy system examined herein is distinct from the systems tested in [18], which featured Styrofoam buoys carved in such a way as to introduce a rotational component in the floats as they rise. The concept of introduced rotation may prove beneficial in reduction of drag forces acting on buoy at the cost of complication due to required swivel connections. In order to fulfil a gap in literature regarding the simplified buoyancy battery apparatus as well as isolate the fundamental charge phenomena, this paper will consider and examine the base storage system, without complication of rotational float motion.

The amount of energy that can be stored and discharged within the buoyancy energy storage system will be dependent on the cable tension, C. The force acting on this cable will be proportional to buoyancy force acting on float as calculated using Archimedes principle. Cable tension can be expressed;

$$C = \rho g V - mg \qquad \textbf{(1)}$$

where V= float volume, ρ=density of fluid, g = gravitational acceleration and m = float mass. The energy that can be charged or discharged from a system can then be expressed in terms of work performed on the cable.

$$E_{Discharge} = C\, Z_{Charge} \qquad \textbf{(2)}$$

Where Z_{CHARGE} = charge depth. The ideal energy storage capacity can then be expressed assuming ideal, incompressible fluid and constant float volume as expressed below.

$$E_{Ideal} = \rho g V Z_{Charge} \quad \textbf{(3)}$$

Using this equation the idealized energy storage values obtainable at given depths and for specific float volumes can be plotted as shown in Figures 3-2a and 3-2b. The energy storage density of BBES can be calculated with equation 3, using a unit volume float and unit float submersion. BBES has an energy density of 0.272 Wh/m^4 when applied in a body of fresh water.

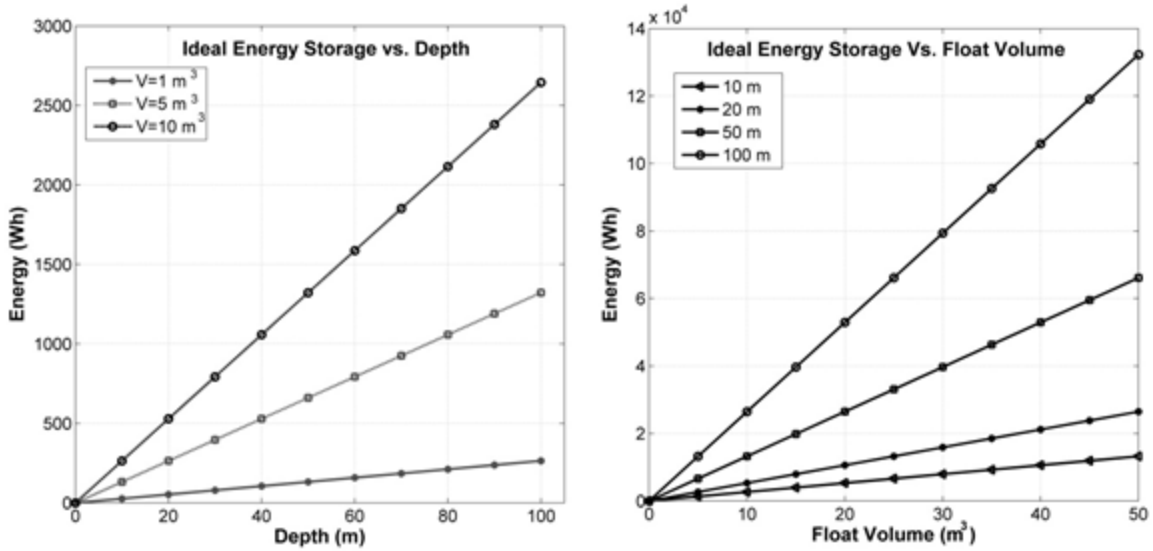

Figure 3-2 – 2a. Ideal Energy vs. Storage Depth. 2b. Ideal Energy Storage vs. Float Depth

Scalability is an important consideration for any energy storage system with intentions of utility-scale application. BBES has very positive scalability characteristics considering that the main components required for storage are air and water, which are some of the most abundant materials on the planet. As calculated above, BBES has a low storage energy density in

comparison to other energy storage technologies, specifically chemical batteries. BBES has high spatial requirements, but this is not problematic as marine real estate exceeds land real estate and has very few competing uses.

This idealized case must be considered in context of inefficiencies which can be expected. These include hydrodynamic losses due to drag, electrical losses and pulley friction losses. The past patent application [17] reported system roundtrip efficiency of 90% which was estimated neglecting drag losses. A generator efficiency of 95%, motor efficiency of 97%, and pulley efficiency of 99% were used in this calculation within the patent although no references or experimental validation was presented. Existing literature on motor [20] and generator [21] efficiencies state that the efficiencies used by the patent are obtainable. The maximum pulley efficiency found in literature is 96% [22].

System Charge Ratio (Cr) and Ambient volume ratio (Ar) are two dimensionless ratios which are of importance for buoyancy system design and evaluation. System charge ratio is defined as the ratio of water depth to float height as expressed in (4) below.

$$Cr = \frac{D-H}{D} \quad \textbf{(4)}$$

Where Cr = charge ratio, D= water depth, and H = float height. This charge ratio is of importance for float design, as the charge ratio defines the vertical distance available for the float to operate.

Ambient volume ratio is defined as the ratio of ambient fluid volume to float volume. For full scale application in large bodies of water such as the Great Lakes and Oceans this will typically

not be a concern as the ratio will be very high. For smaller water bodies, contained systems and experimental analysis, this variable becomes an important value of interest.

$$Ar = \frac{V_a}{V} \quad \textbf{(5)}$$

Where AR = Ambient volume ratio, V_a= ambient fluid volume, and V= float volume. Experimental testing on a small scale was conducted in order to first validate the functionality of the system before investing further time and resources into analysing and developing a larger apparatus.

3.3 - Experimental Analysis

3. 3.1 - Proof of Concept Testing

To first investigate the potential of buoyancy based underwater energy storage a small scale concept model was constructed as depicted in Figure 3-3. A 3D printer was utilized to produce system components in Poly-Lactic Acid (PLA) material. The buoyancy battery is charged by turning the hand crank mechanism which turns the reel. The reel is also connected to a small NEMA 17 stepper motor being driven as a generator, converting the rotational energy of the reel into electrical energy. Properties of the tested scale model are displayed in Table 1. The float utilized was of cylindrical shape. This testing was performed in a cylindrical container made of PVC plastic.

Table 3-1- Testing Specifications

Water Depth	Charge Distance	Ambient Volume	Float Height	Depth Ratio	Float Volume
0.89m	0.7m	$0.028m^3$	0.19m	3.6	$0.0053m^3$

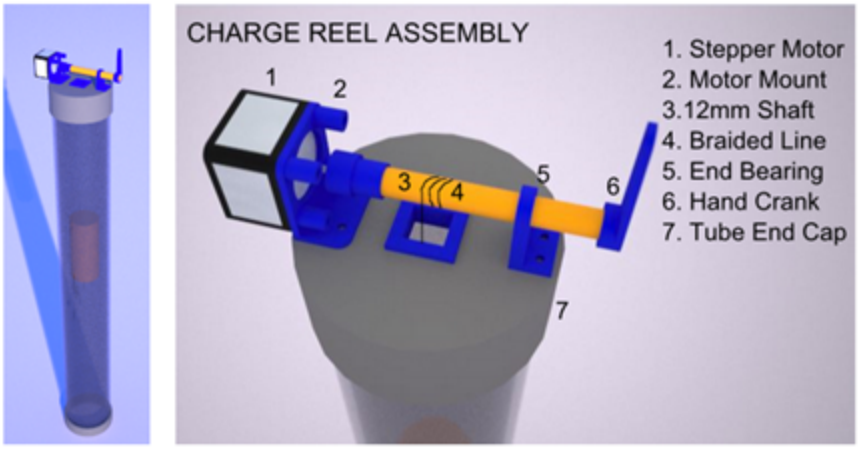

Figure 3-3 – Buoyancy Energy Storage Concept Testing Model

The intention of the proof of concept model was to confirm that the overall operation principle as presented above is functional before proceeding to larger scale testing. The NEMA stepper motor utilized, although very convenient for generating low power levels at low RPM, is far from ideal for use as a generator with efficiencies expected in the 40-50% range. For further efficiency analysis of a container based system a greater volume float and ambient fluid depth should be utilized . Hydrodynamic effects of drag will be different between the container and open water type systems and as such the results from proof of concept testing could not extended to make conclusions regarding open water operation.

The system was tested with several different load levels and discharge time was measured. The voltage drops across the resistive loads were measured and power output calculated.

3.3.2 - Proof of Concept Results

Positive results were obtained for the small proof of concept system. Stored mechanical energy was discharged at various power levels as displayed below.

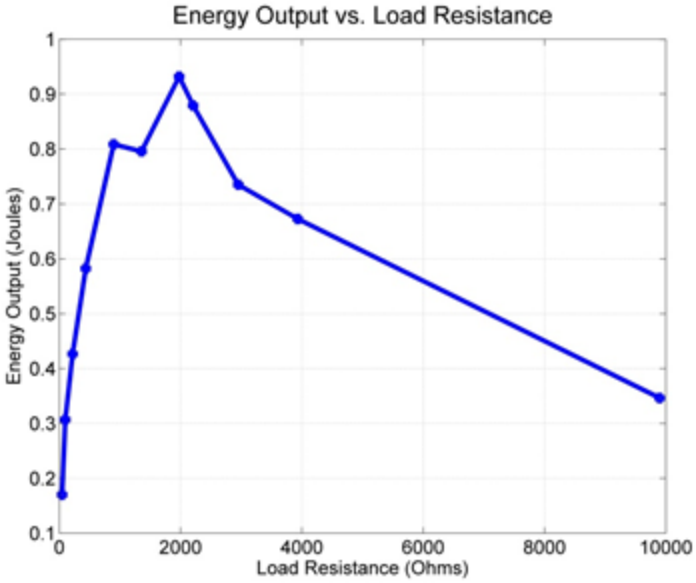

Figure 3-4 – Energy Output vs. Load Resistance for Concept Testing

One of the most important observations from the testing performed was verifying that the buoyancy storage scheme does operate as predicted. It was capable of storing energy for a desired period of time and powering both resistive and lighting loads on discharge.

The obtained results also display that the buoyancy storage technique can be applied within cylindrical containers where water flow is restricted to the annular region between float and container walls.

3.3.3 - Large Tank Testing

Results from the proof-of-concept testing motivated the development of a more elaborate experimental apparatus and larger scale buoyancy energy storage system with a minimum ten times greater float volume. This system was developed for testing within the 25 m^3 offshore resting tank located at the University of Windsor Turbulence and Energy lab.

For more elaborate testing to occur, each component of the buoyancy energy system underwent development and fabrication. Components are discussed below in context of experimental and as well as full application. Figure 3-5 displays the complete buoyancy storage system. Additional properties for offshore tank testing are presented in Table 2.

Table 3-2 - Large Tank Testing Specifications

Water Depth	Charge Distance	Ambient Volume	Float Height	Depth Ratio	Float Volume
2 m	1.67m ± 0.604%	24.5m^3	0.33m ± 0.6%	5.06	0.014m^3

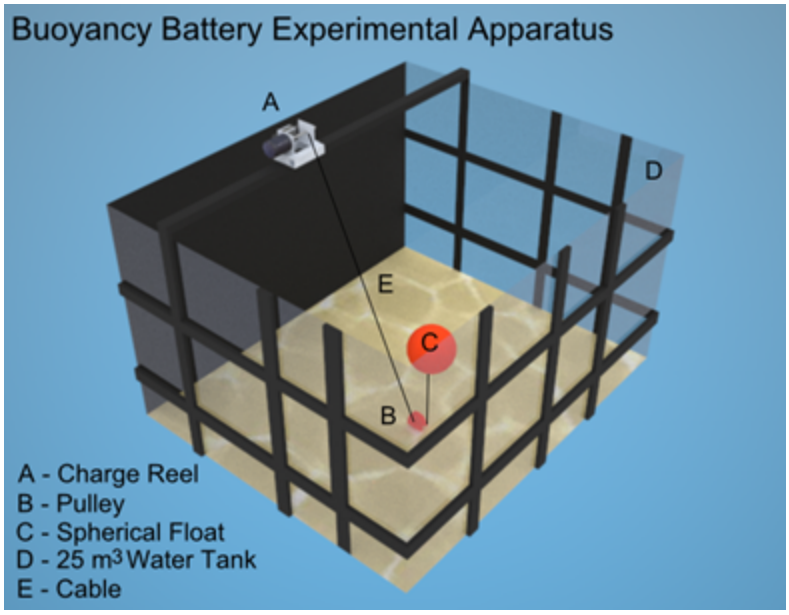

Figure 3-5 – Large tank Testing Apparatus

Charge Reel

The charge reel is the location where linear motion of float is translated into rotational motion through the wrapping of the tension cable around the reel generator shaft. The rotation of the shaft can then be converted into electrical energy by coupling a generator to the charge reel shaft. As previously mentioned, reels are common machinery and thus the developed reel features components adapted from an automotive winch.

Energy is both charged and discharged from the battery system through a common main shaft, thus a design option of utilizing the same electrical generator as both generator and motor is possible. In such a situation very careful selection of generator/motor is required to ensure that it can operate within its optimal speed and torque range for both charge and discharge. Separate charging and discharging electrical motors can also be used, with the advantage of simplifying

electrical control systems as well as independent control of charge and discharge loading characteristics. For utility scale application, generator technology from the wind industry can be adapted for application within a buoyancy system.

The experimental system featured a Windstream 1.5 amp DC generator, originally purposed for small wind turbine application. When driven at manufacturer specified voltage, the generator was unable to act effectively as a motor for submersing the float and thus energy was introduced to the system using a hand crank method. The 25mm main reel shaft used for this experimentation was mounted to a rigid aluminum frame and supported by matching flange bearings. The reel frame was affixed to the rigid wall of tank.

Buoyant potential energy as described in (2) is distributed between the kinetic energy of float, the extracted energy of generator and losses. Thus, the intended operation is that the float proceeds very slowly to the surface, in order ensure a maximum amount of energy is extracted by the generator.

Pulley Anchorage

Subsurface anchorage is a significant challenge facing offshore energy storage technology where storage containers are required to be secured at depth below water surface. At utility-scale energy storage levels, anchorage requirements for these systems become very challenging from both a cost and installation perspective.

The anchorage system for the developed experimental system features an aluminum mounting plate on which a heavy duty rigging pulley was affixed. This was deployed from surface, lowered, and located within tank using the float tension cable. The anchor plate was further dead loaded with two precast concrete cylinders lowered atop the plate as depicted in Figures 3-6a and 3-6b. The anchorage installation procedure used verified that with careful planning a full system installation can be completed from the water's surface. This is significant as it begins to confirm one of main advantages to buoyancy, surface deployment.

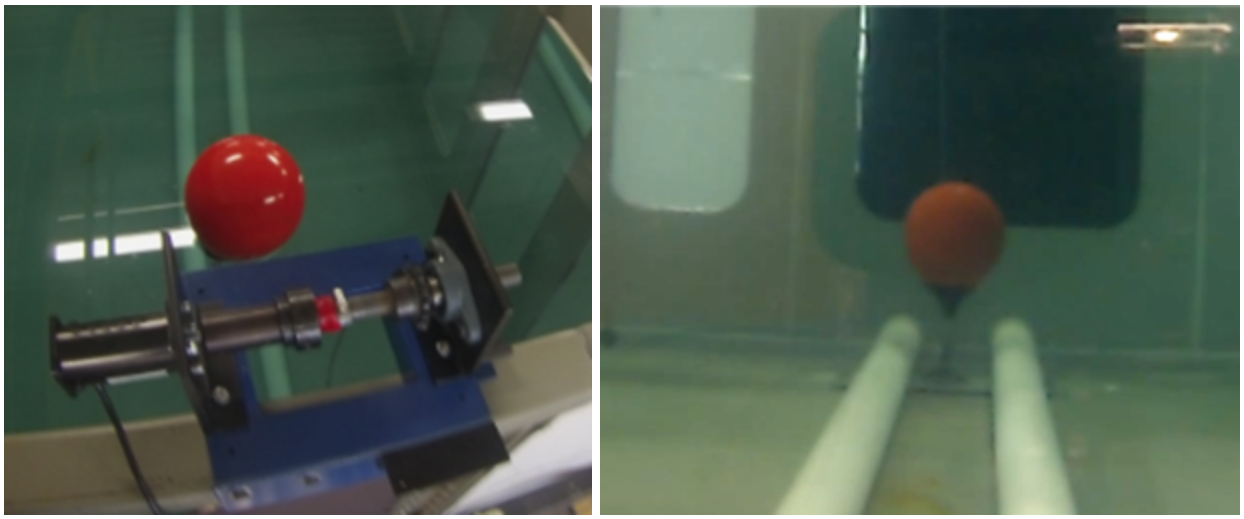

Figure 3-6 – a. Charge Reel Assembly b. Subsurface Anchorage

Float

Float size, shape, and material will each affect the operation characteristics of the buoyancy battery system. The ideal float will rise straight to surface with minimal hydrodynamic losses to both skin friction and shape induced drag. Inflatable, distensible type floats commonly used in marine industry such as buoys, ship docking bumpers, and marine salvage bags have potential

viable application in buoyancy energy storage. The inflatable type float has the advantage of availability and very low weight relative to volume. As an inflatable type float is submerged into the water, the volume of the float will be affected by the hydrostatic pressure and will decrease in volume, resulting in efficiency loss. This can be overcome through pressurization of the inflatable float. Rigid wall tanks, such as those used for the storage of gases, can also be utilized as floats for this system with the advantage of maintaining a constant volume at the expense of increased float weight.

To investigate effects of float symmetry, a non-symmetric "boat bumper" style float was initially tested and filmed during no load discharge cycles. A symmetric marine buoy was also observed under the same conditions as depicted in Figure 3-5. Each float featured a single point connection between the cable and the float which was molded into each floats plastic form.

For each of the no load tests completed the asymmetric float exhibited a highly non-linear displacement path during its rise to the surface. At approximately one third of its discharge height the float began moving sideways direction, resulting in drastic changes of float geometry and angle of attack relative to direction of float travel.

The symmetric float consistently displayed the desired straight trajectory during its rise in the water. In order to simplify geometry considerations associated with float position and motion in water, the symmetric float was used for further quantitative analysis.

3.3.4 - Large Tank Testing Results

The developed experimental system was tested under various loading conditions including both resistive and lighting loads. Five trials of each condition were conducted. Results for maximum power output, float velocity, and discharge time are presented in Figure 3-7. Power was calculated based on measured amperages and resistance for the resistive loads. The resistance of the lighting loads was variable as the bulbs warmed during the test trials. Power output for the lighting tests was calculated using measured voltage and amperage. The lighting loads were used primarily to allow for video capture of the system operating, but the high power outputs exhibited for the single bulb trials warrants its inclusion in this paper. Using generator manufacturer's published power curves the no load RPM was determined to be 1700 RPM.

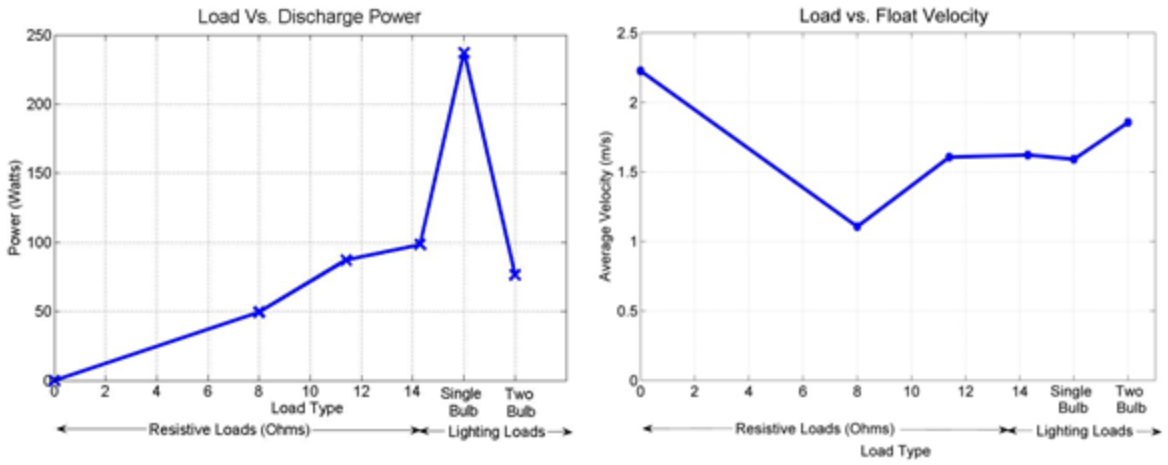

Figure 3-7 – a. Load vs. Discharge Power, b. Load vs. Discharge Velocity

The power output results were in fact much greater than expected by the authors for a float of this size. The maximum achieved average discharge during this initial testing was 237 watts. During this discharge the floats considerable average velocity of 1.6 m/s indicates that the

maximum energy is yet to be fully extracted for the specific float volume. For each test conducted the float was accelerating as it reached the water surface, indicating that charge depth was insufficient for reaching steady state at this load level. These high power levels also resulted in the generator operating at higher-than-recommended power levels resulting in considerable resistive losses within the generator itself. A generator of greater power rating will be required for improved evaluation of maximum discharge power for the spherical float of interest.

For ideal performance with properly matched loading, the float should proceed slowly and come to a stop once it reaches the water surface. This is done in order to minimize energy loss to both float acceleration and surrounding fluid. The kinetic energy remaining in the float as it reaches the surface represents a portion of energy loss and can be referred to as residual kinetic energy loss, $E_{Residual\ Kinetic}$. To further investigate the losses present in the completed testing, the total energy output of the system can be expressed in the equation 6 below.

$$E_{input} = E_{Residual\ Kinetic} + E_{Drag} + E_{Friction} + E_{Output} \quad \textbf{(6)}$$

Where E_{input} = Energy input, E_{Drag} = Energy lost to drag, $E_{Friction}$ = Energy lost to friction, and E_{Output} = Energy extracted from system through generator. For the completed tests time series data was not obtained for amperage and thus total energy output cannot be calculated at this point. Energy will be lost to friction within the bearings of the pulley, as well as reel generator rotating assembly which features the internal generator bearing along with a secondary reel bearing. Although the input energy was not measured explicitly due to the hand crank procedure, it can be estimated for an ideal case by considering equation 2. For the float tested, the required theoretical energy input was 221.7 Newton Meter. Using the measured no-load float speed where the energy output of the system is zero, in conjunction with established Reynolds number vs. drag coefficient curves [23], an estimate for the energy lost to hydrodynamic drag

and bearing friction can be made using equation 7 below. The values of drag loss and kinetic energy are calculated based on float velocity and are displayed for the resistance tests in Table 3-3.

$$(\rho g V - mg)Z = \tfrac{1}{2}(m + m_a)v^2 + \tfrac{1}{2}(\rho A v^2 C_D)Z + E_{Friction} + E_{Output} \qquad \textbf{(7)}$$

Where is m_a added mass, A is frontal area of the float, C_D is drag coefficient and v is float velocity, The Reynolds number of this no-load flow scenario was 6.65 x 10^5 which corresponds to an approximate drag coefficient of 0.15 [23]. The flow is within the drag crisis regime and as such the drag coefficients are appropriately low. All tests were found to be within this drag crisis regime. Energy components and Reynolds numbers for the completed tests are displayed in Table 3-3 below.

Table 3-3 – Components of drag and kinetic energy loss for completed tests. Uncertainties for experimental observations is reported in Appendix D.

Load	Energy Input (N- M)	Average Float Velocity (m/s)	Re Number	Drag Coefficient	Drag Loss (N- M)	Residual Kinetic Energy Loss	Discharge Efficiency (%)
Open circuit	222	2.23	6.65×10^5	0.15	43.87	4.49	N/A
8 Ohm	222	1.11	3.30×10^5	0.20	14.43	1.11	16.85
11.4 Ohm	222	1.61	4.81×10^5	0.16	24.33	2.34	20.4
14.3 Ohm	222	1.62	4.84×10^5	0.18	27.91	2.38	22.8

Using this drag coefficient with relevant float speed and frontal area the drag losses are calculated to be 43.87 Newton Meter representing 19.8% of total input energy. These calculated drag losses represent a worse-case scenario for the system. The addition of electrical loading will work to slow the float, decreasing the effect of drag. This decreased float speed will have an associated increase in drag coefficient as the float will no longer be operating in the drag crisis regime. The residual kinetic energy loss based on the float velocity as it reached the water's surface for the no-load case was 4.49 Newton Meter representing 2% of total energy input. Using calculated values for drag and kinetic energy losses, a friction loss of 175.32 Newton meter is found representing 79.1% of input energy.

In order to better examine the potential round-trip efficiency of BBES a more sophisticated system prototype is required utilizing an electrical input energy analogous to the energy that would be introduced in a real-world energy storage circumstance. Control mechanisms will be required to vary the discharge speed and thus control discharge power output for a given load condition. Greater charge depth ratios are required for precise control of discharge speed.

3.4 - Conclusions and Next Steps

A buoyancy based energy storage system has been described, developed and tested for proof of concept and basic power testing. The simplicity of the storage scheme, along with the fully surface deployable installation makes this an increasingly attractive area for further large scale research. Despite the low energy storage density of the technique, it is highly scalable due to the abundance of its main components air and water. Marine space is highly abundant and waters of

100m depths are available within vicinity of major population centres in North America and around the world.

Two scales of systems have been tested for discharge operation characteristics. Both proof of concept and large tank testing has confirmed the approaches ability to store and discharge energy at various power levels. The larger tested system was fully surface deployed.

The smaller system made with 3D printed components and contained to a cylindrical container, provided first confirmation of the technique's ability to store and discharge energy.

The high power levels achieved during large tank testing for the small float utilized are very promising and motivating for larger scale tests at real world depths. Using results from no-load trials, the components of drag, friction and kinetic energy were calculated. The greatest amount of energy loss was due to friction loss which accounts for 79.1% of the input energy. This could also be due to imbalance and vibration within the reel assembly as it was operating at a high rotational speed of 1700 RPM. Hydrodynamic drag losses, which accounts for 19.8% of the input energy, were found to be significantly greater than kinematic losses (2%). The calculated values represent a worse-case scenario for the system as additional loading will work to slow the float, decreasing the effect of each of the loss components. Although the completed tests cannot be used to determine true operational efficiencies, the no-load energy balance does provide information regarding the distribution of losses and the overall influence of the components on the system's performance.

Greater charge ratios will be essential for future study in order to isolate the steady state performance of the system. For this to be accomplished with the spherical float of interest,

application must be tested in a real-world marine environment. Apparatus improvements including the development of an efficient charging apparatus for evaluation of charge cycle efficiency are also required.

Fundamental analysis is also to be performed within controlled lab setting to obtain greater knowledge of float dynamic behaviour and hydrodynamic factors. This will only be practical for floats much smaller than tested, where steady state operation is achievable within tanks depth. This also calls for research into minimum charge ratio required per unit float volume. Next steps for research include

- Development of efficient charging apparatus for evaluation of full round trip efficiencies
- Application testing in real world marine setting where greater charge depths are highly accessible.
- Fundamental analysis of float behaviour under highly controlled lab setting for small floats with charge ratios at minimum twice those used for testing thus far.

There remains much work to be done before definitive statements regarding maximum experimental efficiency, cost and achievable energy densities are to be made but each of the steps above will further advance the research.

References

[1] A. Cavallo, “Controllable and affordable utility-scale electricity from intermittent wind resources and compressed air energy storage (CAES)”, Energy, Vol. 32, Issue 2, 2007, pp. 120-127.

[2] P. Barker, P. Bing, J.M., “Advances in solar photovoltaic technology: an applications perspective”, Power Engineering Society General Meeting 2005. IEEE , vol. 2, June 2005, pp.1955,1960.

[3] B. Parida, S. Iniyan, R. Goic, “A review of solar photovoltaic technologies”, Renewable and Sustainable Energy Reviews, vol. 15, Issue 3, April 2011, pp. 1625-1636.

[4] V. Devabhaktuni et al. “Solar energy: Trends and enabling technologies”, Renewable and Sustainable Energy Reviews, vol. 19. March 2013, pp. 555-564.

[5] A. Campoccia, L. Dusonchet, E. Telaretti, G. Zizzo, “Comparative analysis of different supporting measures for the production of electrical energy by solar PV and Wind systems: Four representative European cases”, Solar Energy, vol. 83. Issue 3, March 2009, pp. 287-297.

[6] A. Campoccia, L. Dusonchet, E. Telaretti, G. Zizzo, An analysis of feed’in tariffs for solar PV in six representative countries of the European Union, Solar Energy, vol 107, September 2014.

[7] Cimuca, G.O.; Saudemont, C.; Robyns, B.; Radulescu, M.M., "Control and Performance Evaluation of a Flywheel Energy-Storage System Associated to a Variable-Speed Wind Generator," Industrial Electronics, IEEE Transactions on, vol.53, no.4, June 2006, pp.1074,1085.

[8] J.P. Deane, B.P. Ó Gallachóir, E.J. McKeogh, “Techno-economic review of existing and new pumped hydro energy storage plant”, Renewable and Sustainable Energy Reviews, vol. 14, Issue 4, May 2010, pp. 1293-1302.

[9] C. Abbey, G. Joos. "Supercapacitor energy storage for wind energy applications." IEEE Transactions on Industry Applications 43.3 (2007): 769.

[10] H. Lund, G. Salgi, “The role of compressed air energy storage (CAES) in future sustainable energy systems”, Energy Conversion and Management, vol. 50, Issue 5, May 2009, pp. 1172-1179.

[11] H. Lund, G. Salgi, B. Elmegaard, A. N. Andersen, “Optimal operation strategies of compressed air energy storage (CAES) on electricity spot markets with fluctuating prices”, Applied Thermal Engineering, vol. 29, Issues 5–6, April 2009, pp. 799-806.

[12] M. Dicorato, G. Forte, M. Pisani, M. Trovato, "Planning and Operating Combined Wind-Storage System in Electricity Market," Sustainable Energy, IEEE Transactions on , vol.3, no.2, pp.209,217, April 2012

[13] P. Denholm, R. Sioshansi, “The value of compressed air energy storage with wind in transmission-constrained electric power systems”, Energy Policy, vol. 37, Issue 8, August 2009, pp. 3149-3158.

[14] B.Cheung, R. Carriveau, D. S-K. Ting. "Distensible air accumulators as a means of adiabatic underwater compressed air energy storage." International Journal of Environmental Studies vol. 69, 2012 pp. 566-577.

[15] Pimm, A. J., S. D. Garvey, and R. J. Drew. "Shape and cost analysis of pressurized fabric structures for subsea compressed air energy storage."Proceedings of the Institution of Mechanical Engineers, Part C: Journal of Mechanical Engineering Science 225.5 2011, pp. 1027-1043.

[16] J. Maxim. "Commercial grid scaling of Energy Bags for underwater compressed air energy storage." International Journal of Environmental Studies 71.6, 2014, pp. 804-811

[17] Morgan, J.P., “Buoyancy energy storage and generation.” US Patent US 20100107627 A1. 6 May 2010

[18] A. Alami, "Analytical and experimental evaluation of energy storage using work of buoyancy force." *Journal of Renewable and Sustainable Energy* 6.1 (2014):

[19] R. Klar, M Aufleur, M Thene, “Buoyancy Energy – Decentralized energy storage in European Power Plant Park” University of Innsbruck, Unit of Hydraulic Engineering, published online http://www.buoyant-energy.com/files/buoyant_energy_at_a_glance.pdf

[20] Boglietti, Aldo, et al. "International standards for the induction motor efficiency evaluation: a critical analysis of the stray-load loss determination."IEEE Transactions on Industry Applications 40.5 (2004): 1294-1301.

[21] Siemens, “Siemens Air Cooled Generators” http://www.energy.siemens.com/hq/pool/hq/power-generation/generators/sgen-1200a/siemens-generators-sgen-1200a-US-LowRes.pdf. 2016. Accessed Online 9.8.16

[22] Balance Community. “An in depth look at pulley efficiency” http://www.balancecommunity.com/slack-science/an-in-depth-look-at-pulley-efficiency/ Accessed Online 9.8.16

[23] Munson, B. R., D. F. Young, and T. H. Okiishi. "Drag on Spheres"*Fundamentals of Fluid Mechanics. New York: John Wiley & Sons* (1990)

Chapter 4

Integration of Buoyancy Battery Energy Storage With Utility Scale Wind Energy Generation

4.1 - Introduction

Buoyancy Battery Energy Storage (BBES) is a new form of energy storage under development for the improved integration of intermittent energy sources such as wind and solar onto existing electricity grids. BBES utilizes an objects buoyant property to store energy through a force transfer mechanism which couples linear underwater float motion into rotational motion as depicted in Figure 4-1 [1].

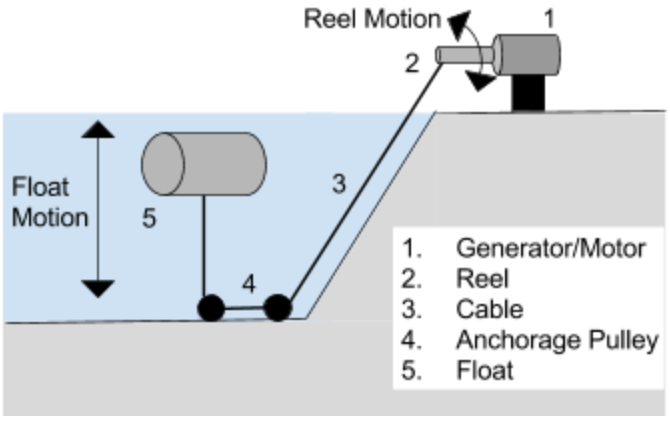

Figure 4-1 - BBES system for open water body.

When applied in an open body of water, the system features subsurface components including the float, numerous transfer pulleys, and the connection cable. The reel generator and associated electronics and controls are surface mounted and interconnected to an intermittent power source

and electricity grid. This approach to storing bulk energy has several potential advantages which make the technique attractive for further research and development.

One challenge currently facing the economic-feasibility of large scale offshore energy systems (both for energy storage and generation) is the deployment costs associated with the transport and installation of equipment. The costs of construction offshore are several times greater than typical terrestrial construction [2]. This is further complicated when sub-surface construction is required and construction diving or ROVs (Robotic Operated Vehicles) are utilized. Due to the layout of system components, BBES has the potential for full surface deployment - the pulley anchorage can be launched and sunk to depth from a barge. Float can be pre-filled with air and towed to their final location. This technique of surface installation has been used for previous experimental BBES systems [1,3].

The system components for BBES are existing equipment in heavy machinery and offshore industries which greatly simplifies the design and development process. By adopting from best practices from offshore oil, and subsurface telecommunication cable installation industries, the development of the system from lab to full application, can be accelerated. Furthermore, due to energy storage depending primarily on volumes of air and water, there are no thermodynamic complications or losses.

Previous experimental analysis [3] has displayed that BBES discharge force is constant with respect to both float depth and time. This confirms that BBES is non-dissipative, meaning that the medium for storage, buoyant potential energy, does not degrade over time and thus the lifespan and cycling fatigue will depend solely on the basic mechanical and electrical components which make up the BBES system assembly. Pulleys, crane reels, electric motors, and electric generators have all been in extensive use for more than 200 years and thus their design and operation is well understood [4]. Many examples exist of electric motors and these mechanical devices still in operation after more than 100 years of operation and thus the potential for BBES to have 50+ year lifespan is highly possible.

One of the most attractive aspects of BBES is scalability. Unlike chemical based batteries, the primary BBES elements required for increased storage capacity are air and water, which are some of the most abundant elements on the planet. This allows for the possibility of utility scale bulk storage on the magnitude of Gigawatt-hours. Presently, energy storage techniques theoretically capable and potentially practical for approaching this level of capacity are limited to pumped hydro, and compressed air energy storage (CAES) [5]. It is the intention of the authors to demonstrate that the much less discussed BBES is also capable of this level of energy storage capacity.

4.2 - BBES Process and Operation

The operational process for BBES involves the conversion between electrical, kinetic and potential energy forms through the aforementioned mechanism and machinery. The process begins with the power source, which would typically be an intermittent, renewable energy generator such as a wind turbine or solar panel array. Currently these systems supply an electricity grid with energy on an "as generated basis". Figure 4-2 below displays power output data from an operational 2.3 MW wind turbine in the Port Alma wind farm located in Tilbury, Ontario, Canada. The typical intermittency is evident in the figure, with power output at a maximum during the early morning hours.

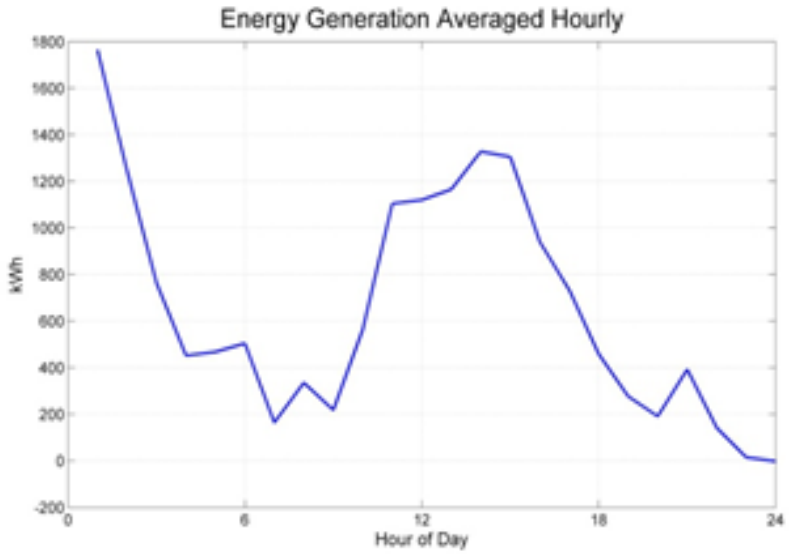

Figure 4-2 - Power output vs. Time for 2.3 MW wind turbine in Port Alma wind farm.

The generators are financially compensated based on the Energy Purchase Price (EPP) established by the local Electricity System Operator (ESO). The EPP is a price for supply of each kWh of electricity, which will fluctuate continuously in relation to the supply/demand balance experienced by the electrical grid as a whole. When expressed as a rate, the revenue earned by can be expressed in equations 1 and 2 below.

$$R = E \times EPP \quad \textbf{(1)}$$

$$RR = P \times EPP \quad \textbf{(2)}$$

Where R = Revenue, RR = Revenue Rate ($/hr), E = Energy generated (kWh), EPP = Energy Purchase Price ($/MWh), and P = Generator Instantaneous Power (MW). By integrating energy storage with a generator system, there are new possibilities for increased revenue generation by controlling and optimizing the revenue rate based on the fluctuating energy purchase price. Generated energy can be diverted to the storage systems at times of low demand (EPP1), storage for a period of time, and discharged at time of high demand (EPP2). EPP market is updated on a 5 minute interval basis. The price opportunity is defined as change in EPP between time of storage and time of discharge

$$\text{PO} = EPP_2 - EPP_1 \quad \textbf{(3)}$$

Where PO = price opportunity, EPP_1 = current energy purchase price, EPP_2 = energy purchase price at time of discharge. The extent of price opportunity will depend on local grid supply/demand conditions but can vary drastically in a daily time period. To demonstrate the drastic variation in EPP and show the potential price opportunity, sample data from the Ontario, Canada electricity grid was obtained from the Independent Electrical System Operator (IESO) [6]. Figure 4-3A displays the daily maximum PO values for 2015. Figure 4-3B displays the Hourly ontario energy price data for select months.

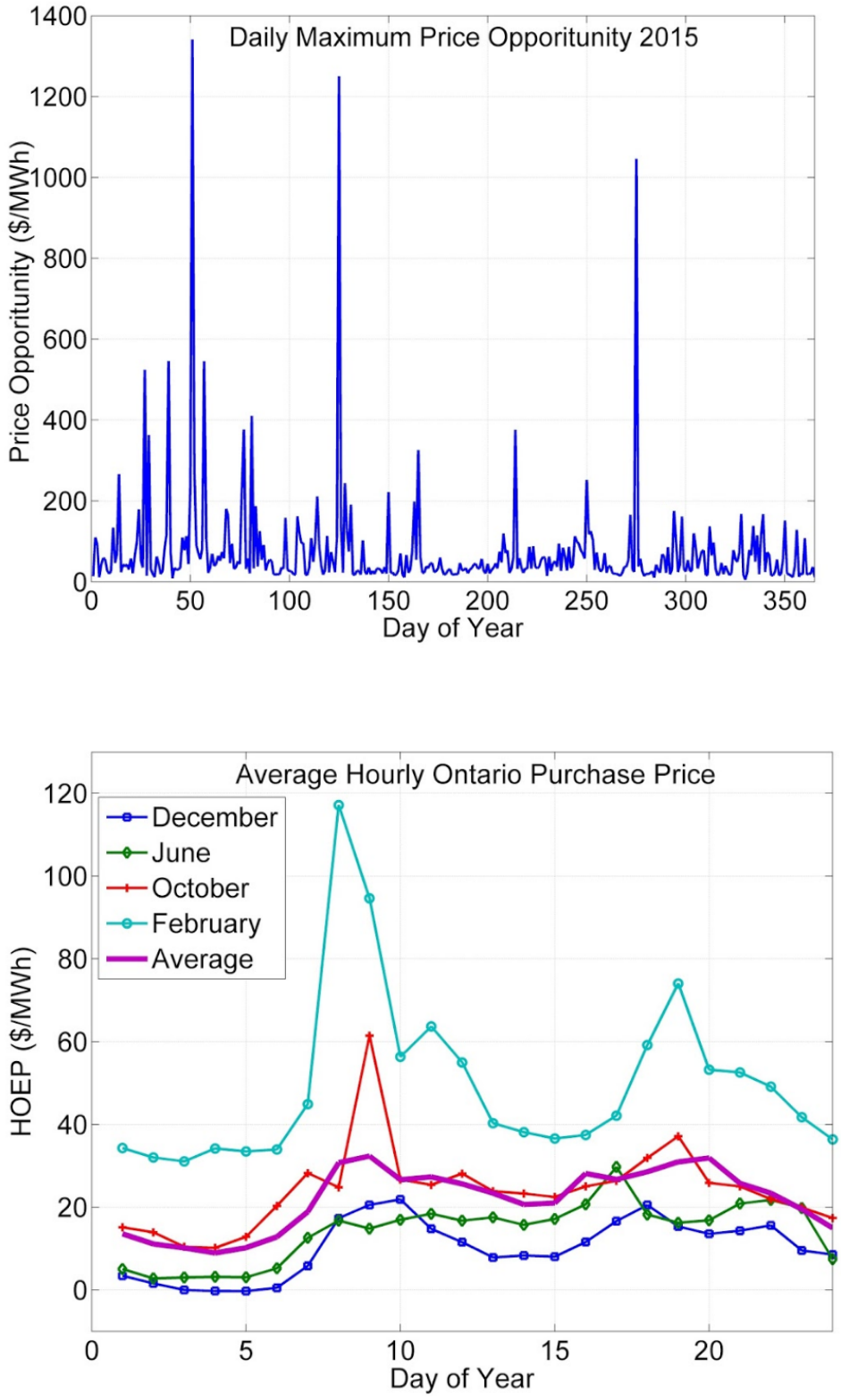

Figure 4- 3- A(top) Maximum Daily Purchase Opportunity for Ontario 2015. B (Bottom) Hourly Ontario energy price data for sample days.

As can be seen from the plots above, there are certain instances where the OHEP is a negative value which seems counter-intuitive. These negative values occur when there is an excess of wind energy capacity available and the grid operators wish to de-incentivize the generation of wind energy [7]. During these periods of negative electricity value, wind turbine farm operators will often shut down their turbine arrays to avoid financial loss and unnecessary turbine wear. It would be during these periods when the application of energy storage can be most beneficial.

There are also significant high Purchase Opportunity events throughout the year where the EPP can increase drastically for a few hours throughout a given day. These events correspond to larger climatic or infrastructure factors. For instance the highest EPP for 2015 occurred on Feb 20 when Ontario's capital city Toronto experienced a drastic cold front, and temperatures dropped to the lowest of the year. High PO events also occur during summer months at times of exceptionally high temperatures, when Ontario residents use air conditioning the most. The average PO for 2015 was $73.23.

The additional revenue created by storage can now be expressed.

$$RS = \eta \times E \times PO \qquad \textbf{(4)}$$

Where RS = additional revenue from storage ($), η = storage system efficiency. When storage is required the charge function is initiated and the energy generated by the power source will be diverted to the reel motor which will rotate the reel, forcing the float below the water surface at a specific velocity. To stop the charge process the power source is diverted back to the grid, a lock is applied to the reel and the float will remain stationary in its position.

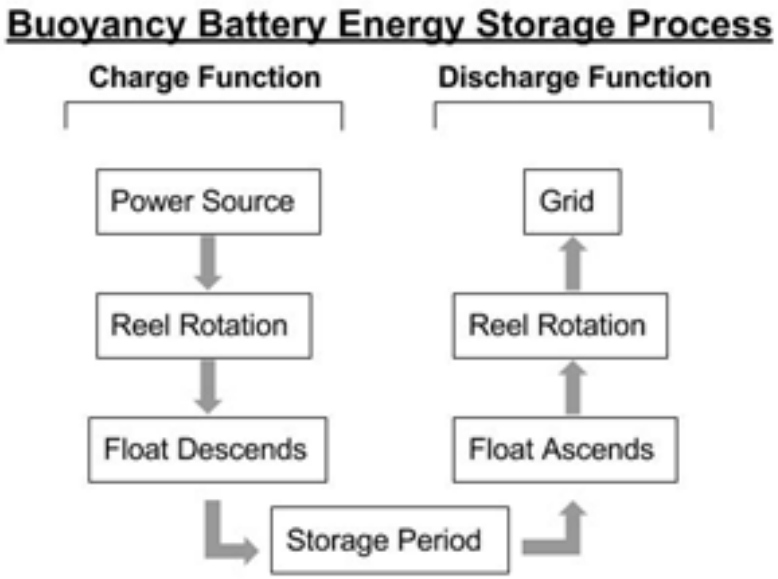

Figure 4-4 – BBES Process

The governing equations for BBES are straightforward with energy storage capacity depending on float volume, water depth, and float drag characteristics. They can be found by considering the force balance on a submerged float as expressed in equation (5) below.

$$F_{net} = \rho V g - mg - \tfrac{1}{2}\rho A U^2 C_d \qquad \textbf{(5)}$$

Where V = float volume, ρ= water density, g=gravitational acceleration, m=float mass, A = float cross sectional area, U = float speed, Cd=float drag coefficient. For steady state operation this net force will be counteracted by an electrical load on the generator. Energy storage can be calculated by considering this net force acting over a distance equal to the water depth z as shown in equation 6. Theoretical maximum power output of the float can also be calculated by considering the net force acting at float velocity U as shown in equation 7. These equations describe the energy and power from the float itself. Additional losses will be encountered when the specific balance of components are added including the electric generator, motor and pulley.

$$E = z(\rho V g - mg - \tfrac{1}{2}\rho A U^2 C_d) \quad \textbf{(6)}$$

$$P = U(\rho V g - mg - \tfrac{1}{2}\rho A U^2 C_d) \qquad \textbf{(7)}$$

4.3 - System Design for Coupling with 2.3 MW Wind Turbine

To provide a starting point for designing a buoyancy storage system capable of integration with a utility scale wind turbine a required energy storage capacity of 1 MWh has been selected. A more sophisticated analysis into the ideal storage capacity for a given wind turbine will consider the daily standard deviation of wind energy generation over an extended time period and is beyond the scope of this paper.

4.3.1 - Float Array

Several options exist for the selection of floats for a BBES system ranging from custom made rigid vessels to readily available lift bags used for marine salvage. Using manufacturer supplied data for from Seaflex Corp, the fleet of readily available lift bags can be considered as a basis for float design [8]. Multiple bags are to be arranged in an interconnected array as a single bag of sufficient lift capacity meeting the 1 MWh is not available. Table 4-1 displays energy storage capacity of each float based on (6) at a relevant water depth of 100m. Although this depth may seem significant, it is important to note that the average depth of the ocean is 3000 meters [9]. The number of floats required, n, is calculated for the desired 1 MWh capacity.

Table 4-1 - Storage capacity for Seaflex Floats ranging between 1 and 35 Tonne.

Float	*L (m)*	*D (m)*	*V (m^3)*	*Mass (kg)*	*E (kWh)*	*n @ 1 MWh*
5T	3.5	1.5	6.18	46	1.67	598.9
10T	3.5	2	10.99	68	2.97	336.3
20T	5	2.3	20.76	120	5.61	177.9
35T	6.5	2.6	34.49	300	9.31	107.4

As shown in table 1 above, many of the considered floats are required in order to meet the desired 1 MWh storage capacity. The exact arrangement of these floats within an array is an interesting topic of future experimental research. One attractive option would be to arrange floats in rows end to end and extend additional rows orthogonally as depicted in Figure 4-5 below.

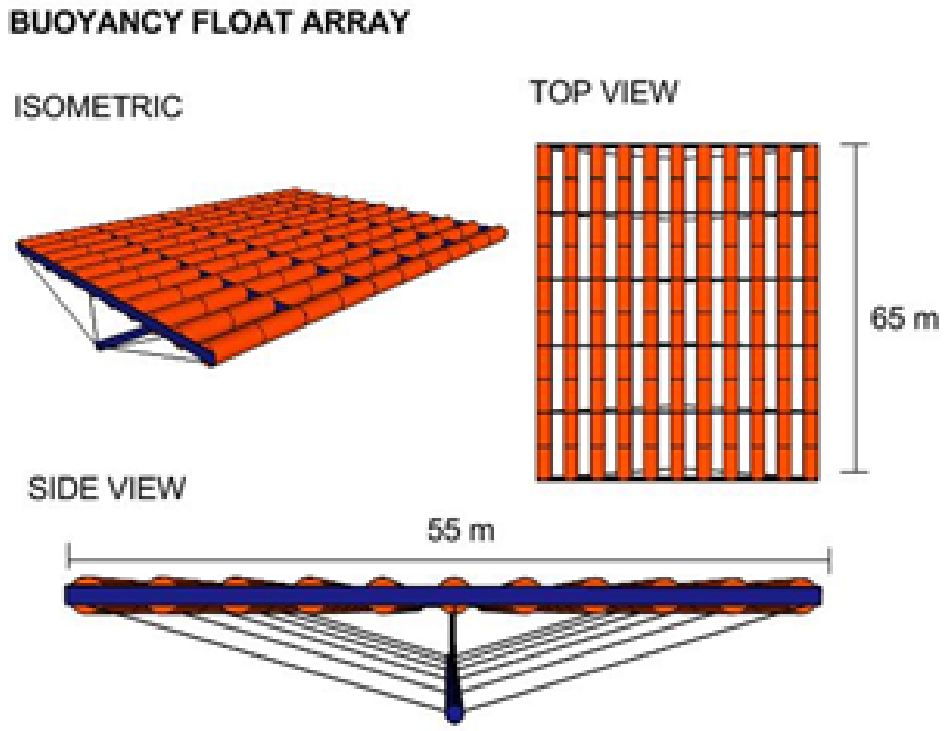

Figure 4-5: Float Array Assembly for 1 MWh Buoyancy Storage System

4.3.2 – Drag Considerations

The float rows are arranged with radial separation in order to prevent interference effects which would increase the hydrodynamic drag losses. The effect of hydrodynamic drag is of importance as it accounts for the fundamental losses of energy to viscous dissipation. The effect of drag is governed by the drag coefficient Cd, which, for bluff bodies such as the selected circular cylinder, will depend on the relevant Reynolds number of the flow. Drag characteristics of circular cylinders has been studied extensively and it has been shown experimentally that at for Reynolds numbers of $3x10^5$ there is a drastic decrease in drag coefficient [10]. This is known as

the drag crisis which is a result of the boundary layer transition from laminar flow with a wide wake, to turbulent flow with a narrowed wake [11]. Using this experimental data, the ideal float speed can be calculated based on the Re number where drag crisis occurs. For this analysis the speed of the drag crisis represents the best case scenario for drag losses and the drag coefficient used is 0.2. In order to determine the full hydrodynamic efficiency range, drag losses are also calculated for a simulated worst case scenario of Cd=12 and speed equal to drag crisis speed. Calculated losses and efficiency range for the floats considered is presented in Table 4-2 below.

Table 4-2: Hydrodynamic Losses for considered floats.

Float	*Max Drag loss (Wh)*	*Drag Loss @ Crisis (Wh)*	*U @ Drag crisis(m/s)*	*Efficiency Range (%)*
5T	35.28	0.58	0.200	97.88 - 99.96
10T	26.46	0.44	0.151	99.10 - 99.98
20T	32.87	0.54	0.130	99.41 - 99.99
35T	37.80	0.63	0.115	99.59 - 99.99

From this table we can observe that since the float is moving very slowly in relation to its size, the hydrodynamic drag losses are very small compared to total energy storage capacity and as such the efficiency range is very high. This implies that a designed BBES system can work effectively through a large range of velocities which gives storage operators flexibility in supplying energy from storage to the grid at variable power levels (by setting the desired float velocity for desired power output). Drag losses for BBES have been a serious point of discussion throughout the storage concept's development and the results from calculations indicate that for the utility sized floats considered, drag losses are virtually negligible.

Having established that there is some flexibility in float velocity, and that overall hydrodynamic is minimally affected by changes in velocity, the design float velocity can be calculated based on

water depth and cycle time. The design cycle time must take into consideration the economic environment into which the stored energy will be transferred. As displayed in Figure 4-3, there are numerous short duration events where price opportunity increases drastically for 1-3 hours. In order to capitalize on these events, the ideal storage system would have a discharge cycle time on scale with these short term events.

4.3.3 - Generator Selection

The storage system requires the ability to transfer a portion of total energy generated by the power source to each the storage system and the grid. This is due to high maximum power levels achievable by the wind turbines during periods of high wind and financial limitations of the storage system generator. It would be impractical for a storage system to require a generator/motor of equal power capacity to the generator. Based on the power curve presented in Figure 4-2, during early morning hours a 1 MWh storage system would be filled in less than one hour. Many MW scale generated options exist, originally purposed for utility scale wind turbines.

4.4 - System Performance Simulation

The parameters for the designed 1 MWh BBES system is summarized in Table 4-3 below.

Table 4-3 - Design parameters of BBES system for simulation.

Parameter	Value
Storage Capacity	1 MWh
Water Depth	100 m
Float Type	Seaflex 35T
Floats in Array	11
Radial Spacing	2.6 m
Marine Footprint	3565 m^2
Design Float Speed	0.027 m/s
Power output @ design float speed	1 MW
Hydrodynamic Efficiency	93.1%

Generator power rating	1 MW
Generator Efficiency	97%
Roundtrip Efficiency	83%

4.4 – System Performance Simulation

4.4.1 – Roundtrip Efficiency

An existing patent on a form of buoyancy energy storage states that a roundtrip efficiency of 97% is possible although no experimental validation is provided [12]. The calculation of round trip efficiency featured in the patent utilized a generator efficiency of 95%, motor efficiency of 97%, and pulley efficiency of 99% were used in this calculation within the patent although no specific references were presented. Existing literature on motor [13] and generator [14] efficiencies state that the efficiencies used by the patent are obtainable. The maximum pulley efficiency found in literature is 96% [15].

Using the calculated hydrodynamic losses for the 35T Seaflex float, along with assigned efficiencies for the motor and generator components the roundtrip efficiency of the system can be calculated using equation 8 below.

$$\eta_{roundtrip} = \eta_{motor} \times \eta_{generator} \times \eta_{charge} \times \eta_{discharge} \times \eta_{pulley} \quad (8)$$

$$\eta_{roundtrip} = 0.97 \text{ x } 0.95 \text{ x } 0.97 \text{ x } 0.97 \text{ x } 0.96 = 0.83$$

Using this calculated data we can now evaluate the performance and revenue generation of the designed storage system with respect to historical energy purchase price data and a set cycling program.

4.4.2 – Diurnal Storage Cycling

Several potential strategies for program cycling exist. The developed BBES system functions on a diurnal cycle with two charge and discharge cycles per 24 hours period. The timing ranges C1 and C2 represent the times of the first and second daily charge. DC1 and DC2 represent times when the battery is discharged to the grid. The optimal timing of these cycles within the day will depend upon the specific behaviour of the energy market. Statistical and time series analysis of historic energy price in order to identify larger scale patterns and trends within energy purchase price should be applied for developing an elaborate storage controller algorithm. This controller would allow for dynamic control of storage programming such that the exact charge and discharge times would be modified daily to suit the market. The development of such a controller is the topic of future publication. Charge and discharge times for the two storage algorithm simulated are presented in Table 4. Storage algorithm M2 was developed by referring to the average daily variation in EPP throughout 2015 and optimizing the curve to find ideal times charge and discharge.

4.4.3 Simulation Results

The performance of the developed system was simulated by evaluating the revenue equation using specific historic energy price data for 2015, along with the specified diurnal storage program and the calculated round trip efficiency.

Table 4-4 - Simulation Results

Program	*C1*	*DC1*	*C2*	*DC2*	*R total ($)*	*R net storage ($)*
M1	3-4	8-9	14-15	19-20	19722	9100
M2	4-5	9-10	14-15	20-21	20648	10337

As displayed, the yearly revenue generation for 2015 through arbitrage is very limited. This is apparent even when using the ideal round trip efficiency of 83% which is high in comparison to achievable efficiencies of existing ES technologies. Based on the calculated revenue, there is no ES technology which would be financially viable even at 100% efficiency. This demonstrates the current challenge facing both prospective ES developers as well as the grid controllers, which is the monetization of the service provided. Through cooperation with the IESO, additional revenue can be generated through ancillary services yet the exact compensation for these services are dependant on exact contracts between the ES developer and the IESO.

4.5 - Open Water Field Testing

Although BBES has been tested experimentally in a lab setting, the system had never been tested in the open water. In order to begin examining the real world application of this system, and gain appreciation for the practical challenges storing energy in the marine environment, open water testing was completed over a three day period in August 2016. It was not the intention of the testing to rigorously evaluate actual system roundtrip efficiency but to validate that float speed and power level can be controlled through loading and that the steady state operation (upon which the simulated 1 MWh system is based) can be achieved.

Testing was completed on a small scale system within a secluded bay in the Georgian Bay region of Lake Huron. A 3 float array was constructed with PVC tubes and radial spacing equal to 1 diameter as depicted in Figure 4-6 A. Scaled cylindrical floats were used, similar to those proposed in the utility system above. The developed charge reel for the open water testing is depicted in Figure 4-6 B.

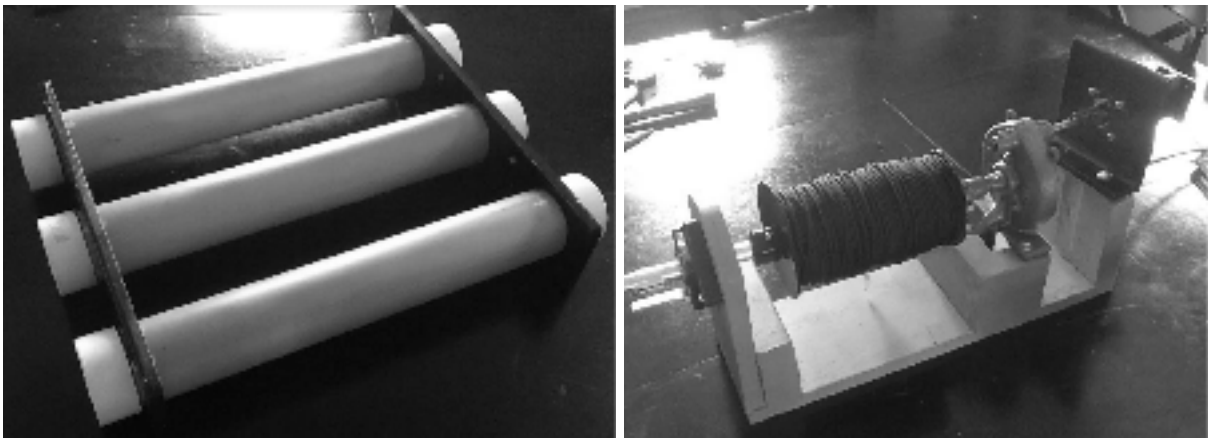

Figure 4-6 - A (Left) 3 float array, B (right) Charge Reel featuring 9 to 1 transmission

One of the challenges faced with experimental performance previously was devising a charge reel system which would effectively load the float such that its velocity would be reduced to a level that results in minimal drag losses. To better accomplish this a transmission was integrated into the reel such that each revolution of the reel would result in 9 revolutions of the generator. 550 Paracord was used as the main float line.

4.5.1 - System Deployment

The system was deployed from a large sailing vessel of 12 m length and a weight of 15 tonnes. Three point anchorage was used to moor the vessel in an effort to reduce error caused by the boat moving and rotating in the wind and waves. The primary ship anchor, a 50 kg, Navy style, was deployed and set into the waterbed. The stern of the ship was then affixed to shore with nylon rope tied to a shore mounted mooring cleat. The BBES pulley was mounted to second hook style anchor weighing 35 kg. The mooring system is depicted in Figure 4-7 below.

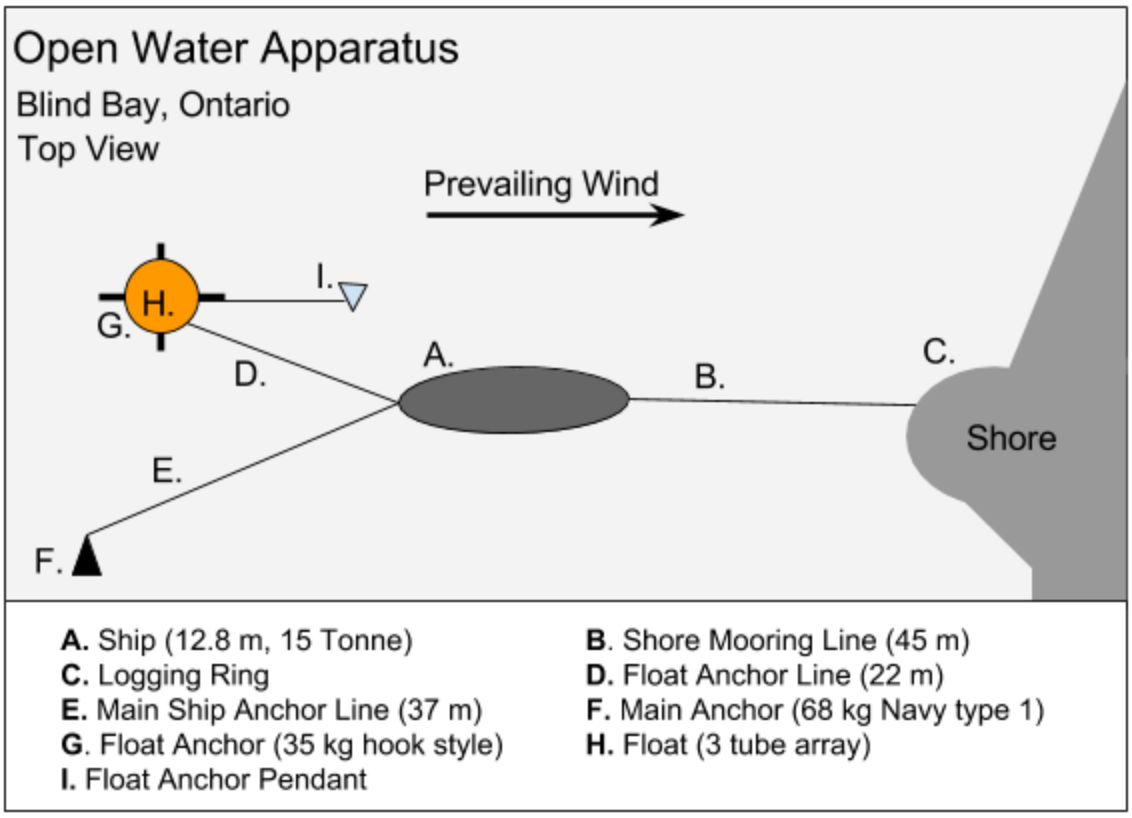

Figure 4-7 - Anchorage and mooring system for open water tests.

With the main anchor and shore line affixed the float line was then rigged through the pulley and the pulley anchor was deployed from a small aluminum boat approximately 20 m ahead of the vessel. A simple survey of the waterbed conditions indicated a layer of vegetation of approximately 0.75 m. To avoid interference with the marine vegetation, the pulley was mounted with a 1 m line. The pulley anchor was carefully and slowly lowered with a secondary line affixing the pulley anchor to the vessel. A removable pendant buoy was mounted to the end of the float line such that the anchorage could be fully set and tensioned before installing the float. This also allowed for anchorage to remain undisturbed underwater during the nighttime when testing was not taking place. With the three mooring points established all the anchor lines were tightened and tied. The charge reel was mounted to the deck of the ship. The pendant buoy was then removed and float attached to the float line for testing.

4.5.2 - Operational Cycle Testing

BBES system cycling was then tested under several resistive load conditions. Voltage and discharge time was measured such that float velocity and power could be calculated. The generator has an internal resistance of 21 ohms. The tests were conducted with a 5.9 m charge depth. The total power output from the float to the generator includes both the measured power output at the external resistors and the power dissipated within the internal resistance of the generator. The theoretical power output for each loading condition can be calculated as the product of the discharge force and discharge velocity. Results for the power output and float velocity are displayed in Figure 4-8 below.

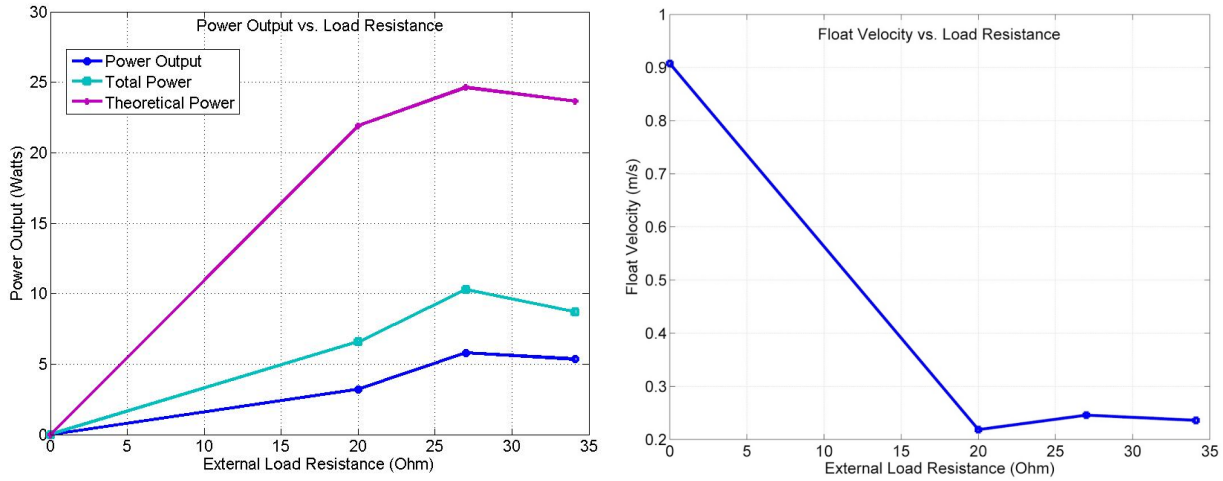

Figure 4-8 - Power output and float velocity for various external resistive loads

A very positive result from the testing is that unlike previous discharge testing, which was unable to achieve steady state float motion [1], the new apparatus was able to limit float velocity to the range of 0.21 to 0.23 m/s. This is significant considering the drag losses which are proportional to the square of float velocity. Due to the improved RPM load matching with the transmission, the floats proceeded with constant velocity through the water.

Due to the high internal resistance of the generator relative to the external load resistance, a large proportion of the total power is dissipated within the generator itself. An additional source of power loss which accounts for some of the difference between the theoretical power output and the total power is the electromagnetic efficiency of the generator in converting the rotational kinetic energy of the reel into electricity. As previously discussed, drag also results in losses to both power and efficiency. Energy will also be lost to residual kinetic energy left in the float as it reaches the surface of the water.

Certain challenges were apparent when testing the system at high resistance, low load. When the system was released after charge, the limited mechanical resistance to rotation at the reel caused it to accelerate rapidly and tangle. Several other high resistances ranging from 500 - 40 Ohm were connected and tested but each exhibited the tangling behavior. No load testing was completed by disconnecting the generator from the transmission and slowly releasing the reel for the first half turn of the reel - the discharge distance and time for the no-load was adjusted accordingly to reflect this release method.

The float line used was 550 paracord, and this was found to be non-ideal due to the high levels of stretch encountered during testing. Even when the reel surge from float line stretch did not result in a tangle, it introduced high vibration loads through the charge reel. These vibrations eventually loosened the low speed shaft couplings and affected the integrity of the transmission mounting points. After the second day of testing the low speed shaft was rebuilt with welded one piece construction. A flex-mount type coupler was added between the low speed shaft and transmission. Tests were repeated with the modified charge reel.

Overall, results from the open water testing is very encouraging as they displayed that with appropriate load matching, float velocity can be effectively controlled and steady state motion can be achieved. Improvements based on observations and results from open water testing include the following;

- For deployment in greater depths a reel winding guide is required to ensure organized winding of float line and prevent tangles at discharge release
- Reel Generator must account for vibration through flex couplers and dampeners at transmission and generator mounting locations
- To reduce reel surge at discharge a float line with minimal stretch is required

4.6 - Concluding Remarks

The concept of Buoyancy Battery Energy Storage has been further developed by considering its application in storing renewable, intermittent wind energy. By considering historic energy purchase price data for the electricity grid in Ontario, Canada and real turbine power output data from the Port Alma Wind Farm, a Buoyancy system has been designed of 1 MWh storage capacity.

Hydrodynamic drag losses for several variations of industrially-available lift bags have been calculated and it was found that drag effects have minimal impact on overall system efficiency. The developed system features 110 floats arranged in an array of float rows separated by a radial distance equivalent to the float diameter. Future work into the ideal radial spacing should be conducted.

Calculations of ideal round trip efficiency of the system have been presented indicating that high efficiency levels are possible when high efficiency components (motor, generator, pulley) are used.

Future work into quantifying the exact project costs associated with BBES is required considering equipment, installation and operation costs. These cost analysis will allow for direct comparison between BBES and competing bulk storage techniques.

As shown through the float array rendering and calculated marine footprint, the BBES systems appropriate for utility scale application are very large, the developed system covers nearly an acre of marine area. Although this is a certainly a challenge from the practical perspectives of structural engineering and economic viability, it is not a theoretical limitation as more than 70% of the planet's surface area is water. Obtaining the volumes of air required to fill the floats is also not a concern.

Using a basic and static algorithm, revenue generation for the energy storage system was tested with historic 2015 HOEP data which revealed that revenue generation potential is very low ($10,337/year). This indicates that, barring drastic increase in HOEP daily price opportunity energy storage facilities are not yet financially viable when generating revenue solely through energy arbitrage.

Open water testing of a small scale BBES system was conducted to verify that steady state float motion could be achieved with proper matching of generator and reel loading. Results indicated that float velocity control is possible. Float line stretch was found to results in surging behavior at the charge reel and thus future testing must feature lines with less elongation to control this effect.

References

[1] K. Bassett, R. Carriveau, and D. S-K. Ting "Experimental Analysis of Buoyancy Energy Storage," IET Renewable Power Generation. In Press.

[2] REN21, "Renewables 2014: Global Status Report." Paris, 2014.

[3] Bassett, K., Carriveau, R., Ting D., "Energy Storage through application of archimedes principle" Journal of Energy Storage. In Press

[4] Brancato, Emanuel L. "Estimation of lifetime expectancies of motors."*Electrical Insulation Magazine, IEEE* 8.3 (1992): 5-13.

[5] Li, Binghui, and Joseph F. DeCarolis. "A techno-economic assessment of offshore wind coupled to offshore compressed air energy storage." *Applied Energy* 155 (2015): 315-322.

[6] IESO Data Directory http://www.ieso.ca/Pages/Power-Data/Data-Directory.aspx. Accessed April 1, 2016

[7] Steel, W., "The what when and how of negative electricity. Prices Cleantechnica "http://cleantechnica.com/2015/10/01/texas-electricity-prices-going-negative/. Accessed April 12, 2016

[8] Unique Group, "Seaflex Enclosed Inflatable Buoyancy Units" https://www.uniquegroup.com/item/137/AirLiftBags/Enclosed-Inflatable-Buoyancy-Units.html. Accessed April 10, 2016.

[9] National Oceanic and Atomospheric Administration, "Ocean Facts", http://oceanservice.noaa.gov/facts/oceandepth.html. Accessed May 17, 2016.

[10] Fluent Inc. "Flow over a cylinder" http://www.wiley.com/college/munson/0471675822/flowlab/templates/cylinder. Accessed April 1, 2016

[11] Singh, S. P., and S. Mittal. "Flow past a cylinder: shear layer instability and drag crisis." *International Journal for Numerical Methods in Fluids* 47.1 (2005): 75-98.

[12] Morgan, J.P., "Buoyancy energy storage and generation." US Patent US 20100107627 A1. 6 May 2010

[13] Siemens, "Siemens Air Cooled Generators" http://www.energy.siemens.com/hq/pool/hq/power-generation/generators/sgen-1200a/siemens-generators-sgen-1200a-US-LowRes.pdf. 2016. Accessed Online 9.8.16

[14] Boglietti, Aldo, et al. "International standards for the induction motor efficiency evaluation: a critical analysis of the stray-load loss determination."IEEE Transactions on Industry Applications 40.5 (2004): 1294-1301.

[15] Balance Community. "An in depth look at pulley efficiency" http://www.balancecommunity.com/slack-science/an-in-depth-look-at-pulley-efficiency/ Accessed Online 9.8.16

Chapter 5

Energy Arbitrage and Market Opportunities for Energy Storage Facilities in Ontario

5.1 - Introduction

Electricity grids are changing on an international scale, as environmental initiatives have resulted in increased focus on environmental impact and sustainability. Fossil-fuel phase out is occurring in varying degrees across the planet and the world's top industrialized nations have agreed to reduce and limit emissions through the phase out of subsidies for fossil fuels, per the Paris agreement of 2015 [1]. Renewables including solar, hydro, and wind have been utilized to meet increasing electricity demands. Renewables are variable in nature, and their output depends on the environmental conditions which change based on daily and seasonal cycles. This is distinct from fossil fuel and nuclear generators which have consistent and predictable energy output for their desired operation period. The long term impact of increased variable generation on essential aspects of grid operation including market electricity price, energy export, and the management of surplus generation are interesting and important areas of study as wind energy penetration rates increase internationally.

Ontario's electrical energy grid is a significant grid for study as it features a diverse mix of both dispatchable and non-dispatchable (Variable) generation as well as interconnection to several other important North American Electricity grids. It is Canada's largest electricity grid supporting a population of 13.6 million people. A growing population along with high yearly temperature variation, and increasing penetration rates of variable generation sources, present significant challenges for this grid. The situation in Ontario may be used as a case study to inform the electrical development of other regions around the world.

The energy market in Ontario has been changing as initiatives for renewable energy beginning in 2008 have resulted in the rapid growth of wind energy generation capacity. This additional capacity help contribute to the phasing out of all coal-based generation facilities in the province. The approximate 36591 MW of currently installed capacity is made up of six generation sources including the baseload generators nuclear and hydro, along with variable generators (VG) wind, biofuel, natural gas and solar energies [2].

Ontario's not-for-profit grid controller organization, the Independent Electricity System Operator (IESO) is responsible for control, dispatch and management of the grid assets along with establishing the Globally Adjusted Energy Price (GAEP). The GAEP is a measure of the true cost to the Province for generating a MWh of energy and is the result of Ontario operating in a closed market, where individual contracts between generators and the IESO exist. This includes purchase agreements with long established nuclear facilities as well as recently installed wind farms and solar arrays. A recent report from the Ontario Ministry of Environment regarding expected global adjustment purchase price for May 30, 2016 through April 1, 2017 indicates global adjustment value of $90.86/MWh and expected wholesale electricity costs of $16.86/MWh [3]. With projection variance the total regulated energy price is reported as $111.41/MWh with global adjustment accounting for approximately 81% of total energy cost.

Presently, control of the dispatchable baseload resources is accomplished through a bidding process completed by each generator asset. These bids are then entered into a Dispatch Scheduling and Pricing Software (DSPS) which calculates economic gain defined as the difference between the perceived worth of the electricity produced and the cost of producing the electricity, when considering additional costs of operating reserves [4]. Dispatch instructions to baseload generators are based on the results of these calculations. Variable generators operate in a different economic market due to their intermittency, and are paid hourly based on energy produced and the Hourly Ontario Energy Price (HOEP). When demand projections exceed actual demand there can be an imbalance known as Surplus Baseload Generation (SBG).

SBG is a condition when production from the base load generators exceeds Ontario's demand. To deal with these situations, energy exports can be scheduled, water can be spilled from hydroelectric dams, or specific baseload variable generators (wind farms) can be curtailed. These situations are non-ideal and represent an imbalance between demand and supply as the result of projected demand exceeding actual demand. Each situation is problematic as the actual cost of producing the electricity is reflected in the global adjustment price paid by the consumer.

Grid-scale energy storage (ES) is one proposed method endorsed by Ontario's IESO for aiding with the regulation of SBG. Through the storage of energy generated by non-dispatchable resources at times of low demand, and discharge of energy onto the grid at times of increased demand, there is opportunity to gain additional utility, or revenue from this energy. Several grid-scale energy storage technologies exist at various stages of implementation and development including Pumped Hydro [5-8], Compressed Air Energy Storage [9-12], Underwater Compressed Air Energy Storage [13-15], Flywheel [16-17], Chemical Batteries [18,19] and Buoyancy [20-21]. A recent request for information from the IESO for prospective energy storage facility proposals indicates a desire to implement ES and there is currently a procurement program seeking 50 MW of energy storage.

It is the intention of this paper to analyze historic Hourly Ontario Energy Price (HOEP) in order to identify patterns and fundamental frequencies within the datasets. This historic data is then used to simulate the revenue generated by a standardized energy storage system operating within the Ontario energy marketplace. The analysis is conducted to help assess market opportunities for prospective ES facilities.

5.2 - Energy Arbitrage Through Grid-Scale Energy Storage

ES technology has the potential to provide a suite of services to the grid. Prospective energy storage facilities stand to provide several services for the grid. The first service, time-shifting involves the storage of surplus baseload generation during times of low demand and dispatch-scheduled discharge onto the grid during a period of high demand. The duration of the time shift can vary from a few hours (daily shifting) to several months (seasonal shifting). Daily shifts work to address SBG, typically at night, when demand can drop as much as 8000 MW and nuclear and hydro generation is more than sufficient to cover Ontario's demand. Seasonal shifts work to address surplus energy during milder months (Spring, Fall) , when demand is low, for utilization during more extreme temperatures (Summer, Winter).

Both types of time-shift will result in financial benefit, the extent of which depends on whether the storage assets are owned by province itself, or by a private company operating under contract with the IESO. Recent publication by IESO indicates that newly installed storage capacity would be done through contract with private companies and thus this paper will examine the impacts of that scenario. The energy for storage is purchased by the storage company at the relevant energy purchase price for that hour P_1, and then sold at a later time P_2. The revenue generated for the storage company, R, through this transaction is dependant on the price difference between P_1 and P_2 as well as the amount of energy exchanged, E, and the roundtrip efficiency of the storage system, $\in$. Revenue generated is expressed in equation 1.

$$R = \in E(P_2 - P_1) \qquad \textbf{(1)}$$

The benefit of this transaction from the Province's perspective relates to loss reduction. During times when the SBG is being controlled through energy export (which occurs constantly throughout each day), there is an economic loss as the province purchases all energy from the IESO at the Global Adjustment rate and then sells it to neighbouring electricity grids at the hourly rate. This transaction is expressed through equation (2) below.

$$L = \epsilon E(GAEP - P_1) \quad \textbf{(2)}$$

Considering the globally adjusted energy price and wholesale energy values presented above, it can be determined that the province suffers an approximate economic loss of $92.83 for each MWh of energy exported. Per market rules, a 1400 MW excess reserve capacity is required at all times for grid resiliency. Any SBG beyond this level represents notable economic loss, thus it is of critical interest and importance to determine and identify factors which influence SBG. In 2015, 16,854 GWh were exported representing approximately $1.56 billion of economic loss.

The total economic benefit considering revenue for the storage company, and recovered losses for the province can then be expressed.

$$B = \epsilon E(P_2 - P_1) + \epsilon E(GAEP - P_1) \quad \textbf{(3)}$$

Hourly energy price has a major influence on the economic feasibility of an energy storage system. HOEP fluctuates in response to demand and a variety of other parameters including daily patterns (sleeping at night, working during day), weather patterns, and generation fluctuation. Typical HOEP data for a six day period July in 2015 is presented in Figure 5-1.

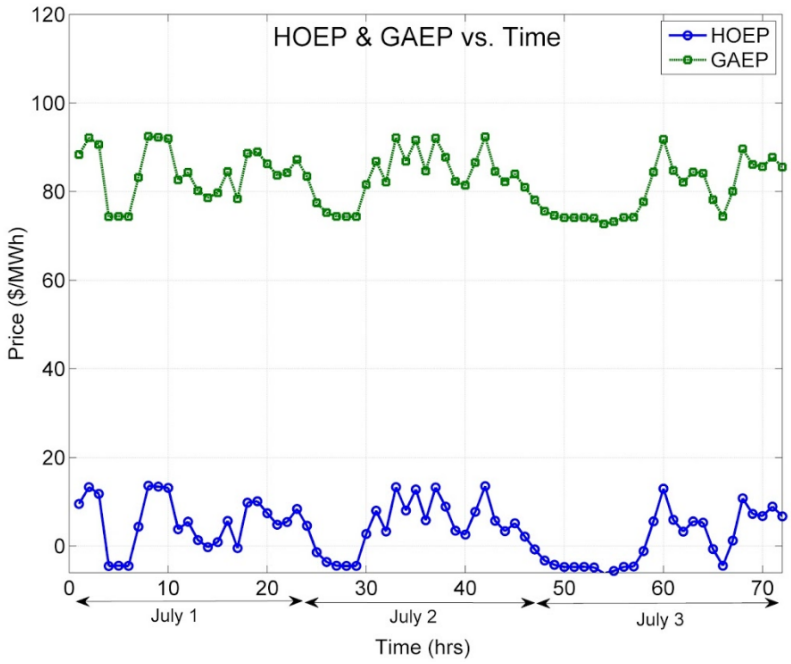

Figure 5-1 - Variations in HOEP and GAEP for three day period July 1 - 3, 2015 .

As displayed in the chart, HOEP varies greatly throughout the day, and GOEP follows the trend offset by $73 for this period of interest. HOEP values can fall to negative values in order to de-incentivize non-dispatchable generators from producing energy during times of SBG conditions. The HOEP determines the ideal times for energy to be stored and discharged. These charge and discharge times can be referred to as an Energy Storage Program (ESP). Determining an optimized ESP starts with characterization of the performance of an ES asset, including total storage capacity, power output at ideal operation, and the system round trip efficiency.

To gain insights into a potential ES market, historic HOEP can be analyzed for trends and patterns. The IESO provides general summaries on its website [22] including averages of HOEP for years, months and quarters. To explore HOEP in the frequency domain the Fast Fourier Transform was employed. Inspection of Figure 1 reveals that the energy price is periodic and several pricing cycles of various duration are evident. The FFT can provide insight into these cycles.

5.3 - Fourier Analysis of HOEP 2005-2015

Fourier analysis was completed for times series HOEP datasets for years 2005 through 2015 in order to study its periodicity. The sampling frequency for the HOEP is 2.777×10^{-4} Hz which corresponds to the one hour period. Several fundamental frequencies were found present at various amplitudes within each year. Fourier plots for 2009 and 2014 are presented in Figure 2A and 2B.

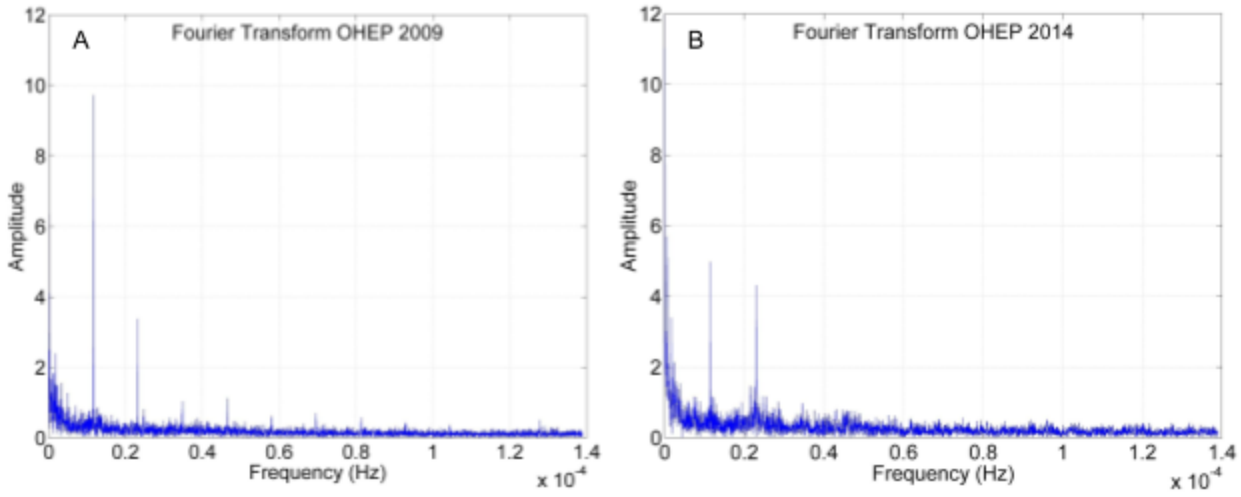

Figure 5-2 - A) FFT plot for 2009 with prominent 24 hr period amplitude B) FFT plot for 2014 with diminished 24 hour period amplitude

As can be seen in the above plot, peaks in the frequency amplitude exist at very low frequencies on scale with daily and seasonal cycles**.** To investigate these low frequency daily and seasonal cycles the FFT data for 0 through 3.0×10^{-5} Hz is isolated in Figure 3 and considered. Frequencies of high amplitude present across the ten year dataset are presented in Table 1.

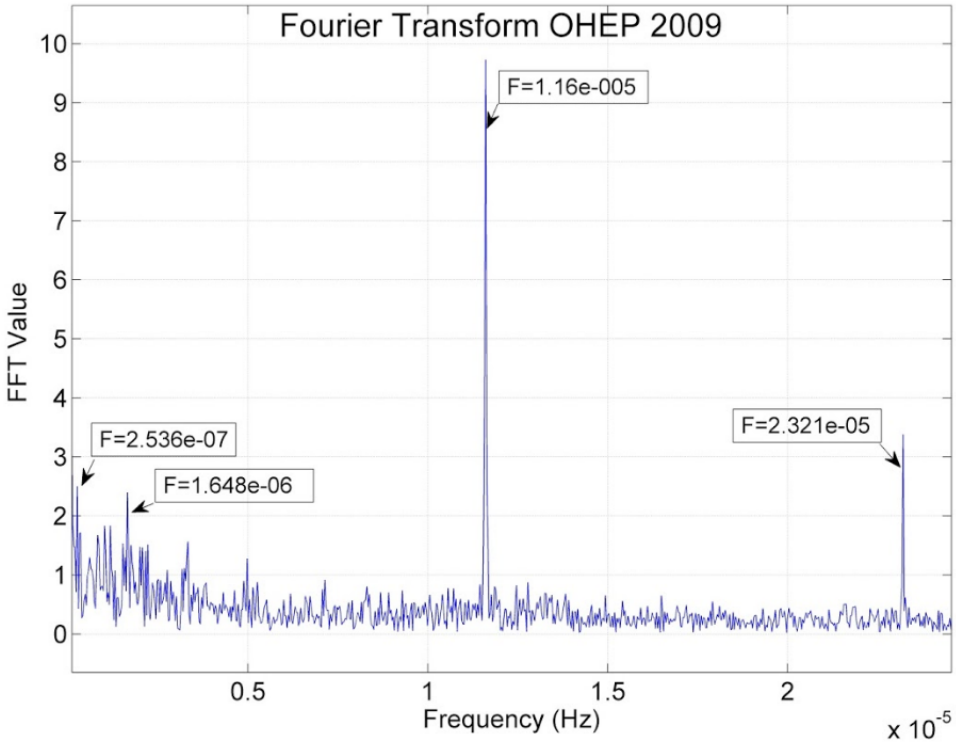

Figure 5-3 - Isolated FFT for low frequency spectrum

Table 5-1 - FFT Amplitude of prominent frequencies within HOEP 2005 - 2015

		FFT Amplitude Per Year										
Frequency (Hz)	**Period**	**2005**	**2006**	**2007**	**2008**	**2009**	**2010**	**2011**	**2012**	**2013**	**2014**	**2015**
3.47E-05	**8 hrs**	1.72	0.911	1.08	1.03	1.038	0.655	0.390	0.676	0.619	0.98	1.11
2.31E-05	**12 hrs**	3.67	2.60	2.84	3.38	3.200	1.45	1.65	1.57	2.35	4.31	3.13
1.16E-05	**24 hrs**	11.7	7.00	8.24	9.72	9.85	4.24	4.04	3.59	3.96	4.98	3.80
3.30E-06	**3.5 days**	2.53	1.61	1.88	1.56	1.566	0.324	0.63	0.402	0.487	1.09	1.23
1.65E-06	**7 days**	4.35	2.43	3.14	2.39	2.43	1.38	1.54	0.384	1.48	3.40	0.791

From Table 1 it can be seen that certain cycle lengths are very prominent in the HOEP dataset. The 24 hour period has the highest amplitude across the entire dataset which corresponds to the

repetitive daily peaks in energy price which occurs as response to a demand spike each evening. The 8 hour period corresponds to the time between morning peak and afternoon peak. The 12 hour period corresponds to the time between evening peak and morning peak the following day. Considering the change in FFT data over the ten year time period there are few obvious trends. The most distinct trend is the reduced amplitude of the 24 hour frequency. The lower 24 hour amplitude does not appear to have resulted in increases in the other ordered intervals considered. This implies that the overall price variation is becoming more stochastic. Insight into the cause for this can be gained by considering the external factors which affect HOEP.

HOEP is intimately linked to the energy consumption and demand patterns of Ontarians. One policy change which occurred during the period of interest is the introduction of time-of-use (TOU) billing. This involved the installation of smart meters across the province, which bills customers based on defined peak, mid-peak, and off-peak periods. Rollout of the TOU program began in 2009 and concluded in 2011. A impact analysis report on the this program found that the introduction of TOU resulted in load-shift behavior from the customers [23]. In an effort to conserve money, energy users consumed less electricity during peak hours and more during off-peaks. This distinct change in consumer behavior affected the HOEP patterns. This can be correlated with the decreased 24 hour amplitude which occurred between 2009 and 2010.

HOEP is also linked to energy supply in Ontario and another important change which occurred during this period was the introduction of wind energy generation into the Ontario energy supply mix. Installation of wind farms in Ontario began in 2006 and wind energy penetration rates have grown consistently to the current level of 11% with 3823 MW. This wind energy has introduced new levels of generator uncertainty to the base load power supply which has in turn affected price variation. New installation of renewables as well as nuclear and natural gas plants is displayed in Figure 5-4.

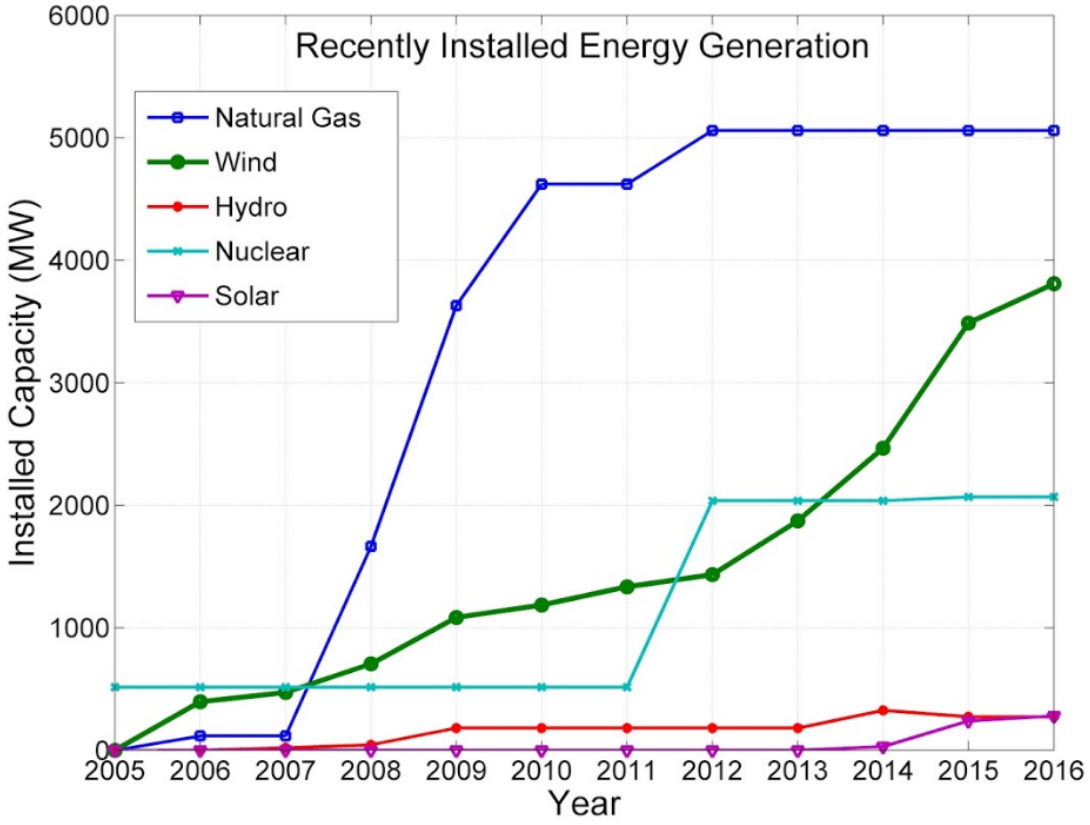

Figure 5-4 - New installations of generator facilities in ontario for 2005 through Q2 2016.

5.4 - Operating Revenue from Static ESP for 2015 HOEP

Per IESO direction, time-shifting energy storage facilities for prospective operation in Ontario require a minimum 0.5MWh and several different technologies are available for application on this scale. Pumped Hydro Storage (PHS) (5), Compressed Air Energy Storage (CAES), Underwater CAES (UWCAES), and developing Buoyancy Based Energy Storage (BBES) (20) all represent potential candidate facilities.

Using the 2015 HOEP data, simulations can be completed to calculate the revenue generated by an energy storage system operating that year. For the sake of scale projections, a standardized 1 MWh, 1 MW, energy storage system was used and revenue was calculated using Equation 1 for various roundtrip efficiencies. A static ESP is an energy storage program which does not vary its daily charge and discharge times throughout the year. A total of 63 revenue simulations were

completed for the simple, standardized system. Early morning charge times (3AM - 7AM) were used and revenue calculated based on discharging that energy over the hours of 8AM-12PM.

To simulate an ideal dynamic ESP, the daily maximum purchase opportunity (PO) was used. The maximum corresponds with charge at the hour of lowest energy price and discharge at time of highest energy price. The revenue from the best performing storage programs and maximum PO program are presented in Table 5-2. Revenue generated daily by each of the ESPs throughout the year is displayed in Figure 5-5.

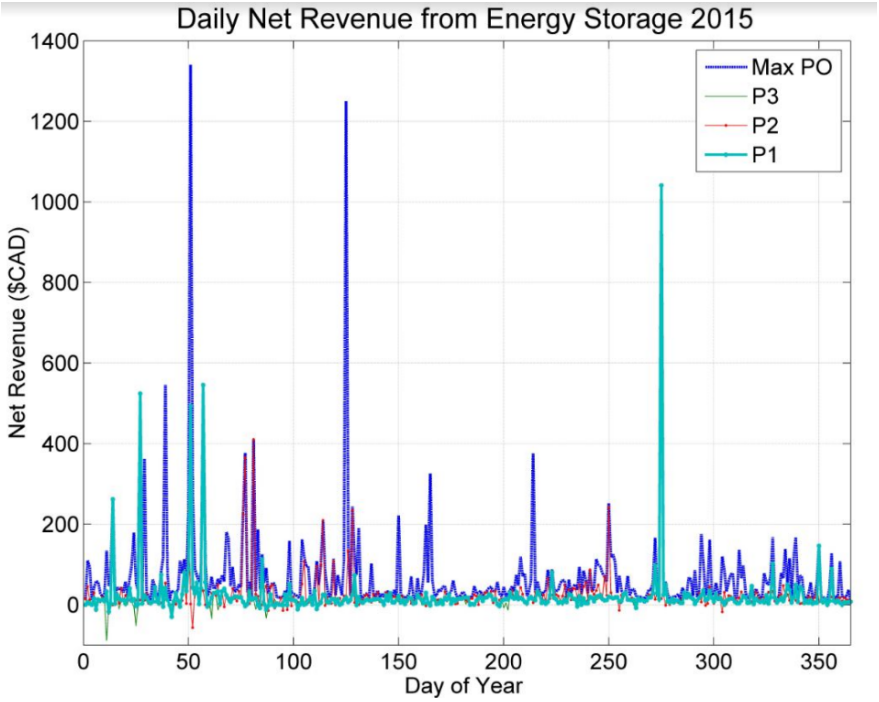

Figure 5-5 - Ideal (Efficiency = 100%) Daily Net revenue from simulated energy storage system for 2015 with high PO events occurring throughout year

Table 5-2 - Results from storage cycling simulations for 1 MW, 1 MWh storage for full 2015 HOEP dataset. Revenue reported in CAD.

Storage Program	Charge Time	Discharge Time	Ideal Storage Revenue	Storage Revenue (80%)	Storage Revenue (70%)	Storage Revenue (60%)
P1	4 AM	9 AM	8407	6726	5885	5044
P2	4 AM	8 PM	8347	6677	5843	5008
P3	3 AM	9 AM	7955	6364	5569	4773
Maximum PO	Variable	Variable	26728	21383	18710	16037

Figure 5-5 reveals that daily revenue values vary greatly throughout the year. Large proportions of the total yearly revenue are made during high PO events which occur on specific days. As the plots for programs P1, P2 and P3 indicate, less than $100 is generated for the majority of days throughout the year.

The maximum PO program, which represents an ESP that perfectly matches charge and discharge times for minimum and maximum HOEP, results in a revenue of $21282 at 80% round trip efficiency. This is a best case scenario for an ES system cycled once daily with the selected parameters.

The revenue for a best case scenario can also be calculated by finding the average of the daily maximum POs throughout the year and multiplying this by the 365 days of operation per year. From this a performance coefficient can be defined indicating the proportion of the revenue for a given ESP to the ideal revenue from the maximum PO program.

$$C = \frac{A}{PO_{MA} x 365} \quad \textbf{(4)}$$

Where A= actual revenue generated by the ESP, PO_{MA} = average of maximum daily Price opportunities for year of interest and C = ESP performance coefficient. For 2015 the average of max PO is 73.23. Using this equation, the performance coefficient of the best performing P1 ESP for 2015 is 0.312.

5.4.1 - Evaluation of Multi-Cycle Storage Programs

In order to increase the revenue of the simulated ES asset, multiple charge and discharge cycles would be completed on a given day. For each subsequent charge, the price opportunity for the transaction decreases. There is a practical limit for the number of cycles which can be completed daily which is based on the power rating of the storage system. For the simulated system, which has a two hour cycle time, the maximum cycles per day is 12, this would result in a situation where energy would be stored one hour then discharged the next. This does not coincide with HOEP patterns where price responds to morning and evening demand peaks. Revenue generated with a multi-cycle, static ESP is expressed in equation 4 below.

$$R = \varepsilon \quad E \quad 365 \quad PO_{MA}(\sum_{i=1}^{12} C_i) \qquad \textbf{(5)}$$

Where ε = system efficiency, i = cycle number, C = performance coefficient for relevant cycle number. The C values can be calibrated based on historic trends within HOEP data. Beginning with the best performing static ESP of charge at 4AM and discharge at 9AM, additional cycles can be added and yearly revenue calculated. Results from multi-cycle simulations are presented in Table 5-3. Revenue is reported is based on 100% roundtrip efficiency for the ES system and the ESP programs shown in Table 3 reflect the best performing of each of the cycle types.

Table 5-3 - Results from Multi-cycle simulations

ESP Operation	Charge Times	Discharge Times	Average R per cycle ($)	Total Ideal Revenue ($)
Single Cycle	4AM	9AM	8407	8407
Dual Cycle	4AM, 2PM	9AM, 8PM	6227	12455
Tri Cycle	4AM, 2PM, 5PM	9AM, 4PM, 8PM	4316	12948
Quad Cycle	4AM,10AM,12PM, 5PM	9AM, 11AM, 12PM, 5PM	2856	11425

As expected the additional revenue added diminishes with each subsequent cycle. Many of the additional cycles could reduce the overall revenue due to negative PO values for certain transactions through the day. The addition of a third storage cycle results in a marginal increase in total revenue. The fourth cycle resulted in an overall decrease in revenue compared to the dual and tri-cycle scenarios. This is indicative of the reduced PO for shorter storage durations. There is a minimum storage time required for sufficient positive changes in energy price to justify the storage transaction.

The ideal number of cycles to be completed by a given storage asset will account for a balance between increased revenue but also wear and tear to the system itself. Well designed systems will have a known system depreciation per cycle and thus, the true revenue of a system will depend on both its revenue through arbitrage transaction but also the decreased value of the system for each cycle performed. Based on the completed simulations, a dual cycle would be most appropriate as it results in the highest average revenue per cycle.

It is important to note that for real-world applications, static ESPs would typically not be used. There is also the option of utilizing IESO published HOEP projections which are posted for each day. These projected curves could be analyzed daily and the storage program defined to optimize revenue based on these projections. Unfortunately, the projected HOEP values do not typically

capture or predict the high PO events which, as demonstrated in Figure 5, accounts for a large proportion of yearly revenue, and could be most advantageous for an ES system.

5.4.2 - Provincial Benefit from Time Shifting

While the potential for revenue generation through arbitrage appears limited, there is additional opportunity to recover losses for the province as previously mentioned. Using monthly historical global adjustment values, this benefit can be calculated for the single and multi-cycle ESPs.

Unlike revenue per cycle, which decreases with each additional cycle per day, the provincial benefit remains constant for each additional cycle. This is due to the Global Adjustment values which remain constant throughout each month. The total energy price is the sum of the global adjustment value and the HOEP as displayed in Figure 1. The provincial benefit remains constant per cycle, assuming that all energy used for the charge is surplus baseload generation which would have otherwise been intended for export and energy discharged is used to meet demand and not exported. Under this assumption the charge and discharge times do not affect provincial benefit.

Based on GAEP rates for 2015, there is a total yearly provincial benefit of $28,965 for a single cycle system.

The future motivation to integrate energy storage onto a grid will be influenced by GAOP as the greater the GAOP, the greater losses the losses when energy is exported from Ontario.

Historic yearly averages of GA over the time period of interest is displayed in Figure 5-6.

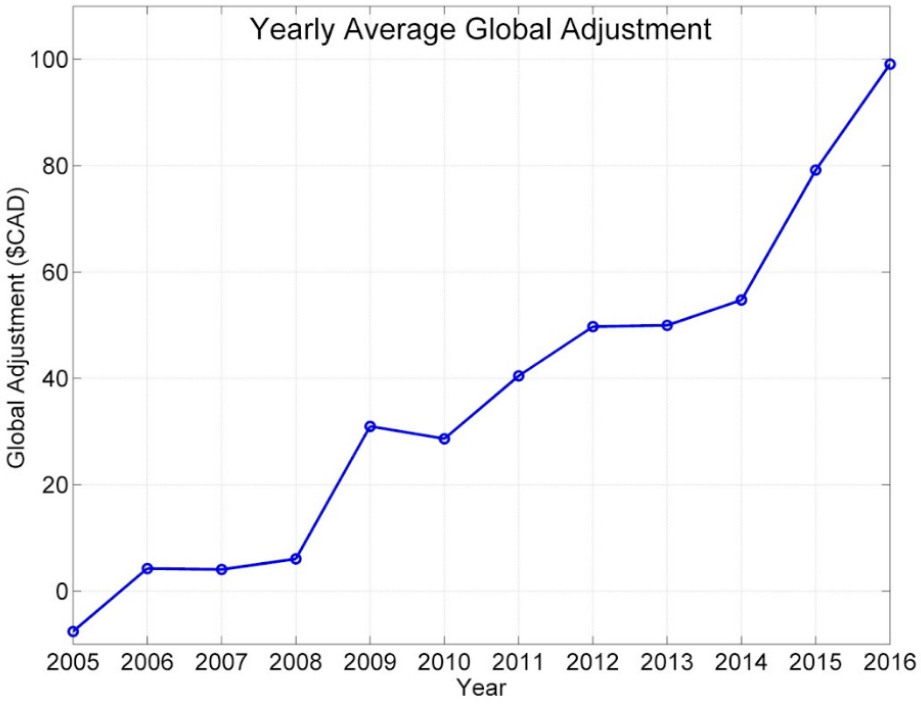

Figure 5-6 - Global Adjustment growth since introduction in 2005. Value for 2016 is year to date value as of July.

Historic GA data indicates a trend of significant growth since its introduction in 2005 when it was a negative value. This growth is a reflection of many different factors but the newly installed generation has had a significant impact on the price. An in depth analysis of the components which make up GA is presented in reference [3]. The growing GA increases the desirability of energy storage from a provincial perspective as a means to reduce losses due to export. Based on year-to-date values of monthly global adjustment the growth trend will continue in 2016 and the provincial benefit of the simulated energy storage system will increase accordingly.

5.5 - Ancillary services

Fortunately, energy storage facilities have the potential to earn additional revenue by providing other services for the grid. In Ontario, these are known as ancillary service and include black start capability, regulation services, reactive support and voltage control [23]. The financial compensation for providing these services is significant, especially in comparison to revenue generated through arbitrage as presented above. For 2015, a total of $66,579,317 was paid out for ancillary services. Based on IESO supplied data, the annual ancillary service revenue of an ES facility can be estimated.

Regulations services are the most appropriate ancillary service which can be provided by ES. Regulation is executed when an energy storage or energy generation facility works under the direction of IESO, increasing or decreasing energy output as required to respond to provincial demand. For example, certain wind farms have been designated for regulation service and can be directed by IESO to reduce their power output through curtailment. Regulation through this means, known as ramp down regulation, works to reduce SBG and financial loss to the province through the previously mentioned GOEP export transaction. Ramp up is another form of regulation which occurs when the provincial demand increases and the IESO must acquire additional energy through available sources. Wind energy cannot be used exclusively for ramp up regulation as there must be sufficient wind at the time of ramp up. Natural gas is used primarily for ramping up in Ontario.

Through coordination with the IESO, energy storage facilities can complete both ramp-up and ramp-down regulation when required by the grid. In 2015 over 45 million was paid for regulation corresponding to $155,798 per year, per MW of regulation control.

Blackstart relates to a generator's ability to discharge energy onto the grid without additional energy supply. An energy storage systems candidacy for black start service depends on the specific ES technology used. Pumped hydro and Buoyancy Energy storage have the potential for

black start service, but only while the systems are charged. How IESO would go about compensating for this part-time black start capability is unclear at this time. In 2015, $1,410,114 was paid out to 4 certified black start facilities in Ontario through monthly fixed payments.

Voltage control relates to controlling the frequency of generated AC voltage. Energy storage systems such as flywheels, which are designed for very short duration storage, can be used to effectively control voltage in a grid. There are two flywheel facilities in Ontario which offer voltage frequency control service. Voltage frequency control is not typically possible for the types of ES systems capable of completing energy arbitrage.

The potential for ES facilities to earn revenue through ancillary services is significant in comparison to the low revenue generated through energy arbitrage. Even including ancillary service payment, the challenge of making an ES facility profitable is a serious one. By adding the revenue from arbitrage and revenue from ancillary regulation service, the simulated 1 MW system produces a total yearly revenue of $176,000.00.

5.6 - Conclusions

Historic HOEP has been investigated using FFT analysis. Results indicate that the frequency corresponding to a 24 hour period was most prominent in the signal, which is consistent with the a priori expectations of daily price peaking in the evening. There also exists other prominent frequencies. Considering the change in FFT amplitudes over the ten year period it appears that changes in HOEP is changing at more random intervals. This may be correlated to the introduction of Time of use billing in 2009 which was found to have modified consumer behavior to shift loads to non-peak hours. There also may be correlation between the integration of wind energy which has grown significantly since 2008.

A 1 MW, 1 MWh storage system has been simulated for operational cycling through 2015 and the revenue generated through the energy arbitrage transaction calculated for various ESPs. Results indicate a gross revenue of $21,686 for such a system cycled once daily, and this revenue represents a best case scenario as the ESP used matched exactly the time of maximum and minimum energy market prices. The best performing static ESP featured a charge time of 4AM and discharge time of 9AM.

Systems operating with multiple daily storage cycles were also considered to determine how additional cycling of the set system would increase yearly revenue. Simulations were completed starting with the best performing single cycle ESP and additional cycles were added and total yearly revenue calculated. The revenue per cycle was found to decrease with each additional cycle per day. The best performing dual cycle program resulted in an average yearly revenue per cycle of $6227 and featured charge times of 4AM and 2PM and discharge times of 9AM and 8PM. The addition of a third cycle resulted in a marginal increase in overall revenue, but the revenue per cycle decreased significantly. Regardless of the ESP and number of daily cycles used, the yearly revenue was very low indicating the significant challenge of making energy storage financially feasible through energy arbitrage in the current market.

5.7 - Policy Implications

Energy Storage facilities have the opportunity to earn additional revenue by providing ancillary services for the grid. The ancillary service of regulation, where IESO can direct the increase or decrease of power level depending on demand curves represents an opportunity for energy storage facilities. Based on 2015 data, an ancillary payment of $155,798 was made per MW per year. ES facilities could also potentially offer blackstart services when charged, but how this service would be financially compensated is not clear at this time.

Developing an economically feasible ES facility for energy arbitrage in Ontario is problematic due to the low financial gain. Daily variations in HOEP are not large enough to result in

acceptable revenue. It is significantly more advantageous for a prospective ES facility to operate in conjunction with the IESO to provide ancillary regulation service.

Grid scale ES technologies are only beginning to be considered for application in Ontario, and the arrangements to be made between the ES operators and the IESO are yet to be seen. The development of energy storage in Ontario will be dependant on these agreements and any additional strategic incentives. Emerging energy policies must provide financial motivation for the integration of energy storage assets. Renewable integration and surplus balance are global issues and the insights gained through fourier analysis and revenue simulation for historic Ontario data can be applied to inform research for other utility grids worldwide.

References

1) The White House. "Leader's statement on the Pittsburgh summit". 2013-04-01. Accessed online 9.12.16
2) IESO, "Ontario's Power Mix" (2016). http://www.ieso.ca/Pages/Ontario%27s-Power-System/Supply-Mix/default.aspx accessed online 9.6.16
3) Board, Ontario Energy. "Regulated price plan price report." *Queens Printer for Ontario, Toronto* (2016).
4) Zareipour, Hamidreza, Claudio A. Cañizares, and Kankar Bhattacharya. "The operation of Ontario's competitive electricity market: overview, experiences, and lessons." *IEEE Transactions on Power Systems* 22.4 (2007): 1782-1793.
5) Rehman, Shafiqur, Luai M. Al-Hadhrami, and Md Mahbub Alam. "Pumped hydro energy storage system: a technological review." *Renewable and Sustainable Energy Reviews* 44 (2015): 586-598.
6) Yang, Chi-Jen, and Robert B. Jackson. "Opportunities and barriers to pumped-hydro energy storage in the United States." *Renewable and Sustainable Energy Reviews* 15.1 (2011): 839-844.
7) Hu, Weihao, Zhe Chen, and Birgitte Bak-Jensen. "Optimal operation strategy of battery energy storage system to real-time electricity price in Denmark."*IEEE PES General Meeting*. IEEE, 2010.
8) Kaldellis, J. K., M. Kapsali, and K. A. Kavadias. "Energy balance analysis of wind-based pumped hydro storage systems in remote island electrical networks." *Applied energy* 87.8 (2010): 2427-2437.
9) Lund, Henrik, and Georges Salgi. "The role of compressed air energy storage (CAES) in future sustainable energy systems." *Energy conversion and management* 50.5 (2009): 1172-1179.
10) Fertig, Emily, and Jay Apt. "Economics of compressed air energy storage to integrate wind power: A case study in ERCOT." *Energy Policy* 39.5 (2011): 2330-2342.
11) Succar, Samir, and Robert H. Williams. "Compressed air energy storage: theory, resources, and applications for wind power." *Princeton environmental institute report* 8 (2008).
12) Drury, Easan, Paul Denholm, and Ramteen Sioshansi. "The value of compressed air energy storage in energy and reserve markets." *Energy* 36.8 (2011): 4959-4973.
13) Cheung, Brian, et al. "Distensible air accumulators as a means of adiabatic underwater compressed air energy storage." *International Journal of Environmental Studies* 69.4 (2012): 566-577.
14) Li, Perry Y., et al. "Compressed air energy storage for offshore wind turbines." *International Fluid Power Exposition, Las Vegas, NV*. 2011.
15) Cheung, Brian C., Rupp Carriveau, and David S-K. Ting. "Parameters affecting scalable underwater compressed air energy storage." *Applied Energy* 134 (2014): 239-247.
16) Lazarewicz, Matthew L., and Alex Rojas. "Grid frequency regulation by recycling electrical energy in flywheels." *Power Engineering Society General Meeting, 2004. IEEE*. IEEE, 2004.
17) Samineni, Satish, et al. "Modeling and analysis of a flywheel energy storage system for voltage sag correction." *IEEE Transactions on Industry applications* 42.1 (2006): 42-52.
18) Divya, K. C., and Jacob Østergaard. "Battery energy storage technology for power systems—An overview." *Electric Power Systems Research* 79.4 (2009): 511-520.
19) Oudalov, Alexandre, Rachid Cherkaoui, and Antoine Beguin. "Sizing and optimal operation of battery energy storage system for peak shaving application." *Power Tech, 2007 IEEE Lausanne*. IEEE, 2007.
20) Bassett, K., Carriveau, R., Ting, D., S-K.,"Energy Storage through application of archimedes principle" Journal of Energy Storage. In Press.
21) "Experimental analysis of buoyancy based energy storage" IET Renewable Power Generation. In Press.
22) IESO, "Public Power Data Directory". (2015). http://reports.ieso.ca/public/. Accessed online 9.3.16
23) Faruqui, Ahmad, et al. "Impact Evaluation of Ontario's Time-of-Use Rates: First Year Analysis." *The Brattle Group. Cambridge, MA* (2013).
24) IESO, "Ancillary Service Market" (2015) http://www.ieso.ca/Pages/Participate/Markets-and-Programs/Ancillary-Services-Market.aspx accessed online 9.3.16

Chapter 6

Experimental Evaluation of Buoyancy Energy Storage Under Mechanical Loading

6.1 - Introduction

Grid-Scale energy storage (ES) is an important technology with the potential to improve the incorporation of intermittent energy sources onto existing electricity grids. Renewable energy forms wind and solar are highly intermittent as their energy output depends on the environmental conditions (sun, wind) which have daily and seasonal cycles. Global trends indicate that renewable energy utilization will continue to grow as fossil fuel based energy generation is phased out. The intermittency of renewable sources add an element of uncertainty to grid control as energy outputs of wind and solar are less predictable that traditional baseload generators nuclear, hydro, coal and natural gas. For sake of grid resiliency and reliability, grid controllers must maintain a minimum excess power capacity on the grid to account for possible surges in demand. When high proportions of renewables are used, the inherent uncertainty in their generation can results in a condition where the grid is running an unnecessarily high energy surplus. This surplus energy must be disposed of through various means such as export to neighbouring grid or spilling water at hydro dams. Each of these disposal means is non-ideal as it represents economic loss for the grid which subsidizes and funds the renewable energy generation in the first place.

Energy storage provides a potential solution to this condition as excess energy can be diverted to an energy storage system, where it can remain for a desired period of time. When demand increases, the energy can be discharged from the storage system in a predictable manner and used to meet demand.

Many different types of energy storage technology exist, each with various advantages, disadvantages and application requirements. One particularly interesting area of energy storage

which has received much attention in recent years - offshore energy storage - is one promising research area. Offshore energy storage looks to utilize the global abundance of marine area, whether it be in oceans, seas or lakes

Several forms of offshore energy storage exist and are in development, yet very few projects have actually been deployed and installed on a utility scale. Underwater compressed air energy storage utilizes waterbed mounted accumulators into which air is pumped and compressed. Energy is discharged by allowing the compressed air to expand through a generator equipped turbine [1]. One existing UWCAES installation is located in Lake Ontario at the city of Toronto, Canada [2].

Ocean Renewable Energy Storage (ORES) is another form of offshore storage currently in development. It features spherical concrete containers mounted at the waterbed which allow water to flow into and out of it through a turbine [3,4].

Buoyancy Battery Energy Storage (BBES) is a new form of offshore storage which utilizes the inherent buoyancy of an object of fixed volume [5-7]. Float motion is converted to electrical energy through a generator reel.

Previous testing [8,9] has confirmed several aspects of buoyancy energy storage operation including

1. Roundtrip efficiency independent of float mass
2. Non-dissipation, cycling will depend on mechanical components
3. Constant discharge force
4. Steady state operation is achievable through proper loading of float
5. Drag effects can be significant at high float speeds
6. Ideal theoretical round-trip efficiency is high at 83%
7. System can be deployed in marine environment from the water surface

Whether the high theoretical round trip efficiency can be approached in an experimental environment is the topic of this paper. Experimental analysis and field testing thus far has focused on discharge performance. Roundtrip efficiencies from these tests have been calculated using measured discharge quantities (power, energy, float velocity, time) and theoretical values for input charge energy. Previous tank testing with a spherical float and direct drive charge reel

yielded a maximum efficiency of 20.5% [6]. Open water testing performed with a cylindrical float array and transmission equipped charge reel yielded 25% efficiency [10].

6.2 - Sources of Energy Loss

As the BBES system is operated, energy is lost to various mechanical, electrical and hydrodynamic sources.

6.2.1 - Residual Kinetic Energy

When BBES is performed in a water body, several types of float motion can be initiated depending on the loading condition used. The most basic form of operation is the the constant loading condition, where a fixed electrical or mechanical load is applied to the float through the float line when the float lock is released. In this case, the float will accelerate towards the surface at a rate proportional to the difference between if the net buoyancy force and the load force. The float will continue to accelerate until it either reaches the water surface or reaches a velocity at which the drag force opposing float motion equalizes the net buoyancy force. The residual energy losses, $E_{Residual}$, for a given float mass is expressed as the standard formula for kinetic energy below.

$$E_{Residual} = \frac{1}{2}mv^2 \qquad (1)$$

Where m is float mass and v is float velocity at exit of water. For the testing subject of this paper, the residual energy loss will include contributions from both the float as well as the load mass.

6.2.2 - Drag Effects

As the float moves through the water volume it will experience the hydrodynamic force of drag opposing its direction of motion. When this drag force persists for a duration, energy is lost through the energy cascade leading to heat within the water. Drag force is a function of float velocity as well as drag coefficient. Drag coefficient for many shapes of interest is related to the flow velocity and thus Reynolds number.

It may prove potentially advantageous to use highly streamlined shapes with very low drag coefficients at the desired float speed, but these custom shapes would be much more expensive to

manufacture. Also, if a rigid float were strong enough one could pull a vacuum and evacuate any air inside of the float, thus reducing weight and increasing net discharge force and energy storage density.

Cylindrical floats are a practical choice as tubular objects are produced and used in industry. For full scale system integration, a developer could leverage advances and existing manufacturing capability of wind turbine tower manufacturing industry. The orientation of cylindrical float either vertical or horizontal, will affect the hydrodynamics of float motion .

6.2.3 - Pulley Losses

The pulleys used at the anchorage will contribute to energy loss through friction. These frictional losses are a function of float velocity. There will be a static as well as dynamic component of pulley friction.

6.2.4 - Electrical Losses

The largest challenge featured thus far with testing has been the efficient conversion of the floats linear motion into electrical energy through the generator. A range of resistive loads have been used to test a direct drive reel generator setup as well as one with a transmission system. A brushed DC generator was used in each of the operational testing trials. The generator used resulted in high electrical losses due to both the high internal armature resistance as well as the electromagnetic conversion efficiency of the device itself.

Optimizing the electrical set-up at such a small scale is problematic due to the limited options of generators in the range of 5-300 watts. Generators of this size are not designed to the same standards of efficiency as proper industrial machinery. For full scale BBES systems, generators with specified and tested efficiencies would be used. Generators of IEC 6 specification have a minimum efficiency of 96% [5].

In order to isolate the mechanical and hydrodynamic aspects of BBES, the electrical side of the system has been removed and the system was tested for the performance in converting buoyancy potential energy to gravitational kinetic energy.

6.3 - Experimental Apparatus

The apparatus used for experimentally testing BBES under mechanical loading is depicted in figure 6-1. The developed experimental apparatus features a conversion pulley set which is mounted rigidly to the tank frame.

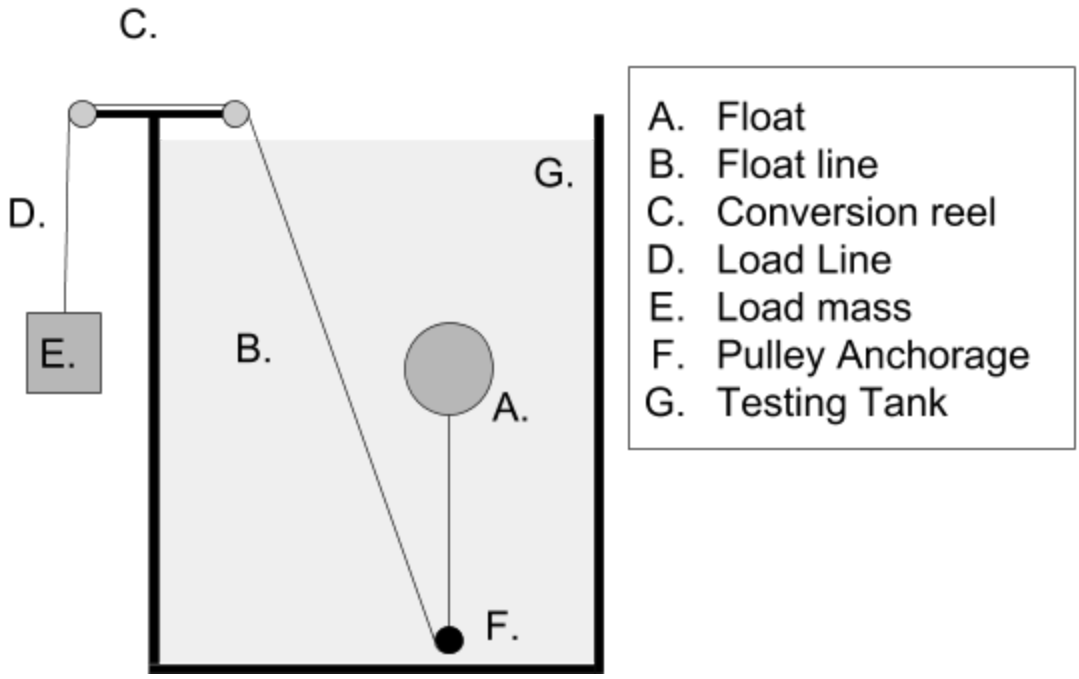

Figure 6-1 - Testing Apparatus used for charge and discharge testing of BBES system under mechanical loading.

The float line passes from the float, through the anchorage pulley and then through the conversion reel. A 14 kg cement block was used as the pulley anchorage.

Several floats of interest were tested to determine the influence of float geometry on discharge performance. Properties for the tested floats are summarized in Table 6-1. The three floats tested for this study are depicted in Figure 6-2.

Table 6-1 - Specifications of Tested Floats

Float	Shape	Dimensions (m)	Volume (m^3)	Mass (kg)
1	Cylinder (Horizontal configuration)	D=0.082 L=0.185	9.95×10^{-4} ±3.0%	0.31±0.01
2	Cylinder (Vertical configuration)	D=0.082, L=0.185	9.95×10^{-4} ±3.0%	0.31±0.01
3	Sphere	D=0.12m	9.05×10^{-4} ±3.0%	0.045±0.002

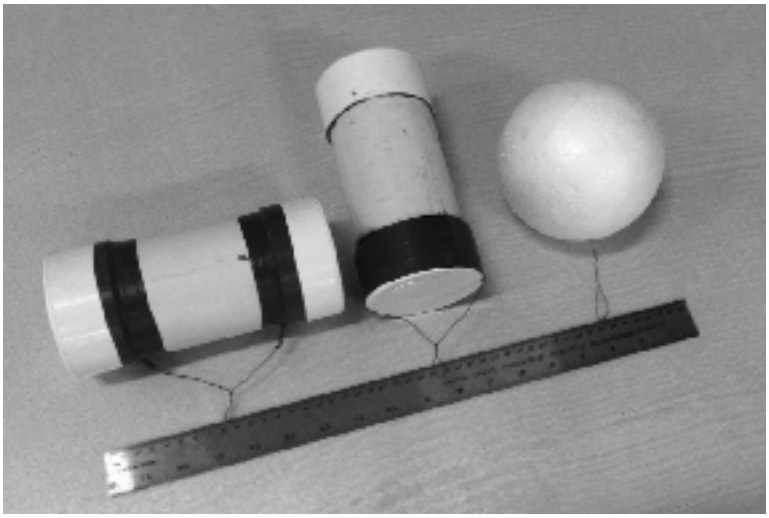

Figure 6-2 - Horizontal Cylinder, Vertical Cylinder, and Spherical floats used for experimentation

The tests were filmed such that charge and discharge durations could be determined as well as float behavior reviewed. Four trials for each load condition were performed.

6.4 - Results and Observations

6.4.1 - Discharge Testing

Discharge testing was completed by releasing the float line from the charge position with a load mass attached. The load mass was varied in order to establish the performance of each specific float throughout its loading range. Discharge testing was completed for static loads and discharge velocity and energy were calculated throughout the loading range. Results from single stage discharge testing is displayed in Figure 6-3 below.

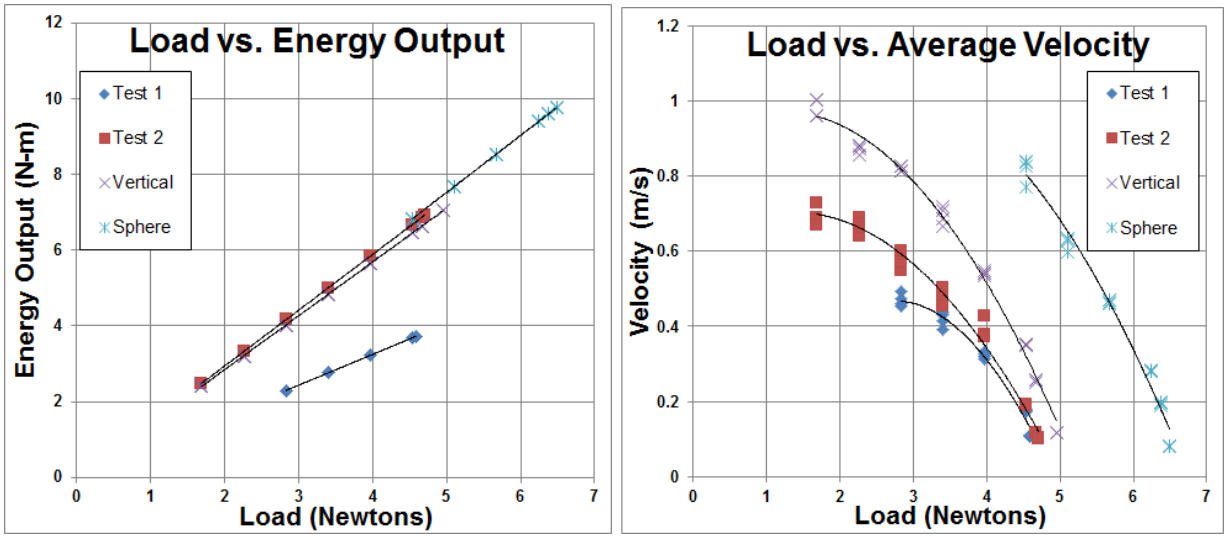

Figure 6-3 - Discharge testing results for energy output and average velocity across loading range.

Test 1 established the baseline for apparatus operation with the pulleys as built. After analyzing the results from the first trials, additional bushings were added to the conversion pulleys in order to reduce friction in the assembly. This improvement is evident in the increased energy output and float velocities achieved for Test 2. These results highlight the sensitivity of the apparatus to frictional losses within the pulleys.

For the second test, where the friction had been considerably reduced compared to Test 1, new float behavior was observed for the horizontally configured float. At low loading levels the float displayed a clear periodic displacement along the axis of the cylinders length. This pattern of motion works to increase the discharge time in comparison to a float which proceeds directly to

the surface. This behavior is consistent with the conservation of energy within the storage system. For the second and proceeding trials where wandering was observed, the frictional losses in the conversion between buoyancy potential energy and gravitational potential energy was low enough that the excess energy needed to be dissipated hydrodynamically through the fluid itself. Wandering motion was also evident for the spherical in the form of 3 dimensional displacement. The path of the sphere was helical in nature for low loading levels. For loading levels below 4.5 Newtons the spherical float moved with such a pronounced helix that it wrapped itself around the other end of the float line, thus fouling the discharge.

The vertical cylinder outperformed the horizontal with significantly higher float velocity and thus power output than the horizontal for equal loading condition. The discharge efficiency can be calculated using the theoretical energy input required to charge the system as expressed below.

$$E_{Ideal} = \rho V g - mg \qquad (2)$$

Using these calculated values the relationship between load, power output and discharge efficiency can be displayed as in Figure 6-4 below.

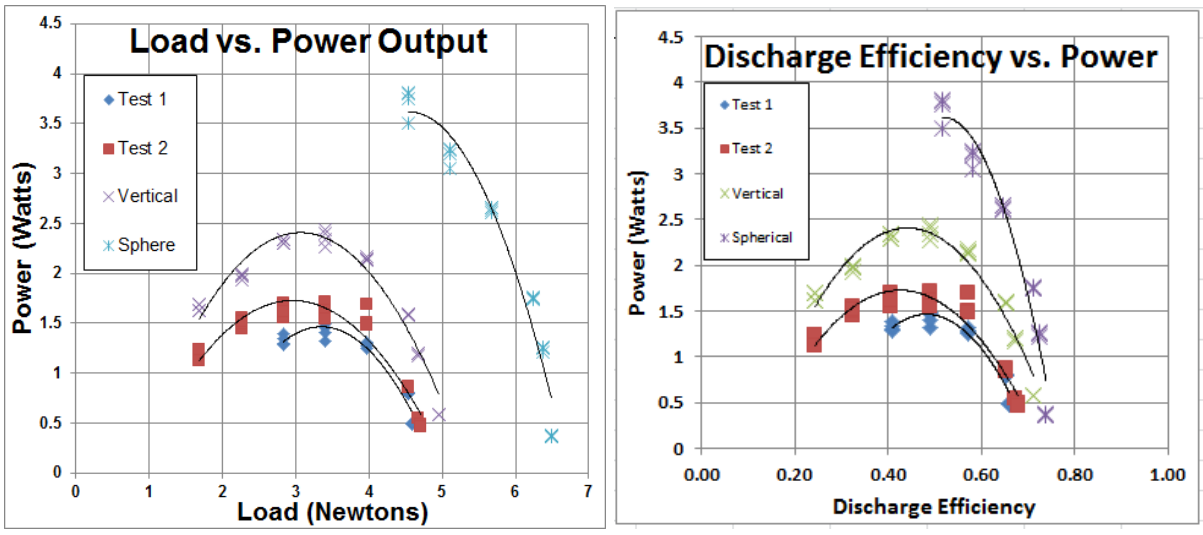

Figure 6-4 - Power curves displaying discharge performance for various floats

Based on these results from discharge testing there is a clear power curve which occurs through the loading range. Power output is dependant on both discharge force as well as discharge

velocity. At low load conditions the high velocity of the float contributes most to overall power. Where the output transitions between speed driven to force driven there is a maximum power point. Differences in the vertical and horizontal float results indicate this curve is affected by hydrodynamic drag forces.

In order to investigate the static efficiency of the experimental apparatus, the power curves can be modelled as a second order polynomial as depicted by the trend lines shown in Figure 6-3. By finding the roots of the trendline curves the maximum theoretical efficiency of the system can be estimated. This provides insight into the apparatus by setting the power output, and thus float velocity to zero - eliminating the effects of hydrodynamics. Results for discharge testing are summarized in Table 6-2. R^2 statistics for the polynomial trend lines used is also displayed.

Table 6-2 - Experimental and theoretically derived efficiencies for discharge testing

Test	**Trendline R^2**	**Maximum Theoretical Discharge Efficiency**	**Discharge Efficiency @ Maximum Power Point**	**Maximum Experimental Discharge Efficiency**
Horizontal 1	0.9411	76.1	50.5	66
Horizontal 2	0.9323	79.7	46.3	68
Vertical	0.9454	82.5	47.6	71
Sphere	0.9554	78.2	55.1	74

In terms of discharge efficiency the vertically configured cylinder performed better than the horizontally configured. The spherical float performed better than the vertical cylinder. These results are a significant improvement over previous experimental and open water testing results. The sphere also had the highest maximum power point. The R^2 values for the trend lines indicate that the polynomial power curves defined for determination of maximum discharge efficiency were a good fit for the data obtained.

6.4.2 - Charge Testing

The charge of the system is completed by adding a load weight greater than the net buoyancy force. The acceleration of the floats submersion will be proportional to the difference between the the load weight and the float net buoyancy force. System charging was completed with various loading conditions and results for energy input and average velocity are displayed in Figure 6-5.

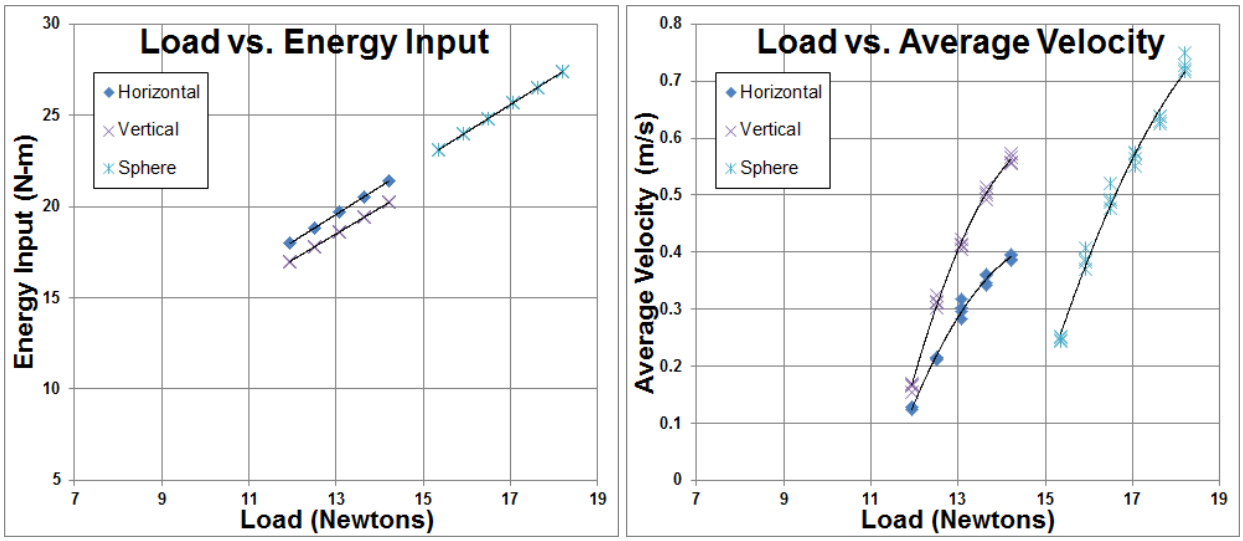

Figure 6-5 - Energy input and average float velocity through loading range for charge testing

The results indicate that the vertical configuration has significantly higher float velocity and thus power input than the horizontal configuration at equal load levels. This is consistent with discharge behavior. The load/ power input and efficiency/power input curves for charge are shown in Figure 6-6.

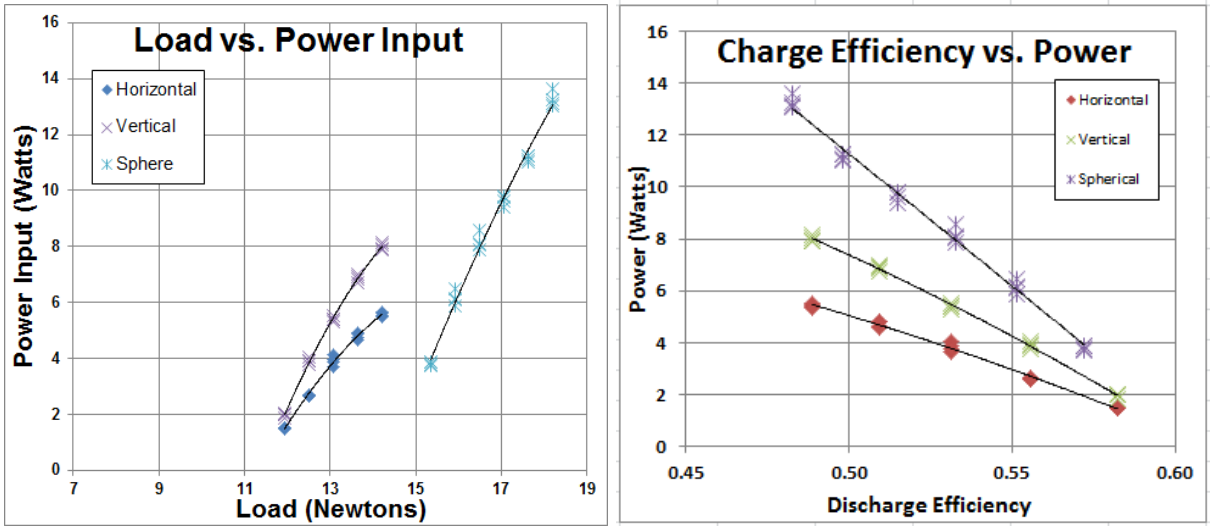

Figure 6-6 - Power and efficiency results for charge testing

Using a similar procedure as that of the discharge efficiency analysis the maximum theoretical charge efficiency can be compared to experimental charge efficiency as displayed in Table 6-3.

Table 6-3 - Experimental and theoretically derived efficiencies for charge testing

Test	**Trendline R^2**	**Maximum Theoretical Charge Efficiency**	**Maximum Experimental Charge Efficiency**
Horizontal	0.9946	61.2	58
Vertical	0.9979	61.5	58
Sphere	0.9926	62	57

6.4.3 - Roundtrip Efficiency

Using results from charge and discharge testing, the roundtrip efficiency obtained with each float can be calculated using equation 3 below.

$$\varepsilon = \frac{Energy\ Output}{Energy\ Input} = \varepsilon_{charge} * \varepsilon_{discharge} \qquad (3)$$

Roundtrip efficiency results are summarized in Table 6-4 below.

Table 6-4 - Roundtrip efficiency results for experiments performed. All efficiencies are reported as a percentage.

Test	Energy Input (N-M)	Energy Output (N-M)	Charge Efficiency	Discharge Efficiency	Experimental Roundtrip Efficiency	Theoretical Max Roundtrip Efficiency
Horizontal	17.56	6.93	58	68	39.44	45.82
Vertical	16.98	7.04	58	71	41.14	47.70
Sphere	23.1	9.77	58	74	42.23	45.60

The difference between the experimental and maximum theoretical roundtrip efficiencies represents the total losses to the other components of loss within the system, namely residual kinetic energy and hydrodynamic drag. These components are very minimal in comparison to pulley losses. This indicated that additional work could be done in reducing these pulley losses and thus a new pulley set-up was built and installed.

6.4.4 - Testing with ball-bearing conversion pulley system

In order to improve roundtrip efficiency, several modifications were made to the experimental system. The float line was reduced in size from the 4 mm diameter paracord used previously to a 0.3 mm diameter braided microfilament line. The anchorage pulley was also changed to a 2.5 cm diameter single sheave rope pulley of 50 kg working capacity. The reel pulleys were changed to 608 type, ABEC 7- equivalent ball bearings with urethane pulley forms.

Charge and discharge testing was repeated using the new apparatus with positive improvements in performance. Results for charge and discharge testing are displayed below. The new efficiency results are shown in Table 6-5.

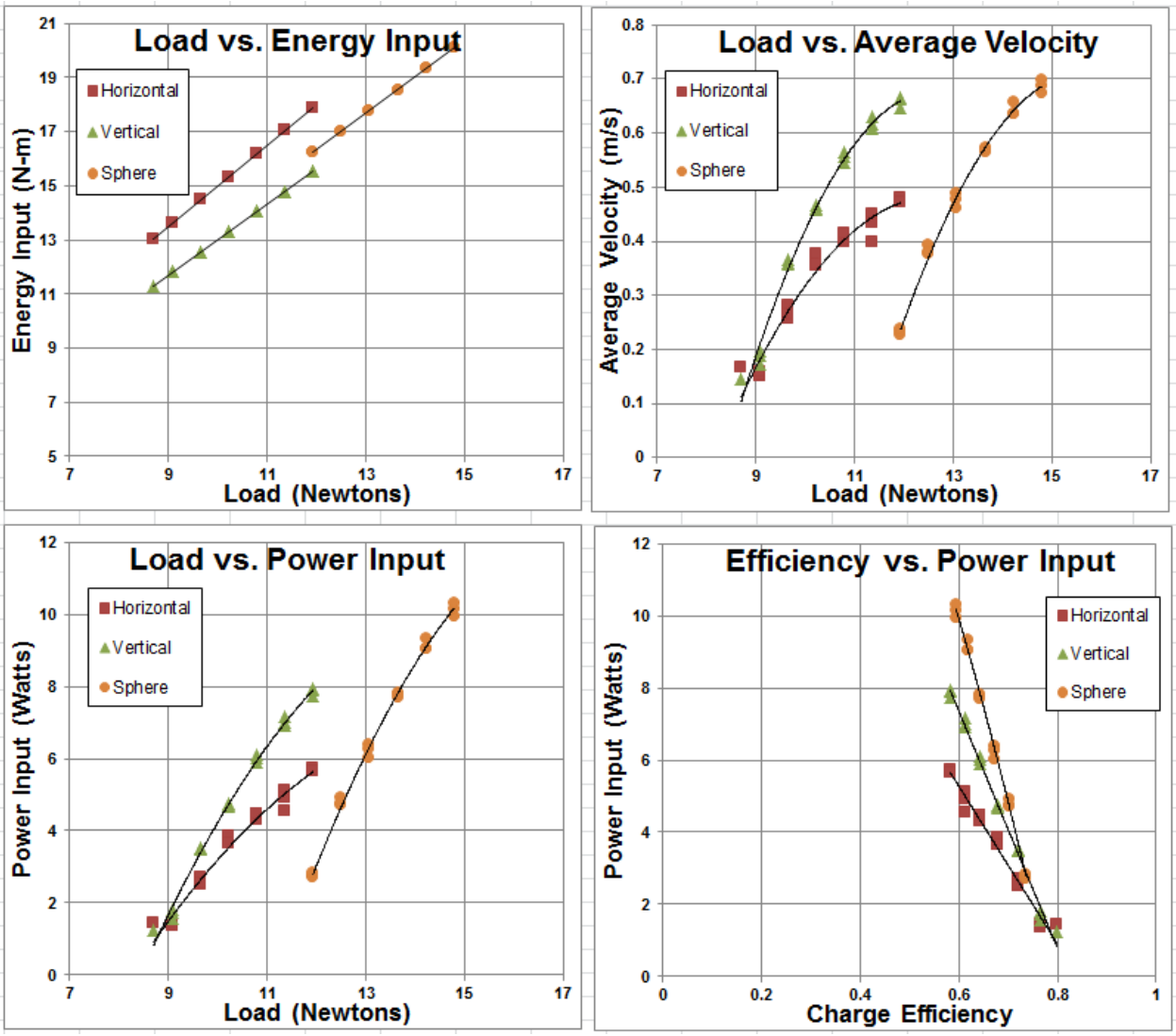

Figure 6-7 - Charge Results for improved experimental system featuring ball-bearing pulleys

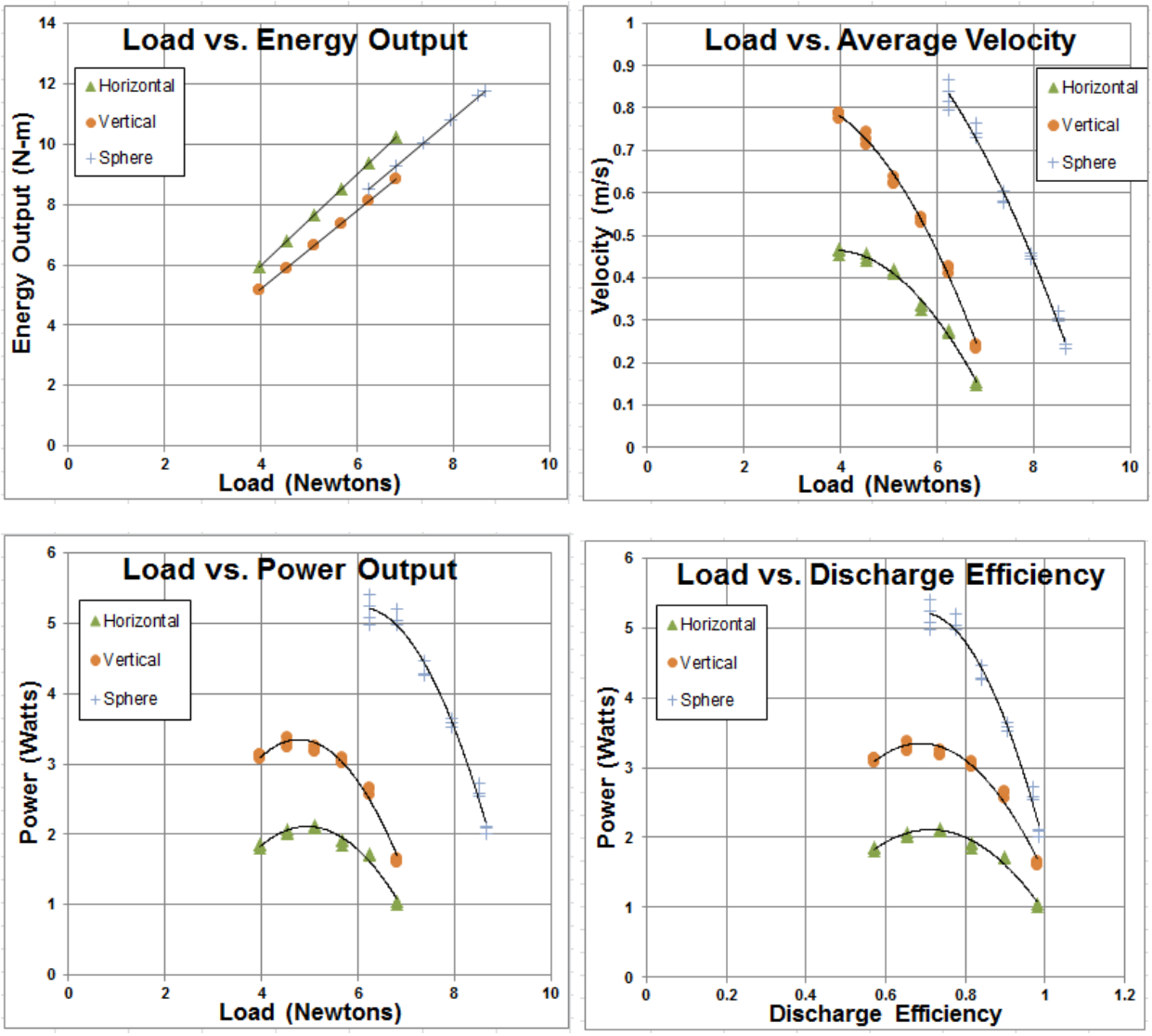

Figure 6-8 - Discharge Results for improved experimental system featuring ball-bearing pulleys

Table 6-5 - Roundtrip efficiency results for experiments performed. All efficiencies are reported as a percentage.

Test	Energy Input (N-M)	Energy Output (N-M)	Charge Efficiency	Discharge Efficiency	Experimental Roundtrip Efficiency
Horizontal	13.05	10.22	79.88	98.03	78.31
Vertical	11.31	8.86	79.88	98.03	78.33
Sphere	16.23	11.76	73.66	98.4	72.45

Results from the repeated tests show significant improvements in both experimental roundtrip efficiency as well as power curve characteristics for each of the floats tested. Power output at maximum efficiency loading has also increased. These results highlight the importance of proper mechanical drivetrain components. One challenge encountered during new trails was oxidization of the subsurface anchor pulley which occurred between the cylinder tests and the sphere test. The cylinders had been tested on the same day, the sphere was tested 30 days later. During that period oxidation appeared the subsurface pulley. The pulley was removed from the water, cleaned and lubricated. Despite these remediation methods, the pulley could not achieve equivalent friction levels which were evident for the cylinder trials. This highlights that the quality of the subsurface pulley has significant effects on the repeatability of the systems performance.

6.5 - Conclusions

Buoyancy energy storage has been tested under mechanical loading of various stages and load masses. Various floats were tested to investigate the influence of float geometry on system performance.

Results from discharge testing represented a significant improvement in performance over previous tests. System performance was found to be highly sensitive to pulley friction and additional bushings within the conversion pulleys resulted in a 2% increase in discharge efficiency. Power output results display a parabolic relationship with loading. By determining a trendline for each trial and solving for the real root, the maximum theoretical efficiency for the system was calculated for each float condition. The vertically configured cylindrical float displayed a 2% improvement over the horizontally configured float of the same volume and mass.

The discovered relationship between efficiency and power output is significant as it highlights that BBES system design must account not only for overall efficiency but also the efficiency for the floats maximum power point.

At low load levels, the horizontally configured float displayed 2 dimensional periodic displacement in the plane parallel to the free surface of the water. The sphere displayed a helical path of motion when discharged under low loading condition. For practical system design, this motion is highly undesirable as it decreases float velocity and thus power.

Results from charge testing stand as a baseline for charge performance as the charge operation had not been studied before these experiments. The system performance for charge was significantly worse than the discharge performance which implies that there is a problem with the pulleys within the apparatus operating well in both directions. Experimental charge efficiencies were practically equal for each of the three floats tested.

Based on charge and discharge performance the roundtrip efficiencies of each float has been calculated. Roundtrip efficiencies were similar across the three float samples in the range of 40%

which is encouraging considering the disproportionately high pulley losses. Experimental results were very close to the determined theoretical maximum efficiencies. Results from first efficiency analysis indicated that the mechanical system was not operating at high efficiency and thus the mechanical components including the float line, anchorage pulley, and reel pulleys were changed in favor of lower friction units. This resulted in drastic increases in roundtrip efficiency and power output performance. The newly obtained 78% experimental roundtrip efficiency is significant in comparison to the efficiencies of competing technologies, particularly UWCAES which has a maximum theoretical efficiency limit of 68% [1].

Evaluating the performance of the BBES system under mechanical loading is highly useful in isolating and comparing float behavior under different loading conditions. Observations from these tests can be used to inform system design when scaled to greater storage and power output capacities.

Future work in improving the efficiency of the apparatus mechanical assembly should be completed, as it was the primary source of loss for both the charge and discharge operation. With an improved pulley configuration, experimental results should confirm that roundtrip efficiencies greater than 80% are possible for BBES. This is consistent with calculated theoretical values for the 1 MWh Buoyancy system described in Chapter 4. Improved mechanical performance will also allow for more accurate evaluation and comparison of performance of advanced float shapes and configurations. Other methods of improving roundtrip efficiency worth investigating include multi-stage loading which would allow for the recovery of residual kinetic energy losses which were present for charge and discharge experiments.

References

[1] Cheung, Brian, et al. "Distensible air accumulators as a means of adiabatic underwater compressed air energy storage." International Journal of Environmental Studies 69.4 (2012): 566-577.

[2] Blackwell R., "Hydrostor launching compressed air power storage off Toronto Island" The Globe and Mail, November 17, 2015.
http://www.theglobeandmail.com/report-on-business/industry-news/energy-and-resources/hydrostor-launches-compressed-air-power-storage-system-off-toronto-island/article27306527/ Accsesed online February 2, 2016

[3] Slocum, A.H.; Fennell, G.E.; Dundar, G.; Hodder, B.G.; Meredith, J.D.C.; Sager, M.A., "Ocean Renewable Energy Storage (ORES) System: Analysis of an Undersea Energy Storage Concept", *Proceedings of the IEEE* , Voume.101, Issue.4, April 2013, Pages 906-924.

[4] Slocum, A., Gregory H., Fennell E. , and Alison S. Greenlee. "Offshore energy harvesting, storage, and power generation system." U.S. Patent No. 8,698,338. 15 Apr. 2014.

[5] Morgan, J.P., "Buoyancy energy storage and generation", US Patent US 20100107627 A1. 6 May 2010

[6] Alami, A., "Analytical and experimental evaluation of energy storage using work of buoyancy force", Journal of Renewable and Sustainable Energy Volume 6, Issue 1, 2014, Pages 131-137.

[7] Alami, A.,, Experimental assessment of compressed air energy storage (CAES) system and buoyancy work energy storage (BWES) as cellular wind energy storage options, Journal of Energy Storage, Volume 1, June 2015, Pages 38-43.

[8] Bassett, K., Carriveau, R., Ting D., "Energy Storage through application of archimedes principle" Journal of Energy Storage. Volume 8, Pages 185-192, November 2016

[9] Bassett, K., Carriveau, R., Ting D., "Experimental Analysis of Buoyancy Energy Storage," IET Renewable Power Generation. Volume 10, Issue 10, Pages 1523-1528, November 2016

Chapter 7

Conclusions and Suggestions for Future Work

7.1 - Summary

Fundamental Properties of BBES which have been established are summarized below.

- BBES has been proven as a functional means of energy storage in the marine environment through lab and field experimentation
- Energy stored is non-dissipative and thus the life of a BBES system will depend on the lifecycle of the specific mechanical and electrical components which make up the system
- Charge and discharge power levels can be controlled through variable loading conditions
- Highly scaleable as primary components air and water are in abundance on the planet
- No thermodynamic processes are required for storage allowing for high theoretical round trip efficiencies in comparison to competing UWCAES technology

The integration and scaling characteristics which have been determined are summarized below.

- A 1 MW, 1 MWh BBES system has been developed featuring a cylindrical float array operating in 100 m water depth
- The developed system has a theoretical round trip efficiency of 82% when using high performance components
- Drag effects can be significant at high float speeds but are minimal for float velocities of interest at utility scale (0.2 m/s)
- Residual energy loss during charge and discharge is minimal but can be eliminated through multi-stage loading

Key points regarding the opportunities for Energy storage facilities to operate in Ontario include;

- Motivation for the integration of grid-scale energy storage in Ontario is related to the reduction in economic loss which occurs when intermittent generation exceeds the required 1400 MW spinning reserve
- Trends indicate that this situation of loss due to excess generation will increase in severity as energy price global adjustment and installation of intermittent generators rise.
- Based on 2015 data, the revenue potential for a facility through energy arbitrage is minimal when trading through hourly ontario energy prices.
- Energy storage facilities can operate to perform regulation services in conjunction with the IESO and data suggests that the income through this service greatly outweighs that of energy arbitrage alone
- There is a significant challenge in monetizing and quantifying the benefits of grid integrated energy storage

Key points from experimental analysis of BBES under mechanical loading are summarized below.

- When tested under mechanical loading, system performance is highly sensitive to friction effects of the pulleys
- At low load condition the horizontally configured cylinder displayed periodic displacement in plane parallel to faces of cylinder
- At low load conditions the spherical float displayed periodic displacement in the form of a helix
- The vertically configured float performs better than the horizontally configured float of the same float volume and mass
- Roundtrip Efficiencies of 78% are obtainable when system composed of high performance mechanical components

7.2 - Suggestions for Future Work

While the research documented in this dissertation represents significant contributions to establishing BBES as a practical and effective form of energy storage, future research in development of the concept is still required. Areas for future work are outlined below

- Expansion of experimental performance dataset to include advanced float geometries for reduced drag losses and improved maximum power point
- Cost and feasibility analysis of various float geometries and float manufacturing methods to determine what shapes and constructions are practical at utility scale energy storage
- Determination of the hydrodynamic performance improvements , if any, which occur when the connection between the float and float line is a swivel connection
- Installation and evaluation of BBES system on a larger scale in controlled outdoor marine environment
- Improved collaboration and coordination between Canadian energy storage researchers and the electrical grid authorities with jurisdiction in order to accelerate integration of grid-scale energy storage

APPENDIX A

Symbols, Abbreviations, and Nomenclature

Chapter 2

A	Float Frontal Area (m^2)
BBES	Buoyancy Battery Energy Storage
CAES	Compressed air energy storage
C	Cable tensions (Newtons)
C_D	Drag Coefficient
D	Water Depth (m)
E	Energy (Joules)
E_{charge}	Charge Energy (Joules)
$E_{discharge}$	Discharge Energy (Joules)
E_{drag}	Drag Energy Loss (Joules)
E_{elec}	Electrical Energy Loss (Joules)
ES	Energy Storage
E_{ideal}	Ideal storage limit (Joules)
FES	Flywheel Energy Storage
F_b	Buoyancy Force (Newtons)
F_d	Drag Force (Newtons)

$F_{discharge}$	Discharge Force (Newtons)
g	gravitational acceleration
I	Current (amps)
J	Joule
m	Float mass (grams)
M	Anchor mass
N	Number of reel revolutions
P	Power (Watts)
P_{charge}	Charge Power level (Watts)
$P_{discharge}$	Discharge Power level (Watts)
Q	Electric motor voltage
r	Reel radius (m)
R	Resistance (Ohms)
RE	Renewable Energy
REV	Charge Revolutions
t	Time (seconds)
t_{charge}	Charge Time
$t_{discharge}$	Discharge Time
T_a	Applied Torque
UWCAES	Underwater compressed energy storage

v	Float volume (m^3)
$V_{ambient}$	Ambient Fluid Velocity (m/s)
V_c	Charge Velocity (m/s)
V_{dc}	Discharge Velocity (m/s)
W	Watt
Wh	Watt hour
Z	Vertical Displacement of float (m)
Z_{charge}	Charge displacement (m)
$Z_{discharge}$	Discharge Displacement (m)
ρ	Ambient fluid density
η	Efficiency

Chapter 3

Ar	Ambient Ratio
C	Cable tension (Newtons)
C_D	Drag Coefficient
D	Water depth
H	Float Height
g	gravitational acceleration
m	Float mass (grams)

v	Float velocity
V	Float volume (m^3)
V_a	Ambient fluid volume
$E_{Discharge}$	Discharge Energy
Z_{Charge}	Charge Distance
E_{Ideal}	Ideal energy storage capacity
ρ	Ambient fluid density
Cr	Charge Ratio
Ar	Ambient Ratio
E_{input}	Input Energy
$E_{Residual\ Kinetic}$	Residual Kinetic Energy
E_{drag}	Drag Energy
$E_{Friction}$	Friction Energy
E_{Output}	Energy output

Chapter 4

BBES - Buoyancy Based Energy Storage

Cd - Drag Coefficient

EPP- Energy Purchase Price

HOEP - Hourly Ontario Energy Price

IESO - Independent energy service operator

M - Float mass

N- Number of floats in array

P - Generator Power

PO - Price Opportunity

R - Revenue

RR - Revenue Rate

RS - Net Storage Revenue

ROV - Robotic Autonomous Vehicle

U - Float Velocity

V - Float volume

η - Efficiency

Chapter 5

A- Actual revenue generated

B- Total benefit

C- ESP performance coefficient

E- Energy

ES- Energy Storage

ESP - Energy Storage Program

FFT- Fast Fourier Transform

GA- Global Adjustment

GAEP- Global Adjustment Energy Price

HOEP - Hourly Ontario Energy Price

IESO- Independent Energy Service Operator

L-	Economic Loss
P-	Price
PO-	Price Opportunity
PO_{MA} -	Maximum Price Opportunity Program
SBG-	Surplus Baseload Generation
VG -	Variable Generator

Chapter 6

$E_{Residual}$	Residual Kinetic Energy
m	Float mass (grams)
v	Float velocity
V	Float volume (m^3)
ρ	Ambient fluid density
Z	Charge distance
ε	Efficiency
ε_{charge}	Charge Efficiency
$\varepsilon_{discharge}$	Discharge Efficiency

Appendix B

Experimental Procedures

Discharge Testing - Chapter 3

1) Generator is connected to resistive load
2) Buoyancy system is charged manually to charge depth of 1.67m.
3) Gopro recording is initiated
4) Buoyancy system is unlocked - float rises
5) Voltage output from generator is recorded
6) Repeat process 3 times for each resistive load and record results

Open Water Testing - Chapter 4

1) Generator is connected to resistive load
2) Buoyancy system is charged by connecting a cordless drill to the output shaft of reel generator
3) Output shaft is connected to the cord reel
4) Load Cell attached to cord
5) Discharge force is measured and recorded
6) Stopwatch is started immediately as buoyancy system is unlocked - float rises
7) Voltage output from generator is recorded
8) Stopwatch is stopped immediately as the float can be seen to penetrate water surface

Mechanical Load Testing - Chapter 6

Charge Testing

1) Float begins from water surface
2) Charge depth is measured
3) Load mass is added until point at which float begins descending
4) Float is returned to water surface
5) High speed recording is initiated
6) Load mass is released - float descends
7) Float is returned to water surface
8) Load mass is increased
9) Load mass is released - float descends
10) Process is repeated for load mass range of interest

Discharge Testing

1) Float begins from fully submerged position
2) Discharge depth is measured
3) Load mass is removed until point at which float begins ascending
4) Float is returned to fully submerged position
5) High speed recording is initiated
6) Load mass is released - float ascends
7) Float is returned to water surface
8) Load mass is decreased
9) Load mass is released - float ascends
10) Process is repeated for load mass range of interest

Appendix C

Data Tables for Experimental Results

C.1 - Data Tables Static Testing

Table C1 - Data for Figure 2-4. Depth vs. Discharge

Depth (m)	Force (N)
0	0
0.1	23
0.2	58
0.3	75
0.4	108.25
0.5	108.9
0.6	108.6
0.7	108.7
0.8	108.5
0.9	108.7
1	108.9
1.1	109.01
1.2	109
1.3	108.8
1.4	108.8
1.5	108.7
1.6	108.9
1.7	108.9
1.8	108.8
1.9	108.7
2	109

Table C2 - Data for Figure 2-5. Discharge force vs. time

Time (hrs)	Force (N)
0.5	38.8
1	38.7
1.5	38.9
2	38.9
2.5	38.7
3	38.8
3.5	38.7
4	38.9
4.5	38.6
5	38.7
5.5	38.8
6	38.9
6.5	38.8
7	38.8
7.5	38.9
8	38.7
8.5	38.8
9	38.9
9.5	38.7
10	38.9

Table C3 - Resistance vs. Discharge Time for proof of concept testing

Resistance (Ohms)	Discharge Time (s)
99	21.1
220	17
436	12
896	8.2
1356	6.1
1976	5.5
2205	4.8
2950	4.1
3930	3.6
9900	2.8

Table C4 - Resistance vs. Maximum Discharge Voltage for proof of concept testing..

Resistance (Ohms)	Discharge Voltage
99	1.2
220	2.35
436	4.6
896	9.4
1356	13.3
1976	18.3
2205	20.1
2950	23
3930	27.1
9900	35

Table C5 - Maximum Output Power vs. Resistance for proof of concept testing.

Resistance (Ohms)	Average Power (Watts)
99	0.0145
220	0.0251
436	0.0485
896	0.0986
1356	0.1304
1976	0.1695
2205	0.1832
2950	0.1793
3930	0.1869
9900	0.1237

Table C6 - Maximum Output Energy vs. Resistance for proof of concept testing.

Resistance (Ohms)	Energy Output (Joules)
99	0.3069
220	0.4267
436	0.5824
896	0.8087
1356	0.7957
1976	0.9321
2205	0.8795
2950	0.7352
3930	0.6727
9900	0.3465

C.3 - Data for Spherical Discharge Testing

Primary observations for spherical discharge testing was voltage output from generator and discharge time. Raw data from trials is presented in table below.

Table C7 - Spherical float testing properties

Parameter	Value
Float Mass	0.454 kg
Float Radius	0.15 m
Float Volume	0.014 m^3
Float Frontal Area	0.07065 m^2
Charge Depth	1.67 m

Three trials were performed for each of the loading conditions raw data from each trial is displayed below.

Table C8 - Results from spherical float discharge testing

Load (OHMS)	Discharge Time	Voltage
0	0.79	93.2
0	0.71	84.9
0	0.74	86.8
8	1.58	17.9
8	1.45	19.7
8	1.49	22.1
11.4	1.08	34.4
11.4	1.01	32.6
11.4	1.06	27.6
14.3	1.06	39.6
14.3	0.99	35.9
14.3	1.1	36.9

Table C9 - Calculated results for discharge testing

Load (OHMS)	Voltage (v)	Power (W)	Discharge Time (s)	Average Velocity (m/s)	Exit Velocity (m/s)
0	88.3	0.0	0.75	2.23	4.45
8	19.9	49.5	1.51	1.11	2.21
11.4	31.5	87.0	1.04	1.61	3.21
14.3	37.5	98.3	1.03	1.62	3.24

C.4 - Data for Open Water Testing

Table C10 - Properties of float array

Parameter	Value
Float Mass	1.31 kg
Tube Radius	0.038 m
Tubes per float	3
Float Volume	0.0115 m^3
Discharge Force	100.2

Table C11 - Results for open water testing

Load Resistance	Voltage (v)	Disharge Duration (s)	Velocity (m/s)	Power (W)	Theoretical Power (W)
0	0	6.5	0.91	0.00	0.00
34.1	13.5	25	0.24	5.34	23.65
27	12.5	24	0.25	5.79	24.63
20	8	27	0.22	3.20	21.90

C.5 - Data for Mechanical Loading Tests Chapter 6

Table C12 - Operating distances for mechanical loading tests

Test	Operating Distance (m)
Original Apparatus	
Test 1 (horizontal)	0.81
Test 2 (horizontal)	1.47
Vertical	1.42
Spherical	1.51
Improved Pulley Apparatus	
Horizontal	1.50
Vertical	1.31
Sphere	1.36

Table C13 - Results for Horizontal Discharge "Test 1"

Horizontal Discharge Test 1

Load (kg)	Load (N)	Time (s)	Discharge (m)	Average Velocity (m/s)	Energy Output (N-M)	Power (W)	Input Energy (N-M)	Discharge Efficiency
0.29	2.83	1.77	0.81	0.459	2.30	1.30	5.64	0.41
0.29	2.83	1.79	0.81	0.454	2.30	1.28	5.64	0.41
0.29	2.83	1.65	0.81	0.492	2.30	1.39	5.64	0.41
0.29	2.83	1.71	0.81	0.475	2.30	1.34	5.64	0.41
0.35	3.40	1.89	0.81	0.430	2.76	1.46	5.64	0.49
0.35	3.40	2.08	0.81	0.390	2.76	1.33	5.64	0.49
0.35	3.40	1.85	0.81	0.439	2.76	1.49	5.64	0.49
0.35	3.40	1.96	0.81	0.414	2.76	1.41	5.64	0.49
0.41	3.97	2.54	0.81	0.320	3.22	1.27	5.64	0.57
0.41	3.97	2.49	0.81	0.326	3.22	1.29	5.64	0.57
0.41	3.97	2.58	0.81	0.315	3.22	1.25	5.64	0.57
0.41	3.97	2.45	0.81	0.331	3.22	1.32	5.64	0.57
0.46	4.54	4.66	0.81	0.174	3.69	0.79	5.64	0.65
0.46	4.54	4.64	0.81	0.175	3.69	0.79	5.64	0.65
0.46	4.54	4.55	0.81	0.178	3.69	0.81	5.64	0.65
0.47	4.58	7.67	0.81	0.106	3.72	0.49	5.64	0.66
0.47	4.58	7.49	0.81	0.108	3.72	0.50	5.64	0.66
0.47	4.58	7.45	0.81	0.109	3.72	0.50	5.64	0.66

Table C14 - Results for Horizontal Discharge "Test 2"

Horizontal Discharge Test 2

Load (kg)	Load (N)	Time (s)	Discharge	Average Velocity (m/s)	Energy (N-M)	Power (W)	Input Energy	Discharge Efficiency
0.17	1.69	2.02	1.47	0.73	2.49	1.23	10.23	0.24
0.17	1.69	2.14	1.47	0.69	2.49	1.16	10.23	0.24
0.17	1.69	2.02	1.47	0.73	2.49	1.23	10.23	0.24
0.17	1.69	2.2	1.47	0.67	2.49	1.13	10.23	0.24
0.23	2.26	2.14	1.47	0.69	3.33	1.55	10.23	0.33
0.23	2.26	2.3	1.47	0.64	3.33	1.45	10.23	0.33
0.23	2.26	2.22	1.47	0.66	3.33	1.50	10.23	0.33
0.23	2.26	2.19	1.47	0.67	3.33	1.52	10.23	0.33
0.29	2.83	2.52	1.47	0.58	4.16	1.65	10.23	0.41
0.29	2.83	2.68	1.47	0.55	4.16	1.55	10.23	0.41
0.29	2.83	2.45	1.47	0.60	4.16	1.70	10.23	0.41
0.29	2.83	2.58	1.47	0.57	4.16	1.61	10.23	0.41
0.35	3.40	2.92	1.47	0.50	5.00	1.71	10.23	0.49
0.35	3.40	3.12	1.47	0.47	5.00	1.60	10.23	0.49
0.35	3.40	3.08	1.47	0.48	5.00	1.62	10.23	0.49
0.35	3.40	3.24	1.47	0.45	5.00	1.54	10.23	0.49
0.40	3.97	3.95	1.47	0.37	5.84	1.48	10.23	0.57
0.40	3.97	3.45	1.47	0.43	5.84	1.69	10.23	0.57
0.40	3.97	3.88	1.47	0.38	5.84	1.51	10.23	0.57
0.40	3.97	3.95	1.47	0.37	5.84	1.48	10.23	0.57
0.46	4.54	7.8	1.47	0.19	6.68	0.86	10.23	0.65
0.46	4.54	7.85	1.47	0.19	6.68	0.85	10.23	0.65
0.46	4.54	7.65	1.47	0.19	6.68	0.87	10.23	0.65
0.48	4.67	12.47	1.47	0.12	6.87	0.55	10.23	0.67
0.48	4.67	12.65	1.47	0.12	6.87	0.54	10.23	0.67
0.48	4.67	12.62	1.47	0.12	6.87	0.54	10.23	0.67
0.48	4.71	14.1	1.47	0.10	6.93	0.49	10.23	0.68
0.48	4.71	14.8	1.47	0.10	6.93	0.47	10.23	0.68

Table C15 - Results for Vertical Discharge Test

Vertical Discharge

Load (kg)	Load (N)	Time (s)	Discharge	Average Velocity (m/s)	Energy (N-M)	Power (W)	Input Energy	Discharge Efficiency
0.17	1.69	1.48	1.42	0.96	2.40	1.62	9.89	0.24
0.17	1.69	1.48	1.42	0.96	2.40	1.62	9.89	0.24
0.17	1.69	1.42	1.42	1.00	2.40	1.69	9.89	0.24
0.17	1.69	1.42	1.42	1.00	2.40	1.69	9.89	0.24
0.23	2.2593	1.62	1.42	0.88	3.21	1.98	9.89	0.33
0.23	2.2593	1.66	1.42	0.86	3.21	1.94	9.89	0.33
0.23	2.2593	1.61	1.42	0.88	3.21	2.00	9.89	0.33
0.23	2.2593	1.63	1.42	0.87	3.21	1.97	9.89	0.33
0.29	2.8286	1.75	1.42	0.81	4.02	2.30	9.89	0.41
0.29	2.8286	1.72	1.42	0.83	4.02	2.34	9.89	0.41
0.29	2.8286	1.75	1.42	0.81	4.02	2.30	9.89	0.41
0.29	2.8286	1.72	1.42	0.83	4.02	2.34	9.89	0.41
0.35	3.3979	2.13	1.42	0.67	4.83	2.27	9.89	0.49
0.35	3.3979	2.07	1.42	0.69	4.83	2.34	9.89	0.49
0.35	3.3979	1.98	1.42	0.72	4.83	2.44	9.89	0.49
0.35	3.3979	2.01	1.42	0.71	4.83	2.40	9.89	0.49
0.40	3.9672	2.63	1.42	0.54	5.64	2.15	9.89	0.57
0.40	3.9672	2.6	1.42	0.55	5.64	2.17	9.89	0.57
0.40	3.9672	2.63	1.42	0.54	5.64	2.15	9.89	0.57
0.40	3.9672	2.65	1.42	0.54	5.64	2.13	9.89	0.57
0.46	4.5365	4.04	1.42	0.35	6.45	1.60	9.89	0.65
0.46	4.5365	4.09	1.42	0.35	6.45	1.58	9.89	0.65
0.46	4.5365	4.05	1.42	0.35	6.45	1.59	9.89	0.65
0.48	4.67	5.55	1.42	0.26	6.64	1.20	9.89	0.67
0.48	4.67	5.67	1.42	0.25	6.64	1.17	9.89	0.67
0.48	4.67	5.55	1.42	0.26	6.64	1.20	9.89	0.67
0.51	4.95	12.02	1.42	0.12	7.04	0.59	9.89	0.71
0.51	4.95	12	1.42	0.12	7.04	0.59	9.89	0.71

Table C16 - Results for Spherical Discharge Test

Sphere Discharge

Load (kg)	Load (N)	Time (s)	Discharge	Average Velocity (m/s)	Energy (N-M)	Power (W)	Input Energy	Discharge Efficiency
0.46	4.54	1.82	1.51	0.83	6.83	3.75	13.22	0.52
0.46	4.54	1.95	1.51	0.77	6.83	3.50	13.22	0.52
0.46	4.54	1.79	1.51	0.84	6.83	3.81	13.22	0.52
0.46	4.54	1.8	1.51	0.84	6.83	3.79	13.22	0.52
0.52	5.11	2.52	1.51	0.60	7.68	3.05	13.22	0.58
0.52	5.11	2.37	1.51	0.64	7.68	3.24	13.22	0.58
0.52	5.11	2.4	1.51	0.63	7.68	3.20	13.22	0.58
0.52	5.11	2.38	1.51	0.63	7.68	3.23	13.22	0.58
0.58	5.68	3.21	1.51	0.47	8.54	2.66	13.22	0.65
0.58	5.68	3.25	1.51	0.46	8.54	2.63	13.22	0.65
0.58	5.68	3.27	1.51	0.46	8.54	2.61	13.22	0.65
0.58	5.68	3.21	1.51	0.47	8.54	2.66	13.22	0.65
0.64	6.24	5.39	1.51	0.28	9.40	1.74	13.22	0.71
0.64	6.24	5.32	1.51	0.28	9.40	1.77	13.22	0.71
0.64	6.24	5.38	1.51	0.28	9.40	1.75	13.22	0.71
0.64	6.24	5.35	1.51	0.28	9.40	1.76	13.22	0.71
0.65	6.38	7.9	1.51	0.19	9.60	1.22	13.22	0.73
0.65	6.38	7.68	1.51	0.20	9.60	1.25	13.22	0.73
0.65	6.38	7.59	1.51	0.20	9.60	1.26	13.22	0.73
0.65	6.38	7.65	1.51	0.20	9.60	1.25	13.22	0.73
0.66	6.49	18.43	1.51	0.08	9.77	0.37	13.22	0.74
0.66	6.49	18.25	1.51	0.08	9.77	0.37	13.22	0.74
0.66	6.49	18.55	1.51	0.08	9.77	0.37	13.22	0.74
0.66	6.49	18.35	1.51	0.08	9.77	0.37	13.22	0.74

Table C17 - Results for Horizontal Charge Test

Horizontal Charge Test 2								
Load (kg)	Load (N)	Time (s)	Discharge	Average Velocity	Energy N-M	Power	Input Energy	Charge Efficiency
1.22	11.94	11.75	1.47	0.13	17.57	1.50	10.23	0.58
1.22	11.94	11.82	1.47	0.12	17.57	1.49	10.23	0.58
1.22	11.94	12.07	1.47	0.12	17.57	1.46	10.23	0.58
1.22	11.94	11.82	1.47	0.12	17.57	1.49	10.23	0.58
1.28	12.51	7	1.47	0.21	18.41	2.63	10.23	0.56
1.28	12.51	6.97	1.47	0.21	18.41	2.64	10.23	0.56
1.28	12.51	7.09	1.47	0.21	18.41	2.60	10.23	0.56
1.28	12.51	7.1	1.47	0.21	18.41	2.59	10.23	0.56
1.33	13.08	4.74	1.47	0.31	19.25	4.06	10.23	0.53
1.33	13.08	4.97	1.47	0.30	19.25	3.87	10.23	0.53
1.33	13.08	5.3	1.47	0.28	19.25	3.63	10.23	0.53
1.33	13.08	5.1	1.47	0.29	19.25	3.77	10.23	0.53
1.39	13.65	4.16	1.47	0.35	20.09	4.83	10.23	0.51
1.39	13.65	4.34	1.47	0.34	20.09	4.63	10.23	0.51
1.39	13.65	4.4	1.47	0.33	20.09	4.56	10.23	0.51
1.39	13.65	4.2	1.47	0.35	20.09	4.78	10.23	0.51
1.45	14.21	3.88	1.47	0.38	20.92	5.39	10.23	0.49
1.45	14.21	3.82	1.47	0.39	20.92	5.48	10.23	0.49
1.45	14.21	3.79	1.47	0.39	20.92	5.52	10.23	0.49
1.45	14.21	3.9	1.47	0.38	20.92	5.37	10.23	0.49

Table C18 - Results for Vertical Charge Test

Vertical Charge								
Load (kg)	Load (N)	Time (s)	Discharge	Average Velocity	Energy (N-M)	Power (W)	Input Energy	Charge Efficiency
1.22	11.94	9.17	1.423	0.16	16.98	1.85	9.89	0.58
1.22	11.94	8.39	1.423	0.17	16.98	2.02	9.89	0.58
1.22	11.94	8.49	1.423	0.17	16.98	2.00	9.89	0.58
1.22	11.94	8.57	1.423	0.17	16.98	1.98	9.89	0.58
1.28	12.51	4.39	1.423	0.32	17.79	4.05	9.89	0.56
1.28	12.51	4.55	1.423	0.31	17.79	3.91	9.89	0.56
1.28	12.51	4.56	1.423	0.31	17.79	3.90	9.89	0.56
1.28	12.51	4.71	1.423	0.30	17.79	3.78	9.89	0.56
1.33	13.08	3.45	1.423	0.41	18.60	5.39	9.89	0.53
1.33	13.08	3.44	1.423	0.41	18.60	5.41	9.89	0.53
1.33	13.08	3.37	1.423	0.42	18.60	5.52	9.89	0.53
1.33	13.08	3.51	1.423	0.41	18.60	5.30	9.89	0.53
1.39	13.65	2.89	1.423	0.49	19.41	6.72	9.89	0.51
1.39	13.65	2.77	1.423	0.51	19.41	7.01	9.89	0.51
1.39	13.65	2.81	1.423	0.51	19.41	6.91	9.89	0.51
1.39	13.65	2.84	1.423	0.50	19.41	6.83	9.89	0.51
1.45	14.21	2.55	1.423	0.56	20.22	7.93	9.89	0.49
1.45	14.21	2.51	1.423	0.57	20.22	8.06	9.89	0.49
1.45	14.21	2.48	1.423	0.57	20.22	8.15	9.89	0.49
1.45	14.21	2.56	1.423	0.56	20.22	7.90	9.89	0.49

Table C19 - Results for Spherical Charge Test

Sphere Charge

Load (kg)	Load (N)	Time (s)	Discharge	Average Velocity (m/s)	Energy (N-M)	Power (W)	Input Energy	Charge Efficiency
1.57	15.35	6	1.51	0.25	23.11	3.85	13.22	0.57
1.57	15.35	6.2	1.51	0.24	23.11	3.73	13.22	0.57
1.57	15.35	5.98	1.51	0.25	23.11	3.86	13.22	0.57
1.57	15.35	6.12	1.51	0.25	23.11	3.78	13.22	0.57
1.62	15.92	4.07	1.51	0.37	23.96	5.89	13.22	0.55
1.62	15.92	3.89	1.51	0.39	23.96	6.16	13.22	0.55
1.62	15.92	3.7	1.51	0.41	23.96	6.48	13.22	0.55
1.62	15.92	3.92	1.51	0.38	23.96	6.11	13.22	0.55
1.68	16.49	3.06	1.51	0.49	24.82	8.11	13.22	0.53
1.68	16.49	2.89	1.51	0.52	24.82	8.59	13.22	0.53
1.68	16.49	3.15	1.51	0.48	24.82	7.88	13.22	0.53
1.68	16.49	3.08	1.51	0.49	24.82	8.06	13.22	0.53
1.74	17.06	2.63	1.51	0.57	25.68	9.76	13.22	0.51
1.74	17.06	2.62	1.51	0.57	25.68	9.80	13.22	0.51
1.74	17.06	2.73	1.51	0.55	25.68	9.41	13.22	0.51
1.74	17.06	2.67	1.51	0.56	25.68	9.62	13.22	0.51
1.80	17.63	2.36	1.51	0.64	26.53	11.24	13.22	0.50
1.80	17.63	2.36	1.51	0.64	26.53	11.24	13.22	0.50
1.80	17.63	2.39	1.51	0.63	26.53	11.10	13.22	0.50
1.80	17.63	2.41	1.51	0.62	26.53	11.01	13.22	0.50
1.86	18.20	2.01	1.51	0.75	27.39	13.63	13.22	0.48
1.86	18.20	2.09	1.51	0.72	27.39	13.11	13.22	0.48
1.86	18.20	2.1	1.51	0.72	27.39	13.04	13.22	0.48
1.86	18.20	2.07	1.51	0.73	27.39	13.23	13.22	0.48

Table C20 - Results for Horizontal Discharge Test - Improved Apparatus

Improved Reel - Horizontal Discharge

Load (kg)	Load (N)	Time (s)	Discharge	Average Velocity (m/s)	Energy (N-M)	Power (W)	Input Energy	Discharge Efficiency
0.40	3.97	3.31	1.5	0.45	5.95	1.80	10.425	0.57
0.40	3.97	3.23	1.5	0.46	5.95	1.84	10.425	0.57
0.40	3.97	3.2	1.5	0.47	5.95	1.86	10.425	0.57
0.40	3.97	3.21	1.5	0.47	5.95	1.85	10.425	0.57
0.46	4.54	3.28	1.5	0.46	6.80	2.07	10.425	0.65
0.46	4.54	3.35	1.5	0.45	6.80	2.03	10.425	0.65
0.46	4.54	3.4	1.5	0.44	6.80	2.00	10.425	0.65
0.52	5.11	3.65	1.5	0.41	7.66	2.10	10.425	0.73
0.52	5.11	3.58	1.5	0.42	7.66	2.14	10.425	0.73
0.52	5.11	3.61	1.5	0.42	7.66	2.12	10.425	0.73
0.58	5.68	4.43	1.5	0.34	8.51	1.92	10.425	0.82
0.58	5.68	4.61	1.5	0.33	8.51	1.85	10.425	0.82
0.58	5.68	4.48	1.5	0.33	8.51	1.90	10.425	0.82
0.64	6.24	5.45	1.5	0.28	9.37	1.72	10.425	0.90
0.64	6.24	5.53	1.5	0.27	9.37	1.69	10.425	0.90
0.64	6.24	5.41	1.5	0.28	9.37	1.73	10.425	0.90
0.70	6.81	9.69	1.5	0.15	10.22	1.05	10.425	0.98
0.70	6.81	10.07	1.5	0.15	10.22	1.01	10.425	0.98
0.70	6.81	9.78	1.5	0.15	10.22	1.05	10.425	0.98

Table C21 - Results for Vertical Discharge Test - Improved Apparatus

Improved Reel - Vertical Discharge

Load (kg)	Load (N)	Time (s)	Discharge	Average Velocity (m/s)	Energy (N-M)	Power (W)	Input Energy	Discharge Efficiency
0.40	3.97	1.68	1.3	0.77	5.16	3.07	9.035	0.57
0.40	3.97	1.65	1.3	0.79	5.16	3.13	9.035	0.57
0.40	3.97	1.65	1.3	0.79	5.16	3.13	9.035	0.57
0.40	3.97	1.65	1.3	0.79	5.16	3.13	9.035	0.57
0.46	4.54	1.75	1.3	0.74	5.90	3.37	9.035	0.65
0.46	4.54	1.82	1.3	0.71	5.90	3.24	9.035	0.65
0.46	4.54	1.79	1.3	0.73	5.90	3.29	9.035	0.65
0.52	5.11	2.09	1.3	0.62	6.64	3.18	9.035	0.73
0.52	5.11	2.04	1.3	0.64	6.64	3.25	9.035	0.73
0.52	5.11	2.08	1.3	0.63	6.64	3.19	9.035	0.73
0.58	5.68	2.39	1.3	0.54	7.38	3.09	9.035	0.82
0.58	5.68	2.45	1.3	0.53	7.38	3.01	9.035	0.82
0.58	5.68	2.41	1.3	0.54	7.38	3.06	9.035	0.82
0.64	6.24	3.18	1.3	0.41	8.12	2.55	9.035	0.90
0.64	6.24	3.08	1.3	0.42	8.12	2.64	9.035	0.90
0.64	6.24	3.04	1.3	0.43	8.12	2.67	9.035	0.90
0.70	6.81	5.35	1.3	0.24	8.86	1.66	9.035	0.98
0.70	6.81	5.46	1.3	0.24	8.86	1.62	9.035	0.98
0.70	6.81	5.55	1.3	0.23	8.86	1.60	9.035	0.98

Table C22 - Results for Spherical Discharge Test - Improved Apparatus

Improved Reel - Spherical Discharge								
Load (kg)	Load (N)	Time (s)	Discharge	Average Velocity (m/s)	Energy (N-M)	Power (W)	Input Energy	Discharge Efficiency
0.64	6.24	1.71	1.36	0.80	8.49	4.97	11.95	0.71
0.64	6.24	1.57	1.36	0.87	8.49	5.41	11.95	0.71
0.64	6.24	1.62	1.36	0.84	8.49	5.24	11.95	0.71
0.64	6.24	1.67	1.36	0.81	8.49	5.09	11.95	0.71
0.70	6.81	1.84	1.36	0.74	9.27	5.04	11.95	0.78
0.70	6.81	1.86	1.36	0.73	9.27	4.98	11.95	0.78
0.70	6.81	1.78	1.36	0.76	9.27	5.21	11.95	0.78
0.75	7.38	2.25	1.36	0.60	10.04	4.46	11.95	0.84
0.75	7.38	2.36	1.36	0.58	10.04	4.25	11.95	0.84
0.75	7.38	2.35	1.36	0.58	10.04	4.27	11.95	0.84
0.81	7.95	3.07	1.36	0.44	10.82	3.52	11.95	0.91
0.81	7.95	2.97	1.36	0.46	10.82	3.64	11.95	0.91
0.81	7.95	3.02	1.36	0.45	10.82	3.58	11.95	0.91
0.87	8.52	4.48	1.36	0.30	11.59	2.59	11.95	0.97
0.87	8.52	4.57	1.36	0.30	11.59	2.54	11.95	0.97
0.87	8.52	4.25	1.36	0.32	11.59	2.73	11.95	0.97
0.88	8.65	5.87	1.36	0.23	11.77	2.00	11.95	0.98
0.88	8.65	5.63	1.36	0.24	11.77	2.09	11.95	0.98
0.88	8.65	5.58	1.36	0.24	11.77	2.11	11.95	0.98

Table C23 - Results for Horizontal Charge Test - Improved Apparatus

Improved Reel - Horizontal Charge

Load (kg)	Load (N)	Time (s)	Discharge	Average Velocity (m/s)	Energy (N-M)	Power (W)	Input Energy	Charge Efficiency
0.89	8.70	9	1.5	0.17	13.05	1.45	10.425	0.80
0.93	9.09	9.96	1.5	0.15	13.64	1.37	10.425	0.76
0.93	9.09	9.85	1.5	0.15	13.64	1.38	10.425	0.76
0.93	9.09	9.45	1.5	0.16	13.64	1.44	10.425	0.76
0.99	9.66	5.81	1.5	0.26	14.49	2.49	10.425	0.72
0.99	9.66	5.32	1.5	0.28	14.49	2.72	10.425	0.72
0.99	9.66	5.66	1.5	0.27	14.49	2.56	10.425	0.72
1.04	10.23	4.21	1.5	0.36	15.34	3.64	10.425	0.68
1.04	10.23	3.97	1.5	0.38	15.34	3.87	10.425	0.68
1.04	10.23	4.18	1.5	0.36	15.34	3.67	10.425	0.68
1.10	10.80	3.75	1.5	0.40	16.20	4.32	10.425	0.64
1.10	10.80	3.63	1.5	0.41	16.20	4.46	10.425	0.64
1.10	10.80	3.61	1.5	0.42	16.20	4.49	10.425	0.64
1.16	11.37	3.76	1.5	0.40	17.05	4.54	10.425	0.61
1.16	11.37	3.32	1.5	0.45	17.05	5.14	10.425	0.61
1.16	11.37	3.46	1.5	0.43	17.05	4.93	10.425	0.61
1.22	11.94	3.15	1.5	0.48	17.91	5.68	10.425	0.58
1.22	11.94	3.13	1.5	0.48	17.91	5.72	10.425	0.58
1.22	11.94	3.17	1.5	0.47	17.91	5.65	10.425	0.58

Table C24 - Results for Vertical Charge Test - Improved Apparatus

Improved Reel - Vertical Charge								
Load (kg)	Load (N)	Time (s)	Discharge	Average Velocity (m/s)	Energy (N-M)	Power (W)	Input Energy	Charge Efficiency
0.89	8.70	9	1.3	0.14	11.31	1.26	9.035	0.80
0.93	9.09	7.53	1.3	0.17	11.82	1.57	9.035	0.76
0.93	9.09	6.85	1.3	0.19	11.82	1.73	9.035	0.76
0.93	9.09	6.59	1.3	0.20	11.82	1.79	9.035	0.76
0.99	9.66	3.61	1.3	0.36	12.56	3.48	9.035	0.72
0.99	9.66	3.55	1.3	0.37	12.56	3.54	9.035	0.72
0.99	9.66	3.62	1.3	0.36	12.56	3.47	9.035	0.72
1.04	10.23	2.82	1.3	0.46	13.30	4.72	9.035	0.68
1.04	10.23	2.79	1.3	0.47	13.30	4.77	9.035	0.68
1.04	10.23	2.84	1.3	0.46	13.30	4.68	9.035	0.68
1.10	10.80	2.3	1.3	0.57	14.04	6.10	9.035	0.64
1.10	10.80	2.33	1.3	0.56	14.04	6.03	9.035	0.64
1.10	10.80	2.38	1.3	0.55	14.04	5.90	9.035	0.64
1.16	11.37	2.11	1.3	0.62	14.78	7.00	9.035	0.61
1.16	11.37	2.06	1.3	0.63	14.78	7.17	9.035	0.61
1.16	11.37	2.14	1.3	0.61	14.78	6.91	9.035	0.61
1.22	11.94	1.95	1.3	0.67	15.52	7.96	9.035	0.58
1.22	11.94	1.96	1.3	0.66	15.52	7.92	9.035	0.58
1.22	11.94	2.01	1.3	0.65	15.52	7.72	9.035	0.58

Table C25 - Results for Spherical Charge Test - Improved Apparatus

Improved Reel - Spherical Charge								
Load (kg)	Load (N)	Time (s)	Discharge	Average Velocity (m/s)	Energy (N-M)	Power (W)	Input Energy	Charge Efficiency
1.22	11.94	6.02	1.36	0.23	16.23	2.70	11.95	0.74
1.22	11.94	5.87	1.36	0.23	16.23	2.77	11.95	0.74
1.22	11.94	5.73	1.36	0.24	16.23	2.83	11.95	0.74
1.28	12.51	3.45	1.36	0.39	17.01	4.93	11.95	0.70
1.28	12.51	3.62	1.36	0.38	17.01	4.70	11.95	0.70
1.28	12.51	3.57	1.36	0.38	17.01	4.76	11.95	0.70
1.33	13.08	2.78	1.36	0.49	17.78	6.40	11.95	0.67
1.33	13.08	2.95	1.36	0.46	17.78	6.03	11.95	0.67
1.33	13.08	2.84	1.36	0.48	17.78	6.26	11.95	0.67
1.39	13.65	2.41	1.36	0.56	18.56	7.70	11.95	0.64
1.39	13.65	2.37	1.36	0.57	18.56	7.83	11.95	0.64
1.39	13.65	2.38	1.36	0.57	18.56	7.80	11.95	0.64
1.45	14.21	2.14	1.36	0.64	19.33	9.03	11.95	0.62
1.45	14.21	2.07	1.36	0.66	19.33	9.34	11.95	0.62
1.45	14.21	2.14	1.36	0.64	19.33	9.03	11.95	0.62
1.51	14.78	2.02	1.36	0.67	20.11	9.95	11.95	0.59
1.51	14.78	1.98	1.36	0.69	20.11	10.15	11.95	0.59
1.51	14.78	1.95	1.36	0.70	20.11	10.31	11.95	0.59

APPENDIX D
Uncertainty Analysis

D.1 - Uncertainty Analysis for discharge testing Chapter 3

Table D -1 - Systematic uncertainty of measured quantities

Measurement	Systematic Uncertainty	Value	Relative Uncertainty	Absolute Uncertainty
Float Mass (kg)	0.05%	0.453	0.50%	0.0023
Water Depth (m)	0.015	1.67	0.90%	0.0150
Discharge Time (s)	0.026	0.75	3.47%	0.0260
Discharge Voltage (v)	0.05%	88	0.50%	0.4400
Float radius (m)	0.0015	0.15	1.00%	0.0015
Resistance (ohm)	0.05	14.3	0.05%	0.0072

Note that only repeated discharge trials have a random uncertainty associated with them

Table D -2 - Random and systematic uncertainty of discharge time

Load (OHMS)	Average Discharge Time	Standard Deviation	Max. Deviation from Average	Random Uncertainty	Systematic Uncertainty	Total Uncertainty
0	0.75	0.04	0.04	5.33%	3.47%	8.80%
8	1.51	0.07	0.07	4.64%	3.47%	8.10%
11.4	1.04	0.04	0.04	3.85%	3.47%	7.31%
14.3	1.03	0.06	0.04	3.88%	3.47%	7.35%

Table D -3 - Random and systematic uncertainty of discharge voltage

Load (OHMS)	Average Voltage	Standard Deviation	Max. Deviation from Average	Relative Random Uncertainty	Systematic Uncertainty	Total Uncertainty
0	88.3	4.35	4.9	5.55%	0.50%	6.05%
8	19.9	2.11	2.2	11.06%	0.50%	11.56%
11.4	31.5	3.52	2.9	9.21%	0.50%	9.71%
14.3	37.5	1.91	1.6	4.27%	0.50%	4.77%

Using the total uncertainties for discharge time and discharge velocity, the total uncertainties associated with the calculated parameters can now be evaluated.

Table D -4 - Total uncertainties of calculated values

Calculation	Systematic Uncertainty	Value	Relative Uncertainty	Absolute Uncertainty
Velocity (m/s)	9.70%	2.23	4.36%	0.0973
Float Volume (cubic m)	3.00%	0.014	3.00%	0.000420
Frontal Area (m sq)	2.00%	0.0765	2%	0.00153
Power (watts)	20.30%	98.34	3.97%	3.90
Input Energy (N-m)	4.40%	221.71	4.40%	9.75
Drag Loss	21.40%	43.87	11%	4.71
Residual Kinetic Energy	19.45%	4.49	8.78%	0.39
Roundtrip Efficiency	33.50%	22.8	33.50%	7.64

D.2 - Uncertainty Analysis for Open Water Tests Chapter 4

Table D -5 - Open Water Systematic Uncertainty of Measured Quantities

Measurement	Systematic Uncertainty	Value	Relative Uncertainty	Absolute Uncertainty
Float Mass (kg)	0.50%	1.313	0.50%	0.0066
Water Depth (m)	0.1	5.9	1.69%	0.1000
Discharge Force (N)	0.50%	100.2	0.50%	0.5010
Discharge Time (s)	0.5	27	1.85%	0.5000
Discharge Voltage (v)	0.05%	13.5	0.50%	0.0675
Resistance (ohm)	0.05	34.1	0.05%	0.0171

Table D -6 - Open Water Systematic Uncertainty of Calculated Quantities

Calculation	Systematic Uncertainty	Value	Relative Uncertainty	Absolute Uncertainty
Velocity (m/s)	3.55%	0.9	3.55%	0.0319
Float Volume (cubic m)	3.00%	0.011538	3.00%	0.000346
Power (watts)	4.05%	5.78	4.05%	0.23
Input Energy (N-m)	2.19%	591.13	4.40%	26.00

D.3 - Uncertainty Analysis for Mechanical Load Testing Chapter 6

Table D -7 - Mechanical Loading Systematic Uncertainty of Measured Quantities

Measurement	Systematic Uncertainty	Value	Relative Uncertainty	Absolute Uncertainty
Float Mass (kg)	0.50%	0.31	0.50%	0.00155
Load Mass (kg)	0.50%	1.51	0.50%	0.00755
Float Volume	3.00%	0.000995	3.00%	0.00002985
Water Depth (m)	0.01	1.51	0.66%	0.01
Discharge Time (s)	0.1	6.02	1.66%	0.1

Table D -8 - Mechanical Loading Systematic Uncertainty of Calculated Quantities

Calculation	Systematic Uncertainty	Value	Relative Uncertainty	Absolute Uncertainty
Velocity (m/s)	2.32%	0.7	2.33%	0.0163
Float Volume (cubic m)	3.00%	0.011538	3.00%	0.0003
Power (watts)	4.05%	10.31	4.05%	0.4176
Input Energy (N-m)	1.16%	20.11	1.17%	0.2346
Output Energy (N-m)	1.16%	11.95	1.17%	0.1394
Discharge Efficiency	7.66%	98	7.66%	7.5090
Charge Efficiency	7.66%	74	7.66%	5.6701
Roundtrip Efficiency	15.32%	72.5	15.32%	11.1103

APPENDIX E

Experimental Equipment

Figure E-1 - Specifications for NEMA17 Stepper motor used for proof of concept testing [1].

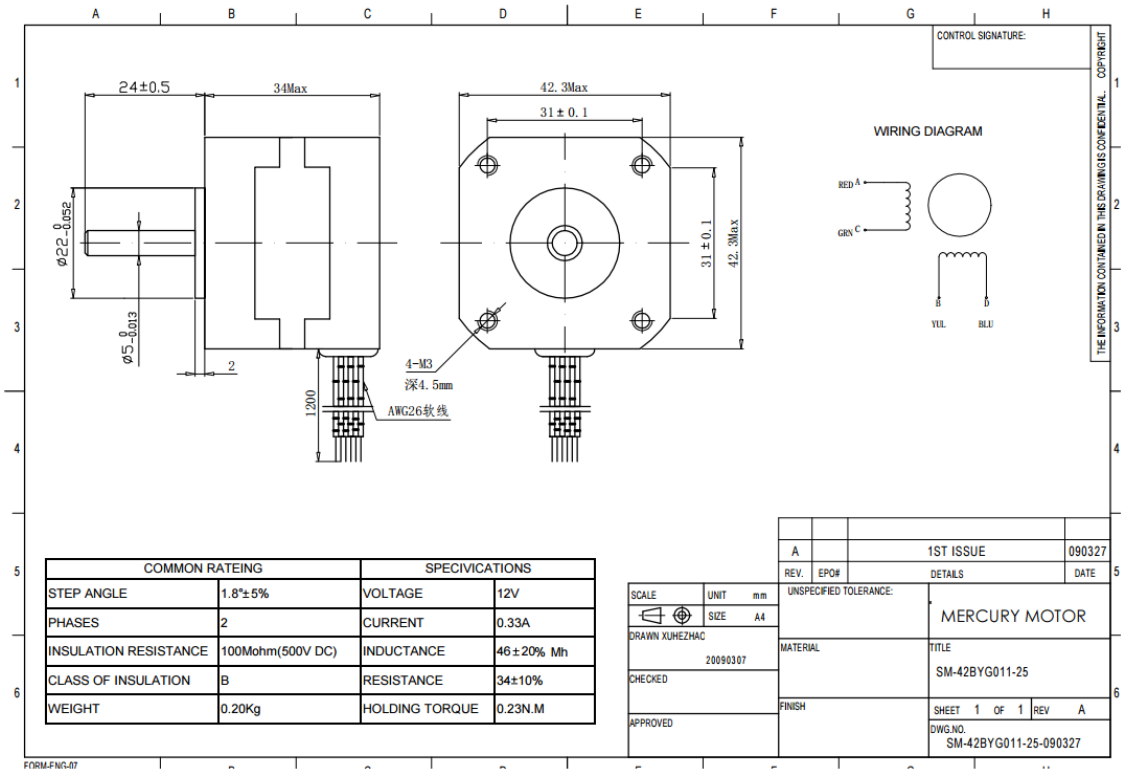

COMMON RATEING		SPECIVICATIONS	
STEP ANGLE	1.8°±5%	VOLTAGE	12V
PHASES	2	CURRENT	0.33A
INSULATION RESISTANCE	100Mohm(500V DC)	INDUCTANCE	46±20% Mh
CLASS OF INSULATION	B	RESISTANCE	34±10%
WEIGHT	0.20Kg	HOLDING TORQUE	0.23N.M

Figure E-2 - Wiring Diagram for 2 phase stepper motor operating as a generator with voltage doubling rectification

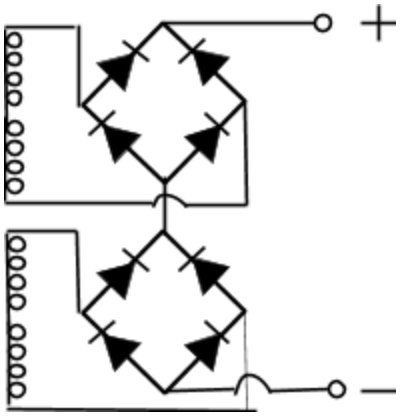

Figure E-3 - Specifications of 1N4001 Diodes used in rectification circuit [2]

1N4001, 1N4002, 1N4003, 1N4004, 1N4005, 1N4006, 1N4007

1N4004 and 1N4007 are Preferred Devices

Axial Lead Standard Recovery Rectifiers

This data sheet provides information on subminiature size, axial lead mounted rectifiers for general−purpose low−power applications.

Features

- Shipped in plastic bags, 1000 per bag
- Available Tape and Reeled, 5000 per reel, by adding a "RL" suffix to the part number
- Available in Fan−Fold Packaging, 3000 per box, by adding a "FF" suffix to the part number
- Pb−Free Packages are Available

Mechanical Characteristics

- Case: Epoxy, Molded
- Weight: 0.4 gram (approximately)
- Finish: All External Surfaces Corrosion Resistant and Terminal Leads are Readily Solderable
- Lead and Mounting Surface Temperature for Soldering Purposes: 260°C Max. for 10 Seconds, 1/16 in. from case
- Polarity: Cathode Indicated by Polarity Band

ON Semiconductor®

http://onsemi.com

LEAD MOUNTED RECTIFIERS
50−1000 VOLTS
DIFFUSED JUNCTION

CASE 59−10
AXIAL LEAD
PLASTIC

MARKING DIAGRAM

A = Assembly Location
1N400x = Device Number
x = 1, 2, 3, 4, 5, 6 or 7
YY = Year
WW = Work Week
• = Pb−Free Package

MAXIMUM RATINGS

Rating	Symbol	1N4001	1N4002	1N4003	1N4004	1N4005	1N4006	1N4007	Unit
†Peak Repetitive Reverse Voltage Working Peak Reverse Voltage DC Blocking Voltage	V_{RRM} V_{RWM} V_R	50	100	200	400	600	800	1000	V
†Non−Repetitive Peak Reverse Voltage (halfwave, single phase, 60 Hz)	V_{RSM}	60	120	240	480	720	1000	1200	V
†RMS Reverse Voltage	$V_{R(RMS)}$	35	70	140	280	420	560	700	V
†Average Rectified Forward Current (single phase, resistive load, 60 Hz, T_A = 75°C)	I_O	1.0							A
†Non−Repetitive Peak Surge Current (surge applied at rated load conditions)	I_{FSM}	30 (for 1 cycle)							A
Operating and Storage Junction Temperature Range	T_J T_{stg}	−65 to +175							°C

Figure E-4 - Specifications of Windstream Permanent Magnet DC Generator Model # 443540 [3]

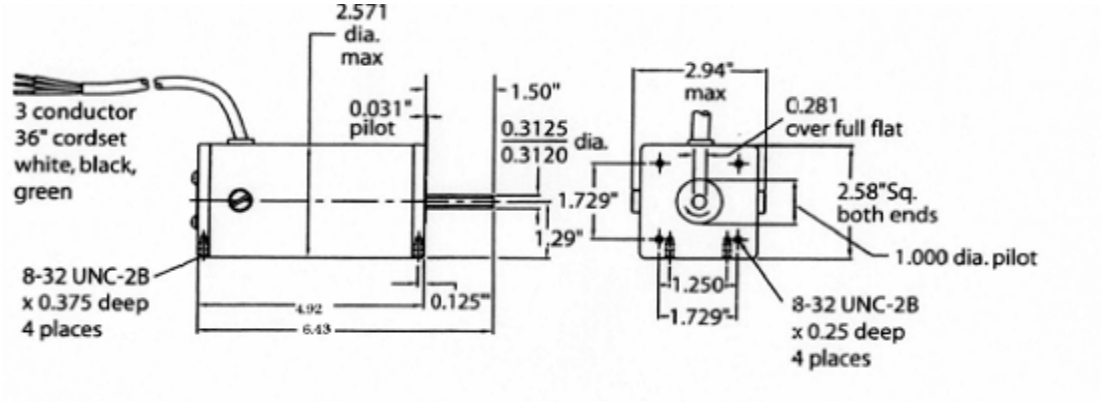

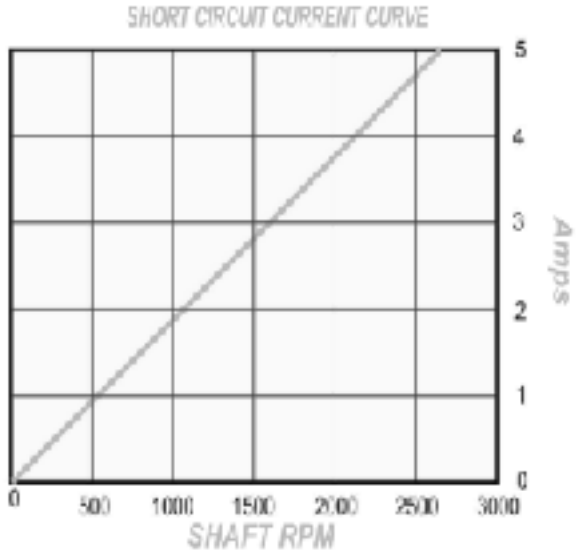

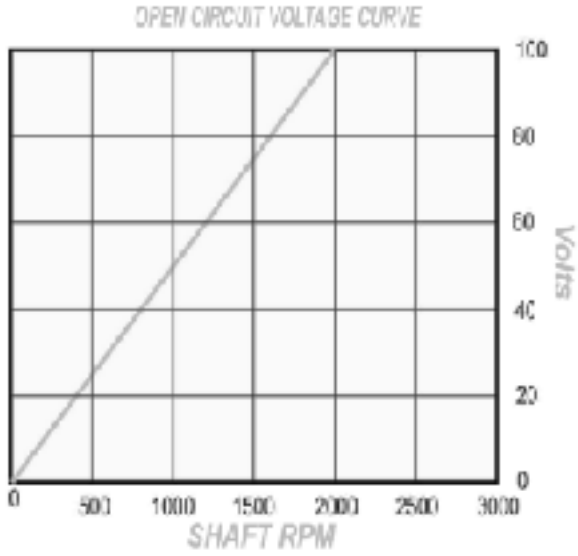

Figure E-5 - Construction Drawing of Fabricated Charge Reel Frame

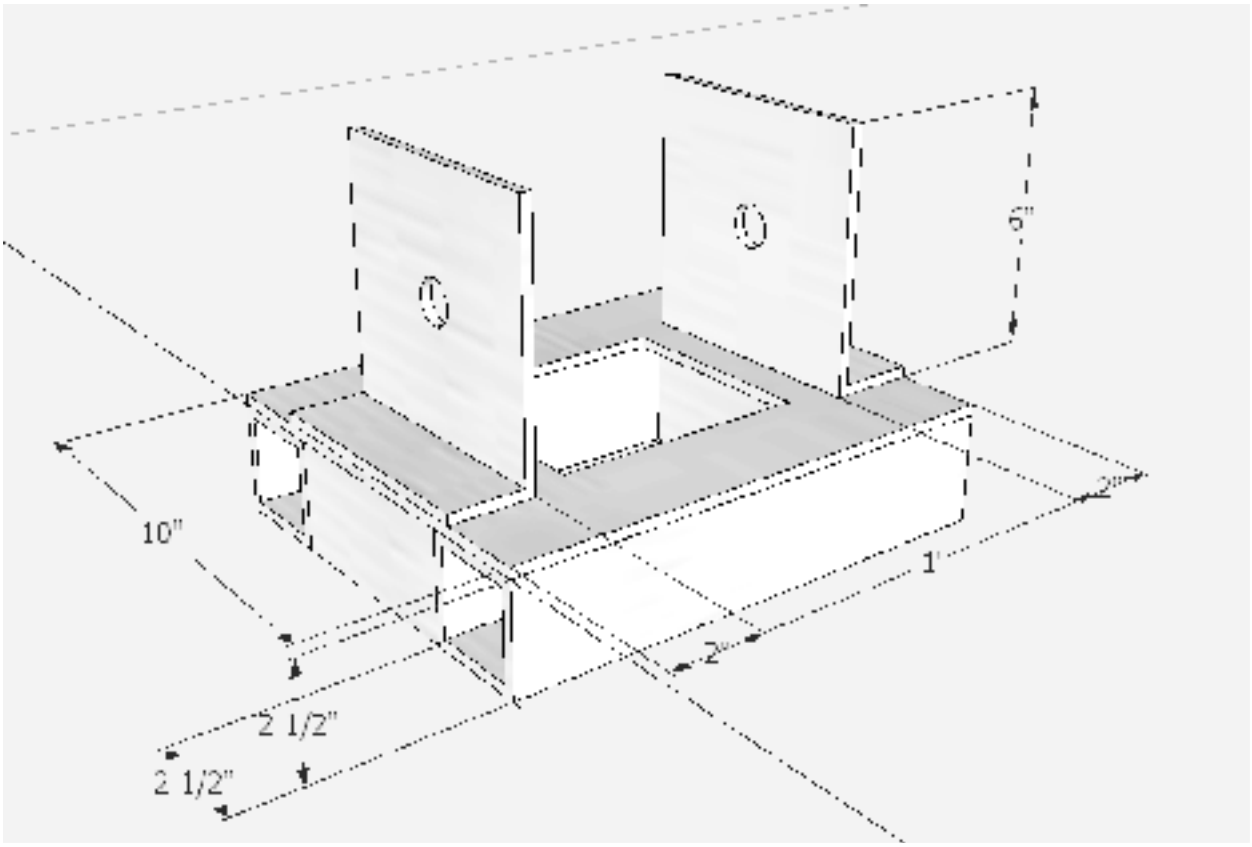

Figure E-6 - Specifications of 4 bolt flange bearing used on charge reel [4]

Weight & Package Dimensions

- **Weight (lbs)** 1.56
- **Package (L x W x H)** 4.0 x 4.0 x 1.7 in.

Attributes & Specifications

Inside Diameter	1 in.
Max. Radial (Downward) Load	3,000 lb
Max. Axial (Thrust) Load	1,500 lb

Figure E-7 - Assembly model of subsurface anchorage

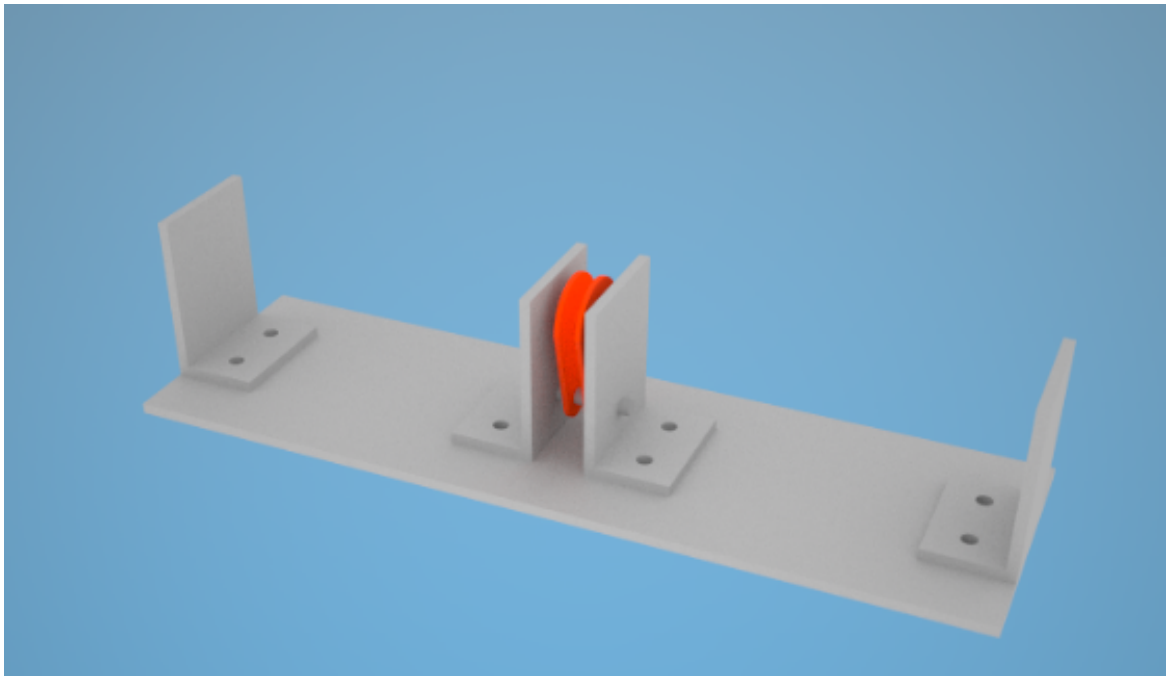

Figure E-8 - Pulley component specifications used for large tank testing [5]

Product Reference	Winching Component
Type	Pulley Block
Vertical Capacity	2,000 lb
Horizontal Capacity	4,000 lb
Pulley Diameter	1-3/4 in.
Max. Cable Diameter	3/16 in.
Brand	Powerfist

Figure E-9 - Specifications for galvanized aircraft cable used as float line in large tank testing [6]

Galvanized Aircraft Cables

Diameter in Inches	Construction	Minimum Break Strength/Lbs.	Rated Load/Lbs.	WT. Per 100 Ft./ Lbs.
1/16	7 x 7	480	100	.8
3/32	7 x 7	920	180	1.6
1/8	7 x 7	1,700	340	2.8
1/8	7 x 19	2,000	400	2.9
5/32	7 x 7	2,600	520	4.3
5/32	7 x 19	2,800	560	4.5
3/16	7 x 7	3,700	740	6.2
3/16	7 x 19	4,200	840	6.5
7/32	7 x 19	5,600	1,120	8.6
1/4	7 x 19	7,000	1,400	11.0
9/32	7 x 19	8,000	1,600	13.9
5/16	7 x 19	9,800	1,960	17.3
3/8	7 x 19	14,400	2,880	24.3

Figure E10- Recording Specifications for GOPRO Hero 3 Silver Edition Camera used for Large tank testing and mechanical load testing [6].

Specification	Value
Resolution	720p
Vertical Lines	720
Frames Per Second	60 (60Hz)
Sampling Period	0.0166 Seconds

CAMERA SETTINGS

The HERO3 Silver Edition offers the following Video Capture modes:

Video Resolution	NTSC fps	PAL fps	Protune	Field of View (FOV)	Screen Resolution
1080p	30fps	25fps	Yes	Ultra Wide, Medium, Narrow	1920x1080 16:9
1080p	24fps	24fps	Yes	Ultra Wide, Medium, Narrow	1920x1080 16:9
960p	48fps	50fps	Yes	Ultra Wide	1280x960 4:3
960p	30fps	25fps	Yes	Ultra Wide	1280x960 4:3
720p	60fps	50fps	Yes	Ultra Wide	1280x720 16:9
720p	30fps	25fps	No	Ultra Wide	1280x720 16:9
WVGA	120fps	100fps	No	Ultra Wide	800x480 16:9

Figure E-11 - Specifications of new anchorage pulley [8]

KingChain Single Sheave Rope Pulley with Swivel Eye, 1”

Safe Working Load 88lbs

Figure E-12 - Specifications for micro braided polyfilament line model #2110400150Y used for ball bearing conversion reel testing. [9]

Powerpro Micro-Filament Braided Fishing Line

Model #2110400150Y

Diameter - 0.3mm

Test strength - 40lbs

References

1) Mercury Motor, 12v Stepper Motor, Accessed online. https://www.adafruit.com/product/324
2) 1N4001 Diode. Accessed Online. https://cdn-shop.adafruit.com/datasheets/1N4001-D.PDF
3) Windstream Power Inc. http://windstreampower.com/products-page/permanent-magnet-dc-generators/443540-permanent-magnet-dc-generator/
4) NBR 1'' Flange Bearing https://www.princessauto.com/en/detail/1-in-4-bolt-standard-duty-flange-mount-bearing-assembly/A-p3870219e
5) Pulley Block. https://www.princessauto.com/en/detail/4-000-lb-pulley-block/A-p8489163e
6) Galvanized Aircraft cable specifications
7) Gopro Hero 3 Silver Edition User's Manual. https://gopro.com/content/dam/help/hero3plus-silver-edition/manuals/UM_H3PlusSilver_ENG_REVB_WEB.pdf,

APPENDIX F

F.1 - Derivation of Round Trip Efficiency Chapter 2 Equation 19

Equation presents the roundtrip efficiency of a buoyancy energy storage system. This equation includes electrical resistive losses within the generator/motor as well as the hydrodynamic losses due to drag force.

Resistive Energy Loss

$$P_{Resistive} = I^2 R \qquad (1)$$

where I = amperage, R=Resistance

$$E_{Resistive} = P_{Resistive} \times t \qquad (2)$$

$$E_{Resistive} = I^2 R\, t \qquad (3)$$ *substitution from (1)

Where t = discharge time

$$t = \frac{Z}{V} \qquad (4)$$

Where Z=discharge distance, V=float velocity

$$I = \frac{P_{Output}}{Q} \qquad (5)$$

Where P_{Output} = Buoyancy Output Power, Q = Generator resistance

$$P_{Output} = CV \qquad (6)$$

Where C = Cable tension, V = float velocity

$$I = \frac{CV}{Q} \qquad (7)$$*substitution from (6)

$$E_{Resistive} = \left(\frac{CV}{Q}\right)^2 R\, t \qquad (8)$$*substitution for amperage (5)

$$E_{Resistive} = \left(\left(\frac{CV}{Q}\right)^2 R\right)\frac{Z}{V} \qquad (9)$$*substitution for time (4)

$$E_{Resistive} = \frac{C^2 V R Z}{Q^2} \qquad (10)$$

This equation represents the resistive electrical losses for a discharge of a buoyancy energy storage system. For the intentions of this derivation the charge and discharge of the system utilizes the same electromotive device and as such the resistance is equal for both charge and discharge. Thus the total electrical loss for a buoyancy roundtrip can be expressed as twice the value of equation (10).

$$E_{Resistive} = \frac{2C^2VRZ}{Q^2} \qquad (11)$$

Hydrodynamic Energy Loss

$$F_{Drag} = \frac{1}{2}\rho C_D A V^2 \qquad (12)$$

Where F_{Drag} = Drag Force, ρ =water density, C_D = drag coefficient, A =float frontal area,

$$E_{Drag} = \frac{1}{2}\rho C_D A V^2 Z \qquad (13)$$

Equation (13) expresses the drag loss experienced for a buoyancy discharge. For the intentions of this derivation the float is assumed to be symmetric about a horizontal axis such that it will have the same drag coefficient for each direction up or down. It is also assumed that the float velocity for charge and discharge is equal. Using these assumptions the total energy loss for a roundtrip cycle can be expressed.

$$E_{Drag} = \rho C_D A V^2 Z \qquad (14)$$

Roundtrip Efficiency

$$\eta = \frac{Energy\ Output}{Energy\ Input} \qquad (15)$$

$$E_{Input} = CZ \qquad (16)$$

$$E_{Output} = CZ - E_{Resistive} - E_{Drag}$$

$$E_{Output} = CZ - \frac{2C^2VRZ}{Q^2} - \rho C_D A V^2 Z \qquad (17)\ \text{*Factor out CZ}$$

$$E_{Output} = CZ\left(1 - \frac{2CVR}{Q^2} - \frac{\rho C_D A V^2}{C}\right) \qquad (18)$$

$$\eta = \frac{CZ\left(1-\frac{2CVR}{Q^2}-\frac{\rho C_D A V^2}{C}\right)}{CZ} \qquad (19)$$

$$\eta = 1 - \frac{2CVR}{Q^2} - \frac{\rho C_D A V^2}{C} \qquad (20)$$

Which is how the equation in presented in Chapter 2 Equation 19.

Vita Auctoris

Kyle Bassett was born in 1987 in Scarborough, Ontario. He was raised in small town named Ballentre. He completed high school at Cardinal Carter Catholic High School in Aurora. Following that he attended the University of Windsor where he obtained a B.A.Sc in Mechanical Engineering in 2009. During this undergraduate study he began research into renewable energy, wind turbines and structural health monitoring. He completed his M.A.Sc. in mechanical engineering in 2010. Following his Master's degree he lived in a remote village of Nicaragua, researching and developing new wind turbine technologies for application in developing countries. In 2015 he returned to academia in pursuit of a PhD in civil engineering, now with a new area of research - energy storage. He anticipates completion of the PhD early 2017.